UNIVERSIDADE DE SÃO PAULO
INSTITUTO DE QUÍMICA
Programa de Pós-Graduação em Ciências Biológicas (Bioquímica)

LORENNA ROCHA REIS

Investigation of the events leading to NETs release using high resolution proteomics

Versão corrigida da Tese defendida

São Paulo

Data de depósito na SPG:

28/04/2023

LORENNA ROCHA REIS

Investigação dos eventos que levam à liberação de NETs usando proteômica de alta resolução

Tese apresentada ao Instituto de Química da Universidade de São Paulo para obtenção do Título de Doutor em Ciências (Bioquímica)

Orientadora: Profa. Dra. Graziella Eliza Ronsein

São Paulo
2023

Universidade de São Paulo
Instituto de Química

"Investigação dos eventos que levam à liberação de NETs usandoproteômica de alta resolução"

LORENNA ROCHA REIS

Tese de Doutorado submetida ao Instituto de Química da Universidade de São Paulo como parte dos requisitos necessários à obtenção do grau de Doutora em Ciências obtido no Programa Ciências Biológicas (Bioquímica) - Área de Concentração: Bioquímica.

_____

Profa. Dra. Graziella Eliza Ronsein(Orientadora e Presidente)

APROVADO(A) POR:

_____

Profa. Dra. Flavia Carla MeottiIQ - USP

_____

Profa. Dra. Leda Quercia Vieira (por videoconferência)
UFMG

_____

Prof. Dr. André Zelanis Palitot PereiraUNIFESP - SJC

SÃO PAULO
01 de junho de 2023

Ficha Catalográfica elaborada eletronicamente pelo autor, utilizando o programa desenvolvido pela Seção Técnica de Informática do ICMC/USP e adaptado para a Divisão de Biblioteca e Documentação do Conjunto das Químicas da USP

Bibliotecária responsável pela orientação de catalogação da publicação:

R375i

Reis, Lorenna Rocha
Investigation of the events leading to NETs release using high resolution proteomics / Lorenna Rocha Reis. - São Paulo, 2023.
111 p.

Tese (doutorado) - Instituto de Química da Universidade de São Paulo. Departamento de Bioquímica.
Orientador: Ronsein, Graziella Eliza

1. NETosis. 2. NETs. 3. NADPH oxidase. 4. PMA. 5. ionomycin. I. T. II. Ronsein, Graziella Eliza, orientador.

Marlene Aparecida Vieira - CRB - 8/5562

Aos meus irmãos queridos Larissa e Callebe,
com todo meu amor e admiração

AGRADECIMENTOS

Desde do início da minha jornada no instituto de química da USP me senti acolhida. Como foi bom desfrutar do dia a dia de trabalho com tantas pessoas companheiras, dispostas a ajudar e fazer a pesquisa acontecer. Tenho certeza que ciência não se faz sozinha, apesar dessa tese ser a respeito do meu trabalho, ele só foi possível devido à ajuda e as trocas de conhecimento que tive com meus companheiros de laboratório e aos amigos que colecionei na jornada.

Meu primeiro agradecimento vai pra professora Graziella, que acreditou em mim desde o início, mesmo eu vindo de outra universidade e tendo que aprender muito, antes de começar o básico. Nunca vou esquecer do seu espírito alegre, compreensivo e sempre de braços abertos para ajudar. Grazi, você é uma pesquisadora excelente, cresci muito debatendo nossas teorias, foi um privilégio, obrigada.

O doutorado me deu uma irmã de alma, que esteve comigo desde o primeiro experimento no laboratório. Amanda querida, você é com certeza uma das minhas alegrias diárias, mesmo não nos vendo mais com frequência. Aprendi e cresci muito com você, obrigada por deixar meus dias mais leves. Um obrigada especial à Clarice por fazer minha grande amiga mais feliz, o que também me deixa mais feliz.

Ao meu querido amigo Doug, que sempre foi uma pessoa de grande ajuda na pesquisa, mas conforme conheci mais, encontrei um grande parceiro de alegrias e aventuras. À minha querida Bianca, que me contagiou com sua doçura e trouxe companhia aos dias frios de HPLC. Um obrigada à vocês dois, por tantos momentos felizes no bar e fora dele.

Foram tantas pessoas que fizeram meus dias mais ensolarados e alegres. Aos meus colegas de laboratório, Rafa, Stella, André, Luiza, Elle, Rebeca e Gaby, obrigada pelas conversas, risadas e almoços felizes. Muito obrigada à Rai, Bianca, Bea, Laurinha, Peter, Litiele e Carol, lembro com muito carinho dos nossos cafés, conversas e peripécias no laboratório. Rai, muito obrigada por me introduzir ao mundo dos neutrófilos, foi muito bom poder contar com você. Um obrigada aos meus parceiros de biologia molecular, Heloísa, Alex, João Vitor e João Paulo, nossa troca sempre foi muito enriquecedora, vocês são brilhantes. Hellen, obrigada por partilhar um pouco do seu vasto conhecimento, você sempre foi muito solícita e didática nas explicações. Muito obrigada Arthur e Nathália pelas conversas gostosas.

A vida no laboratório foi muito mais fácil com a ajuda da Fê, Agda, Mari, Edilaine, Fernando e Izaura, muito obrigada, além de aprender muito com vocês também compartilhei boas conversas que vou guardar. Mari, você foi primordial pra meus experimentos no Lumos, te agradeço por toda a atenção e cuidado. Fê, que privilégio foi aprender de HPLC e massas com você.

Um obrigada aos professores que passaram pela minha jornada e compartilharam seu conhecimento, em especial à professora Flávia Meotti, Marisa Medeiros, Paolo Di Mascio e Giuseppe Palmisano.

Agora da minha vida fora do laboratório, meu primeiro agradecimento vai para meus irmãos que sempre acreditaram em mim e me apoiaram mesmo de longe. Muito obrigada também mãe, sei que você estava torcendo de longe pelo meu sucesso. Amo vocês.

Um obrigada mega especial ao meu companheiro de vida, Rafa, que me acompanhou e acompanha nas subidas e descidas dessa aventura maluca que é viver. Obrigada por ser calmaria enquanto eu sou tempestade. Obrigada por me apoiar e ser ombro amigo independente da situação. Obrigada também à minha sogra Sil e ao Marcos, por serem tão queridos comigo e obrigada cacau, basta olhar pra você que eu fico feliz. Amo vocês.

Aos amigos que lá de Brasília mandam suas boas energias, muito obrigada Laís e Bruna por trazerem alegria, amor e companheirismo de longe. Muito obrigada minha amiga Kelfany, por lembrar de mim com memes, faz o meu dia. Muito obrigada também aos meus amigos Pedro, Hiago, Nay e Kat, pelas conversas sempre muito boas no whatsapp.

Com certeza, eu não sou a mesma Lorenna de quase 6 anos atrás quando entrei no doutorado, aprendi e cresci muito pelo caminho. Devo uma parte disso a vocês mencionados aqui. Obrigada por tudo.

APOIO FINANCEIRO

FAPESP – Fundação de Amparo à Pesquisa do Estado de São Paulo
CAPES – Coordenação de Aperfeiçoamento de Pessoal de Nível Superior
CNPq – Conselho Nacional de Desenvolvimento Científico e Tecnológico

Agradeço também à Fundação de Amparo à Pesquisa do Estado de São Paulo (FAPESP, processo no 2017/17270-1) pela bolsa concedida.

“Cause, I'm in love
With my future
Can't wait to meet her”
(My future, Billie Eilish)

RESUMO

Reis, L. R. **Investigação dos mecanismos intrínsecos à liberação de NETs por meio de proteômica** 2023. 171p. Tese - Programa de Pós-Graduação em Ciências Biológicas (Bioquímica). Instituto de Química, Universidade de São Paulo, São Paulo.

A fim de matar patógenos invasores, neutrófilos liberam redes extracelulares de DNA juntamente com proteínas citotóxicas, conhecidas como NETs (*do inglês*, neutrophil extracelular traps), em um processo chamado NETosis. Estudos mostram que os mecanismos de NETosis podem ser dependentes de cada estímulo. Assim, o estímulo forbol-12-miristato-13-acetato (PMA) leva à liberação de NETs por meio da ativação da NADPH oxidase, enquanto a NETosis causada por ionóforos de cálcio, como a ionomicina, ocorre sem ativação da NADPH oxidase. Independentemente do estímulo, uma série de mudanças bioquímicas e estruturais precisam ocorrer nos neutrófilos antes do evento de liberação de NETs, incluindo a descondensação da cromatina e a degranulação de proteínas citotóxicas. Tais eventos não estão totalmente compreendidos, mas estudos recentes mostraram que proteínas citotóxicas associadas as NETs podem agravar patologias e causar danos vasculares. Neste trabalho, utilizamos estudos de proteômica, microscopia com células vivas (*do inglês*, live imaging) e com células fixadas para investigar os eventos iniciais da NETosis por dois ângulos diferentes. Primeiro, foi realizada uma investigação das alterações bioquímicas que ocorrem antes da liberação de NETs após o tratamento com ionomicina. Assim, a microscopia com células vivas mostrou que os neutrófilos tratados com ionomicina perdem rapidamente seu núcleo polimórfico. Além disso, o fracionamento celular juntamente com os estudos proteômicos apontaram para profundas mudanças bioquímicas observadas dentro e ao redor do núcleo dos neutrófilos após 2 minutos de tratamento com ionomicina, tais como a reorganização do citoesqueleto, a redistribuição nuclear de proteínas relacionadas à remodelação da

actina e a citrulinação de proteínas ligantes de actina e de proteínas estruturais nucleares. Na sequência, foi realizada uma comparação da resposta dos neutrófilos a três estímulos diferentes, a saber, PMA, ionomicina e o peptídeo *N*-formilmetionil-leucil-fenilalanina (fMLP). Curiosamente, a liberação de NETs ocorreu após 30 minutos de tratamento com ionomicina e apenas após 90 minutos de estimulação com PMA. Monitoramos as células por até 120 minutos e o peptídeo quimiotático fMLP não induziu a liberação de NETs. Além disso, apenas os neutrófilos tratados com fMLP e PMA ativaram a NADPH oxidase. A análise das proteínas secretadas pelos neutrófilos após cada tratamento mostrou que os neutrófilos tratados com PMA e fMLP liberaram mais proteínas relacionadas à adesão e migração de neutrófilos e regulação positiva da atividade do superóxido. Em contraste, os neutrófilos tratados com ionomicina apresentaram um secretoma mais citotóxico, devido ao enriquecimento de proteínas dos grânulos azurófilicos. Em conclusão, ao explorar os eventos que ocorrem antes da liberação de NETs, nossos estudos revelaram mediadores bioquímicos envolvidos no processo e mostraram que, apesar de levarem ao mesmo resultado final, PMA e ionomicina desencadeiam respostas diferentes em neutrófilos estimulados.

Palavras-chave: NETosis, NADPH oxidase, NETs, proteômica, PMA, ionomicina

ABSTRACT

Reis, L. R. **Investigation of the intrinsic mechanisms to NETs release through proteomics.** 2023.171p. Thesis - Graduate Program in Biochemistry. Instituto de Química, Universidade de São Paulo, São Paulo.

Neutrophil extracellular traps (NETs) are webs of DNA and cytotoxic proteins released by neutrophils to kill pathogens through a process called NETosis. Studies have shown that the mechanisms of NETosis might be stimulus-dependent. Thus, the stimulus phorbol-12-myristate-13-acetate (PMA) lead to NETs release through activation of the NADPH oxidase, while NETosis caused by calcium ionophores such as ionomycin, occurs without NADPH oxidase activation. Regardless the stimulus, a series of biochemical and structural changes need to occur in neutrophils before the event of NETs release, including chromatin decondensation, and degranulation of cytotoxic proteins. These events are not fully understood, but recent studies have shown cytotoxic proteins associated with NETs can aggravate pathologies and cause vascular damage. Here, we used proteomics studies, live imaging, and fixed microscopy to investigate the early events of NETosis from two different angles. First, an investigation of the biochemical changes that occur upon ionomycin treatment before NETs release was undertaken. Thus, live imaging microscopy showed ionomycin-treated neutrophils rapidly lose their polymorphic nucleus. Moreover, cell fractionation together with proteomic studies pointed to profound biochemical changes seen in and around neutrophil nucleus after 2 minutes of ionomycin treatment, such as cytoskeleton reorganization, nuclear redistribution of actin-remodeling related proteins, and citrullination of actin-ligand and nuclear structural proteins. Second, a comparison of the neutrophils' response to three different stimuli, namely PMA, ionomycin, and the peptide *N*-formylmethionyl-leucyl-phenylalanine (fMLP) was undertaken. Interestingly, the release of NETs occurred after 30 minutes of ionomycin treatment, and after 90

minutes of PMA stimulation. We monitored the cells for up to 120 minutes and the chemotactic peptide fMLP did not induce NETs release. Moreover, only fMLP- and PMA-treated neutrophils activated NADPH oxidase. The analysis of neutrophils' secreted proteins after each distinct treatment showed that PMA and fMLP-stimulated neutrophils released more proteins related to neutrophil adhesion and migration, and positive regulation of superoxide activity. In contrast, ionomycin-treated neutrophils had a more cytotoxic secretome, given the enrichment of proteins from azurophilic granules. In conclusion, by exploring the events that happen before NETs release, our studies revealed biochemical mediators involved in this process, and showed that despite leading to the same final outcome, PMA and ionomycin trigger different responses in stimulated neutrophils.

Keywords: NETosis, NADPH oxidase, NETs, proteomics, PMA, ionomycin

SUMMARY

Introduction

Neutrophils are the most abundant cells of the innate immune system and are essential for host defense against pathogens [1]. Upon arriving at the site of infection, the neutrophil has several strategies in order to eliminate bacteria, fungi and viruses. Among the strategies used are the ingestion of microorganisms by phagocytosis in association with reactive oxygen species (ROS) [2] and cytotoxic proteins from their granules, and the action of these proteins in the extracellular environment linked to a discrete production of ROS, known as degranulation [3] (Figure 1).

Figure 1. Defense strategies of activated neutrophils. Figure created on BioRender website.

However, neutrophils have an additional defense mechanism to trap and eliminate pathogens, the release of neutrophil extracellular traps (NETs). NETs were first described by Brinkman *et al.*, in 2004 [4], and they consist of chromatin fibers coated with cytotoxic proteins from cytosol, nucleus, and granules, such as histones, neutrophil elastase (NE), and myeloperoxidase (MPO) [4], [5]. Neutrophils release NETs through a regulated type of cell death, distinct from necrosis and apoptosis, known as NETosis [4], [6].

A variety of stimuli, including drugs, bacterial toxins, microbes, and cytokines, can lead neutrophils to NETosis [7]. Nevertheless, studies indicate that NETosis

mechanisms are stimulus-dependent [8]. Among the sterile stimuli that trigger the release of NETs, phorbol 12-myristate 13-acetate (PMA) and ionomycin, a calcium ionophore derived from *Streptomyces* species, are widely used and possibly indicate two distinct mechanisms of NETosis [8], [9]. Furthermore, sterile stimuli can activate neutrophils without triggering the release of NETs. An example is the peptide *N*-formylmethionyl-leucyl-phenylalanine (fMLP), a potent chemotactic agent capable of promoting, among other actions, the degranulation of neutrophils [10], [11].

As previously described [2], [12], reactive oxygen species produced by activated neutrophils are an important part of their antimicrobial response. The main source of ROS in neutrophils comes from the enzyme NADPH oxidase [12]. Thus, upon phosphorylation of its cytosolic and granular components, NADPH oxidase becomes activated in the phagosome membrane or in the plasmatic membrane in a stimulus-dependent manner [13], [14]. Upon activation, NADPH oxidase catalyze the monovalent reduction of molecular oxygen to the superoxide anion radical $O_2^{-\cdot}$ [12], [15]. In agreement, chronic granulomatous disease patients, who have a genetic defect in NADPH oxidase and thus fail to produce ROS from these enzyme in phagocytes [16], are more susceptible to infections and are unable to generate NETs, especially after the activation of neutrophils with PMA [6], [9]. The presence and origin of ROS are suggested to be determinant factors in the distinction of NETosis triggered by PMA and ionomycin [8], [9], [17].

Upon treatment of neutrophils with the PMA compound, NADPH oxidase is assembled in the plasmatic membrane, as it mimics the action of the second cellular messenger diacylglycerol (DAG) [18]. Thus, PMA activates protein kinase C (PKC) by increasing its affinity for Ca^{2+} and phospholipid. PKC is responsible for phosphorylating the p47phox, p67phox, and p40phox components of NADPH oxidase [14].

Consequently, the superoxide generated quickly dismutates to hydrogen peroxide, which becomes substrate for MPO [12]. The joint action of H_2O_2/MPO promotes the dissociation of a complex from the membrane of azurophilic granules containing MPO, NE, and other proteins [19]. Once in the cytosol, NE cleaves F-actin filaments and then translocates to the nucleus, where it promotes chromatin decondensation by degrading histones [5].

On the other hand, NETosis triggered by ionomycin proves to be quick and independent of ROS from NADPH oxidase [8], [20]. However, this mechanism seems to trigger the generation of mitochondrial ROS and the activation of the SK3 potassium conductance channel [20]. Treatment of neutrophils with ionomycin increases intracellular calcium to concentrations above 1 uM, whereas under physiological conditions the concentration is around 80 nM [21]. This intense influx of calcium results in hyperactivation of protein arginine deiminases (PADs) [22], including PAD4, which is responsible for converting arginine residues into citrulline in histones [23]. As a result, the electrostatic interaction between histones and DNA is altered, leading to chromatin decondensation.

Chromatin behavior during NETosis has been described in three phases [24]. The first phase comprises the biochemically active phase where there is ATP consumption and the structure of the nucleus remains constant. The next phase begins with the entropic expansion of chromatin and disruption of the nuclear membrane, consequently, DNA expands into the cytoplasm. Next, occurs the release of NETs into the extracellular environment, characterizing the third phase. Within 60 min after activation with PMA, NE is described in the nucleus, where it acts by degrading histones, i.e., initiating the second phase of NETosis [19], [24]. In contrast, after

treatment with ionomycin, the second phase of NETosis is described within 45 min [24] and it is unclear if NE is involved.

In addition to its role in fighting infections [1], [25], the exacerbated and uncontrolled release of NETs can intensify certain pathologies such as diabetes [26], thrombosis [27] and autoimmune diseases [28]–[30]. However, little is known about the signaling mechanisms intrinsic to NETosis, hence it is critical to study such mechanisms [31].

Thus, in the first chapter of this work, we developed a detailed study on the cellular events that occur before the release of NETs using ionomycin as a NETosis inducer. Therefore, we used microscopic imaging of fixed and live cells, in order to capture images of neutrophils from the initial moments to the final stage of rupture of the plasmatic membrane and NETs release into the extracellular environment. Furthermore, using cell fractionation and proteomic studies, we were able to identify the biochemical mediators involved in the process of ionomycin-induced NETosis. Finally, a careful study of modifications by mass spectrometry evaluated the presence of citrullination in neutrophil proteins after activation by ionomycin.

As discussed above, there is evidence that different stimuli trigger different NETosis processes, with their own biochemical mediators and which may or may not depend on the generation of reactive oxygen species. However, the different mechanisms and mediators that trigger the release of NETs are not fully understood. Therefore, in the second chapter of this thesis, we seek to characterize the formation of NETs induced by different stimuli, dependent or not on the generation of reactive oxygen species. Thus, we evaluated the generation or not of NETs triggered by three sterile stimuli, PMA, ionomycin and fMLP. We measured the dependence of NADPH oxidase activation on NETS generation by neutrophils treated with each of the three

stimuli. Using live cell microscopy, we also evaluated the kinetics of DNA networks release against each stressor. Finally, using proteomics, statistics, and data analysis techniques, we identified the proteins secreted into the extracellular medium after activation with each stimulus. The knowledge of the secreted proteins allowed us to identify the different biochemical processes that precede the final event of cell death with the release of DNA and cytotoxic proteins to the external environment.

References

[1] E. Kolaczkowska and P. Kubes, “Neutrophil recruitment and function in health and inflammation,” *Nat. Rev. Immunol.*, vol. 13, no. 3, pp. 159–175, 2013, doi: 10.1038/nri3399.

[2] C. C. Winterbourn and A. J. Kettle, “Redox reactions and microbial killing in the neutrophil phagosome,” *Antioxid Redox Signal*, vol. 18, no. 6, pp. 642–660, 2013, doi: 10.1089/ars.2012.4827.

[3] P. Lacy, “Mechanisms of Degranulation in Neutrophils,” *J Allergy Clin Immunol*, vol. 2, no. 3, pp. 98–108, 2006, doi: 10.2310/7480.2006.00012.

[4] V. Brinkmann, “Neutrophil Extracellular Traps Kill Bacteria,” *Science (80-.).*, vol. 303, no. 5663, pp. 1532–1535, 2004, doi: 10.1126/science.1092385.

[5] V. Papayannopoulos, K. D. Metzler, A. Hakkim, and A. Zychlinsky, “Neutrophil elastase and myeloperoxidase regulate the formation of neutrophil extracellular traps,” *J. Cell Biol.*, vol. 191, no. 3, pp. 677–691, 2010, doi: 10.1083/jcb.201006052.

[6] T. A. Fuchs *et al.*, “Novel cell death program leads to neutrophil extracellular traps,” *J. Cell Biol.*, vol. 176, no. 2, pp. 231–241, 2007, doi: 10.1083/jcb.200606027.

[7] A. B. Guimarães-Costa, M. T. C. Nascimento, A. B. Wardini, L. H. Pinto-Da-Silva, and E. M. Saraiva, “ETosis: A microbicidal mechanism beyond cell death,” *J. Parasitol. Res.*, vol. 2012, no. 929743, pp. 1–11, 2012, doi: 10.1155/2012/929743.

[8] E. F. Kenny *et al.*, “Diverse stimuli engage different neutrophil extracellular trap pathways,” *Elife*, vol. 6, no. e24437, pp. 1–21, 2017, doi: 10.7554/eLife.24437.

[9] H. Parker, M. Dragunow, M. B. Hampton, A. J. Kettle, and C. C. Winterbourn, “Requirements for NADPH oxidase and myeloperoxidase in neutrophil extracellular trap formation differ depending on the stimulus,” *J. Leukoc. Biol.*, vol. 92, no. 4, pp. 841–849, 2012, doi: 10.1189/jlb.1211601.

[10] P. E. R. Follin, A. Johansson, and C. Dahlgren, “Intracellular Production of Reactive Oxygen Species in Human Neutrophils Following Activation by the Soluble Stimuli FMLP : Dioctanoylglycerol and Ionomycin,” vol. 9, pp. 29–37, 1991.

[11] J. A. Nick, G. L. Johnson, and G. S. Worthen, “Common and distinct intracellular signaling pathways in human neutrophils utilized by platelet activating factor and FMLP . Find the latest version :,” vol. 99, no. 5, pp. 975–986, 1997.

[12] C. C. Winterbourn, A. J. Kettle, and M. B. Hampton, “Reactive Oxygen Species and Neutrophil Function,” *Annu. Rev. Biochem.*, vol. 85, pp. 765–792, 2016, doi: 10.1146/annurev-biochem-060815-014442.

[13] G. T. Nguyen, E. R. Green, and J. Mecsas, “Neutrophils to the ROScue : Mechanisms of NADPH Oxidase Activation and Bacterial Resistance,” vol. 7, no. August, 2017, doi: 10.3389/fcimb.2017.00373.

[14] F. R. Sheppard, M. R. Kelher, E. E. Moore, J. D. Nathan, A. Banerjee, and C. C. Silliman, “Structural organization of the neutrophil NADPH oxidase : phosphorylation and translocation during priming and activation Abstract : The reduced nicotinamide adenine,” *J. Leukoc. Biol.*, vol. 78, no. 5, pp. 1025–1042, 2017, doi: 10.1189/jlb.0804442.

[15] S. A. Belambri, R. Houssam, and R. Margarita, “NADPH oxidase activation in neutrophils: Role of the phosphorylation of its subunits,” *Eur. J. Clin. Invest.*, vol. 48, no. January, pp. 1–9, 2018, doi: 10.1111/eci.12951.

[16] M. J. Stasia and X. J. Li, “Genetics and immunopathology of chronic granulomatous disease,” *Semin. Immunopathol.*, vol. 30, no. 3, pp. 209–235, 2008, doi: 10.1007/s00281-008-0121-8.

[17] D. N. Douda, M. A. Khan, H. Grasemann, and N. Palaniyar, “SK3 channel and mitochondrial ROS mediate NADPH oxidase-independent NETosis induced by calcium influx,” *Proc. Natl. Acad. Sci.*, vol. 112, no. 9, pp. 2817–2822, 2015, doi: 10.1073/pnas.1414055112.

[18] M. Castagnag and T. Yoshimi, “Direct Activation of Calcium-activated, Phospholipid-dependent Protein Kinase by Tumor-promoting Phorbol Esters,” *J. Biol. Chem.*, vol. 257, no. 13, pp. 7847–7851, 1982, doi: 10.1038/nrc2592.

[19] K. D. Metzler, C. Goosmann, A. Lubojemska, and A. Zychlinsky, “A Myeloperoxidase-Containing Complex Regulates Neutrophil Elastase Release and Actin Dynamics during NETosis,” *CellReports*, vol. 8, no. 3, pp. 883–896, 2014, doi: 10.1016/j.celrep.2014.06.044.

[20] D. N. Douda, M. A. Khan, H. Grasemann, and N. Palaniyar, “SK3 channel and mitochondrial ROS mediate NADPH oxidase-independent NETosis induced by calcium influx,” *Proc. Natl. Acad. Sci. U. S. A.*, vol. 112, no. 9, pp. 2817–2822, 2015, doi: 10.1073/pnas.1414055112.

[21] R. Gennaro, T. Pozzant, and D. Romeo, “Monitoring of cytosolic free Ca2+ in

C5a-stimulated neutrophils: Loss of receptor-modulated Ca2+ stores and Ca2+ uptake in granule-free cytoplasts," *Proc. Natl. Acad. Sci.*, vol. 81, no. March, pp. 1416–1420, 1984, doi: 10.1073/pnas.81.5.1416.

[22] E. Tarcsa, L. N. Marekov, G. Mei, G. Melino, S.-C. Lee, and P. M. Steinert, "Protein Unfolding by Peptidylarginine Deiminase," *J. Biol. Chem.*, vol. 271, no. 48, pp. 30709–30716, 1996, doi: 10.1074/jbc.271.48.30709.

[23] Y. Wang *et al.*, "Histone hypercitrullination mediates chromatin decondensation and neutrophil extracellular trap formation," *J. Cell Biol.*, vol. 184, no. 2, pp. 205–213, 2009, doi: 10.1083/jcb.200806072.

[24] E. Neubert *et al.*, "Chromatin swelling drives neutrophil extracellular trap release," *Nat. Commun.*, vol. 9, no. 3767, pp. 1–13, 2018, doi: 10.1038/s41467-018-06263-5.

[25] H. L. Wright, R. J. Moots, R. C. Bucknall, and S. W. Edwards, "Neutrophil function in inflammation and inflammatory diseases," *Rheumatology*, vol. 49, no. 9, pp. 1618–1631, 2010, doi: 10.1093/rheumatology/keq045.

[26] S. L. Wong *et al.*, "Diabetes primes neutrophils to undergo NETosis, which impairs wound healing," *Nat. Med.*, vol. 21, no. 7, pp. 815–819, 2015, doi: 10.1038/nm.3887.

[27] A. S. Savchenko *et al.*, "Neutrophil extracellular traps form predominantly during the organizing stage of human venous thromboembolism development," *J. Thromb. Haemost.*, vol. 12, no. 6, pp. 860–870, 2014, doi: 10.1111/jth.12571.

[28] M. Parenza *et al.*, "Neutrophil extracellular traps mediate transfer of cytoplasmic neutrophil antigens to myeloid dendritic cells toward ANCA induction and associated autoimmunity.," *Blood*, vol. 120, no. 15, pp. 3007–18, 2012, doi: 10.1182/blood-2012-03-416156.

[29] E. Villanueva *et al.*, "Netting Neutrophils Induce Endothelial Damage, In ltrate Tissues, and Expose Immunostimulatory Molecules in Systemic Lupus Erythematosus □," 2020, doi: 10.4049/jimmunol.1100450.

[30] J. C. Jennette, H. Xiao, and R. J. Falk, "Pathogenesis of Vascular Inflammation by Anti-Neutrophil Cytoplasmic Antibodies," *Front. Nephrol.*, vol. 3, pp. 1235–1242, 1985, doi: 10.1681/ASN.2005101048.

[31] H. R. Thiam, S. L. Wong, D. D. Wagner, and C. M. Waterman, "Cellular Mechanisms of NETosis," *Annu. Rev. Cell Dev. Biol.*, vol. 36, pp. 191–218, 2020, doi: 10.1146/annurev-cellbio-020520-111016.

CHAPTER 1: Citrullination of actin-ligand and nuclear structural proteins, cytoskeleton reorganization and protein redistribution across cellular fractions are early events in ionomycin-induced NETosis

Abbreviations

(NETs) – Neutrophil extracellular traps

(PAD4) – Peptidylarginine deiminase 4

(ELANE) – Neutrophil elastase

(MPO) – Myeloperoxidase

(LPS) – Lipopolysaccharides

(ROS) – Reactive oxygen species

(PR3) – Proteinase 3

(CTSG) – Cathepsin G

(fMLP) – Formil- methionyl-leucyl-phenylanine

(AZU1) – Azurocidin

(ACTB) – Beta-actin

(VIM) – Vimentin

(CFL1) – Cofilin 1

(ANXA1) – Annexin A1

(ARHGDIB) - Rho GDP-dissociation inhibitor 2

(GAPDH) – Glyceraldehyde-3-phosphate dehydrogenase

(TMSB4X) – Thymosin beta-4

(S100P) – Protein S100P

(ANXA3) – Annexin A3

(OLFM4) – Olfactomedin-4

(ANXA6) – Annexin A6

(ACTC1/ACTA1/2) – Alpha-cardiac actin, alpha-actin-1, alpha-actin-2

(PFN1) – Profilin-1

(CAP1) – Adenylyl cyclase-associated protein 1

(TALDO1) – Transaldolase

(PKM) – Pyruvate kinase

(PGD) – 6-phosphogluconate dehydrogenase

(G6PD) – Glucose-6-phosphate 1-dehydrogenase

(AIF1) – Allograft inflammatory factor 1

(CNN2) - Calponin-2

(CORO1A) – Coronin

(HCLS1) – Hematopoietic lineage cell-specific protein

(LASP1) - LIM and SH3 domain protein 1

(LSP1) - Lymphocyte-specific protein 1

(VASP) – Vasodilator-stimulated phosphoprotein

(TLN1) – Talin-1

(ADSS) - Adenylosuccinate synthetase isozyme 2

(H1FX) – Histone H1.10

(LBR) – Lamin-B receptor

(LMNB1) – Lamin-B1

(IF) – Intermediate filament

Abstract

Neutrophil extracellular traps (NETs) are web-like structures of DNA coated with cytotoxic proteins and histones released by activated neutrophils through a process called NETosis. NETs release occurs through a sequence of highly organized events leading to chromatin expansion and rupture of nuclear and cellular membranes. In calcium ionophore-induced NETosis, the enzyme peptidylargine deiminase 4 (PAD4) mediates chromatin decondensation through histone citrullination, but the biochemical pathways involved in this process are not fully understood. Here we use live-imaging microscopy and proteomic studies of the neutrophil cellular fractions to investigate the early events in ionomycin-triggered NETosis. We found that before ionomycin-stimulated neutrophils release NETs, profound biochemical changes occur in and around their nucleus, such as, cytoskeleton reorganization, nuclear redistribution of actin-remodeling related proteins, and citrullination of actin-ligand and nuclear structural proteins. Ionomycin-stimulated neutrophils rapidly lose their characteristic polymorphic nucleus, and these changes are promptly communicated to the extracellular environment through the secretion of proteins related to immune response. Therefore, our findings revealed key biochemical mediators in the early process that subsequently culminates with nuclear and cell membranes rupture, and extracellular DNA release.

Keywords: Neutrophil extracellular traps, nucleus, actin remodeling, citrullination, proteomics, neutrophils.

1. Introduction

Neutrophils constitute the host's first line of defense [1], employing several defense strategies to neutralize viruses, fungi, and bacteria [2]. Thus, generation of reactive oxygen species, degranulation and phagocytosis are well-known mechanisms used by neutrophils. Another killing strategy discovered more recently involves the release of extracellular DNA networks known as neutrophil extracellular traps (NETs) [3]. NETs consist of chromatin fibers coated with cytotoxic proteins released from the cytosol, nucleus and granules, including histones, neutrophil elastase (ELANE) and myeloperoxidase (MPO) [4], [5]. NETs are the result of a programmed type of cell death named NETosis, distinct from necrosis or apoptosis [3], [6].

A variety of stimuli can trigger NETosis, such as bacteria, fungi, platelets, or small compounds such as lipopolysaccharides (LPS), monosodium urate crystals, bacterial ionophores or phorbol esters [7], [8]. Evidence shows that NETosis mechanisms are stimulus-dependent [9], [10], and the main difference between them is the dependence on NADPH oxidase activation and reactive oxygen species (ROS) production [11], [12]. However, regardless of the mechanism, the decondensation of chromatin is a requirement for NETosis [13]. The chromatin decondensation during NETosis has been described to occur due to the loss of attractive forces between the DNA and modified histones, caused by neutralization of positive charges in histone tails. Two suggested mediators for this effect are the enzyme protein-arginine deiminase type-4 (PAD4), which catalyzes the deamination of arginine residues in citrulline [14], and the joint action of NE, proteinase 3 (PR3), and cathepsin G (CTSG), proteases which can cleave histones [15]. However, there is no consensus regarding which one, or even if both mediators are the drivers of chromatin decondensation and its expansion through the cytosol after neutrophil activation with different stimuli [16].

Moreover, an increase in intracellular calcium, either by mobilization of intracellular calcium stores [11], [17] or via influx from the extracellular medium [11], [13] was also proven to be crucial for NETosis, once the chelation of intracellular or extracellular calcium impaired the process. In this context, treatment of neutrophils with calcium ionophores promote an influx of calcium from the extracellular medium similar to the intracellular calcium oscillations triggered by bacterial pore-forming toxins [18], [19]. Furthermore, neutrophil activation by ionomycin, a calcium ionophore derived from the species *Streptomyces*, leads to PAD4 activation unraveling the ROS-independent mechanism of NETosis [11], [17].

After the *in vitro* activation of neutrophils, a series of morphological changes are observed, such as the disassembly of actin filaments (f-actin) [20], [21], shedding of microvesicles [21], remodeling of vimentin [21], microtubules disassembly [21], [22], endoplasmic reticulum vesiculation [21], granules disintegration [15, 18], chromatin decondensation [3], [20], nuclear envelope permeabilization [21], [23], DNA release in the cytosol [6], plasma membrane permeabilization and rupture [21], [24], and NETs release [3]. Nonetheless, Neubert *et al* [23], showed that the biochemical active phase of NETosis occurs before chromatin expansion and the morphological changes seen after that phase are driven by mechanical forces, with the active processes being secondary. Thus, the investigation of the biochemical pathways leading to chromatin swelling are key to understand NETosis. Yet, the key mediators of these morphological changes are not fully understood. Therefore, to investigate NETosis in the context of high intracellular calcium concentration, human neutrophils treated with the calcium ionophore ionomycin were tracked by live-imaging microscopy and subjected to proteomic studies after cellular fractionation. We have shown that soon after treatment, biochemical changes occur in their nuclei, and this active process is immediately

communicated to the extracellular environment. Also, we revealed altered protein remodeling across cell fractions, and citrullination of multiple proteins involved in cytoskeleton organization, as well as in chromatin and nuclear structure, thus providing potential mediators for the nucleoskeleton and cytoskeleton organization process taking place in and around the nucleus.

2. Materials and Methods

2.1 Materials

Dextran, Hystopaque, ammonium bicarbonate, tris(hydroxymethyl)aminomethane hydrochloride (Tris-HCl), sodium deoxycholate (SDC), dimethylsulfoxide (DMSO), ionomycin, paraformaldehyde, ethylene-bis(oxyethylenenitrilo)tetraacetic acid (EGTA), phenylmethanesulfonyl fluoride (PMSF), 1,4-piperazinediethanesulfonic acid (PIPES), adenosine 5' – triphosphate disodium salt ($ATP(Na)_2$), *cOmplete* protease inhibitor cocktail, benzonase nuclease, and trifluoroacetic acid (TFA) were obtained from Sigma (St. Louis, MO, USA). SYTOX™ green, Hoechst 33342, Prolong Diamond, and Pierce™ BCA protein assay kit were purchased from Invitrogen (Waltham, MA, USA). Dithiothreitol (DTT) and iodoacetamide were purchased from Bio-Rad laboratories (Hercules, CA, USA). Poly-D-Lysine, acetonitrile, acetone and 0.1% formic acid were obtained from Merck (Darmstadt, Germany). Trypsin was obtained from Promega (Madison, WI, USA).

2.2 Neutrophil Isolation

Human neutrophils were obtained from heparinized blood of healthy volunteers. Neutrophils were separated from blood by Dextran sedimentation followed by density centrifugation with Hystopaque 1.077 g/mL. Contaminating erythrocytes were lysed with a hypotonic solution, and neutrophils were resuspended in PBS with 5.5 mM

glucose or RPMI medium without phenol red [25]. Bright-field microscopy with May-Grünwald-Giemnsa stain was used to check for the presence of eosinophils, and the sample was considered appropriate if eosinophils were <5% of the cells. Blood collection was approved by the Research Ethics Committee of the Faculty of Pharmaceutical Sciences at University of São Paulo (CAAE 60860016.5.0000.0067).

2.3 Fluorescence microscopy

Neutrophils were allowed to settle on 0.001% poly-D-lysine coated glass coverslips for 20 min at 37 °C. Then, cells were treated with 0.005% v/v DMSO (vehicle), fMLP 1 µM or ionomycin 6.7 µM for 90 minutes at 37 °C, and subsequently fixed with 4% paraformaldehyde. After fixation, cells were washed with Tris-HCl buffer pH 7.4, and stained with 500 nM SYTOX Green. Coverslips were mounted over the glass slides using Prolong Diamond, and visualized with a fluorescence microscope (Zeiss Axiovert 200) with a 20x/0.4 objective using excitation and emission wavelengths of 485 nm and 520 nm, respectively. Images were taken by an Axiocam HR R3 camera device.

2.4 Live-imaging microscopy

Neutrophils ($1{,}5x10^5$) in phenol-red free RPMI 1640 medium supplemented with 1% of antibiotic and 2 µM Hoechst 33342 were allowed to settle on a 24-well plate coated with 0.001% of poly-D-lysine for 20 min at 37 °C. Next, neutrophils were treated with 6.7 µM ionomycin or the vehicle followed by addition of 500 nM SYTOX Green [12]. Cells were monitored using a 20x objective on a Leica DMi8 epifluorescence microscope coupled with the LASX Application Software (Leica Microsystems). Fluorescent images for Hoechst 33342 and SYTOX Green were automatically acquired every 2 min, for a total of 120min at 37°C with 5% CO_2.

2.5 Quantification of nuclei and NETs

The method of quantification described here was based on previously established methods [13], [26]. Images obtained from the live-imaging cell microscopy were loaded into the ImageJ software (version 1.52p) and converted to an 8-bit binary image. The local threshold was adjusted by the *Phansalkar* or *Bernsen* functions, and the cells that touched each other were separated by the function watershed. Then, the total number of cells was counted, and classified according to size in μm^2, circularity and loss of plasma membrane integrity (SYTOX Green positive cells) (Table 1). Based on these criteria, cells were divided in those containing a polymorphic nucleus, a spherical nucleus, those with a decondensed nucleus, and those with NETs, following the quantification criteria described in Table 1. The percentage of cells with decondensed nuclei but without loss of cellular membrane integrity (Hoechst 33342 positive and SYTOX Green negative) was obtained by counting all cells > 94 μm^2 and subtracting those cells presenting NETs (Hoechst 33342 positive and SYTOX Green positive). Polymorphic cells correspond to the subtraction of cells with a spherical nucleus, decondensed nucleus, or with NETs from total cells.

Table 1. Criteria for quantification of neutrophils based on nuclear shape by live-imaging.

	Total cells	**Polymorphic nucleus**	**Spherical nucleus**	**Decondensed nucleus**	**NETs**
Hoechst 33342	Positive	Positive	Positive	Positive	Positive
SYTOX Green	Positive	Negative	Negative	Negative	Positive
Auto-local threshold	Phansalkar	Phansalkar	Bernsem	Phansalkar	Phansalkar
Size (μm^2)	> 26	26 – 94	26 - 50	> 94	> 94
Circularity (0.0 – 1.0)	0.0 – 1.0	0.0 – 1.0	0.94 – 1.00	0.0 – 1.0	0.0 – 1.0

2.6 Cell lysis and fractionation

Neutrophils ($5x10^6$) were incubated with 0.005% v/v DMSO (vehicle), 6.7 µM ionomycin, or fMLP 1 µM for 2 min at 37 °C, kept on ice, and the secretome was collected and concentrated to 30% of the initial volume at 4 °C. Subsequently, the cells were resuspended in ice-cold disruption buffer (100 nM KCl, 3 mM NaCl, 3.5 mM $MgCl_2$, and 10 mM PIPES, pH 7.2). Next, 1 mM $ATP(Na)_2$ and 0.6 mM PMSF were added to the cells, and the cells were lysed by nitrogen cavitation [27] at 4 °C and 375 psi for 5 min, followed by addition of 1.5 mM EGTA. To minimize sample processing time, each replicate was individually processed up to the cell lysis.

The cell lysate obtained after nitrogen cavitation was centrifuged in 3 cycles of 5 min at 400 x *g* at 4 °C to obtain the nuclear fraction (pellet). Supernatants were used to obtain the organelles and soluble protein fractions. The organelles fraction was separated from soluble proteins through centrifugation at 79,000 x *g* for 30 min at 4 °C [28]. The remaining supernatant, containing the soluble proteins fraction, was concentrated to 30% of the initial volume at 4 °C using a vacuum concentration system. Nuclear and organelles fractions were lysed with 0.2% SDC in 100 mM ammonium bicarbonate in the presence of 0.5x (v/v) cOmplete protease inhibitor. cOmplete was also added to the secretome and soluble proteins fractions. Proteins were precipitated with 1:4 v/v acetone and NaCl 100 mM overnight at – 20 °C, centrifuged at 13,000 x *g* for 10 min at 4 °C, and resuspended in 100 mM ammonium bicarbonate with 0.2% SDC. DNA aggregates were digested twice with 0.1 U/µL benzonase nuclease for 45 min at 37 °C.

2.7 Sample preparation for mass spectrometry

The concentration of proteins in each fraction (secretome, nucleus, organelles and soluble proteins) was measured by the bicinchoninic acid assay (BCA). Ten µg of

proteins from each fraction were reduced with 5 mM DTT for 1h at 37 °C, alkylated with 15 mM iodoacetamide for 30 min in the dark at 25 °C, and the excess of iodoacetamide was quenched with 2.5 mM DTT for 15 min at 25 °C. Next, proteins were digested with two sequential additions of trypsin (1:40 w/w), for 4 h at 37 °C, and overnight at 37 °C. Digestion was stopped with 0.5% v/v TFA at 37 °C for 30 min, followed by centrifugation at 14,000 x *g* for 30 min. Half of the volume of the supernatant was used for desalting the samples using the stage tip protocol [29]. Samples were lyophilized and stored at -80 °C until the injection into the mass spectrometer. Before injection, each sample was resuspended in 100 µL of formic acid 0.1%.

2.8 LC-MS/MS measurements

The peptides were separated and analyzed in a Nano EASY-nLC 1200 (Thermo Fisher Scientific, Bremen, Germany) coupled to an Orbitrap Fusion Lumos mass spectrometer (Thermo Fisher Scientific, Bremen, Germany). First, each sample was injected into a trap column (nano Viper C18, 3 µm, 75 µm × 2 cm, Thermo Scientific) with 12 µL of solvent A (0.1% formic acid) at 500 bar. Then, the peptides were eluted onto a C18 column (nano Viper C18, 2 µm, 75 µm × 15 cm, Thermo Scientific) at a flow rate of 300 nL/min. Peptides were eluted from the column using a linear gradient of solvent A (0.1% formic acid in water) and solvent B (0.1% formic acid in 20:80 water: acetonitrile, v/v), starting with 5−28% B for 80 min, followed by an increase to 40% B for 10 min. Next, column wash was accomplished with an increase of solvent B percentage to 95% in 2 min, followed by 12 min with this solvent proportion. Re-equilibration of the system with 100% solvent A was performed before each injection.

After ionization under positive electrospray conditions, the eluted peptides were analyzed in a data-dependent acquisition mode. The most intense ions detected after

a full scan (400-1600 *m/z*) at a 120,000 resolution, were filtered for fragmentation by the quadrupole with a transmission window of 1.2 *m/z*, followed by HCD fragmentation with a normalized collision energy of 30, and detection of the fragments by the orbitrap mass analyzer with a 30,000 resolution. A new cycle of MS followed by MS2 events occurred at every 3 s. Monocharged ions or ions with undetermined charges were excluded from fragmentation.

2.9 Data analysis

Raw files of all proteomic experiments were processed using MaxQuant software [30]. Proteins were identified through the Andromeda algorithm [31] against the Homo sapiens Uniprot database (downloaded March, 2022; 20,401 entries). Error mass tolerance for precursors and fragments were set to 4.5 ppm and 20 ppm, respectively. Cysteine carbamidomethylation was selected as a fixed modification and methionine oxidation, deimination of arginine residues (citrullination) and *N*-terminal acetylation were selected as variable modifications. The deimination of the arginine residues (R) was set as an increase of + 0.98401 Da with a neutral loss of HCNO (43.0058 Da) [32]. A semi-tryptic digestion mode was set, with a maximum of 2 missed cleavages allowed. A maximum FDR of 1% was allowed both for peptides and proteins identification, and for proteins, FDR was calculated using a decoy database created from the reverse ordination of the protein sequences in the Uniprot database. Protein abundances were obtained from normalized chromatographic peak integrations calculated by MaxQuant through LFQ algorithm [33]. The protein was considered present if at least two peptides (one of them being unique) were detected. Match between runs option was enabled and the other parameters were kept as default.

Neutrophils from three different volunteers were used for proteomic analyses. For each subject, the neutrophils were divided in 4 different replicates for ionomycin

treatment and 4 replicates for control (DMSO only). All the fractions (secretome, nucleus, organelles and soluble proteins) from each volunteer were run in MaxQuant simultaneously. Alternatively, for comparisons within a specific fraction, raw files from all the samples of the volunteers in the fraction of interest (secretome or nucleus) were run in MaxQuant at the same time (n=4 for ionomycin treatment, and 4 for controls). The proteins were analyzed using Perseus software (version 1.6.15.0) [34] and data was plotted using GraphPad Prism (version 6.01) or R (version 1.2.5019). Volcano plots were made with the web app VolcaNoseR (https://huygens.science.uva.nl/VolcaNoseR/) [35]. Pathway enrichment analysis was performed combining enriched and unique proteins of each group using the web app WebGestalt (http://www.webgestalt.org/) under over-representative analysis with FDR < 0.05 and default parameters [36]. The enriched biological processes were summarized by weighted-set cover.

Before statistical analysis, the LFQ intensities were loaded into the Perseus software, filtered for reverse peptides and potential contaminants, and $\log_2$ transformed. Missing values were filtered using the criteria of at least 3 valid values in each group. Proteins were considered unique to a group in a given fraction if they had at least 3 valid values in one group and 0 or 1 valid value in the other.

To compare protein abundance across different fractions, for each protein, we calculated the percentage in each fraction in relation to the total (sum of the protein abundance in all 4 fractions). Only proteins common to all 4 fractions were selected for this analysis.

Before analysis of citrullinated proteins, false-positive peptides with citrullinated arginine in the C-terminal were manually excluded from the data. A citrullinated peptide was included in the analysis if it belonged to a protein present in at least 2 out of 3

individuals. Similarly, a peptide was reported as differentially regulated if it was found significantly altered in at least 2 subjects. Peptides present in a single individual are identified in supporting tables. For clarity, peptides and their miscleavages were compiled in a single lane in supporting tables presenting citrullinations. Common proteins had to have at least 2 valid values in both groups, while exclusive proteins had to have at least 2 valid values in one group and none in the other.

Protein symbols (all capital letters, not italicized) are based on gene symbols as recommended by the Human Genome Organization Gene Nomenclature Committee [37].

2.10 Statistical Analysis

Control and ionomycin live-imaging quantification data were evaluated separately through analysis of variance (ANOVA), followed by post hoc Tukey test of each nucleus type over time using R.

For proteomic analyses of nucleus and secretome, as well as the analysis of citrullinated peptides, the comparisons between groups (control and ionomycin) in each fraction was performed with an unpaired t-test. The p-value was adjusted for multiple comparisons applying an FDR of 0.05. These analyses were performed in R and Perseus.

For percentages in each fraction, after a t-test, proteins with adjusted P value <0.05 and with mean ratio of ionomycin/control >2 or <0.5 in at least one fraction each, were considered significantly different.

2.11 Data Statement

The data supporting the findings of this study are available from the corresponding author upon reasonable request.

3. Results

3.1 Ionomycin treatment induces early chromatin changes culminating in neutrophil NETosis

The neutrophil's response to ionomycin treatment was first assessed by fluorescence microscopy using SYTOX Green. Confirming previous studies [12], [17], treatment of human neutrophils with 6.7 µM ionomycin for 90 min at 37 °C produced large scaffolds of extracellular DNA, known as NETs (Figure 1A). In contrast, neutrophils that received only vehicle (DMSO) got a few spontaneous NETs, but the majority of the cells were still polymorphonuclear (Figure 1A).

Next, we sought to evaluate the progression of NETosis in neutrophils treated with ionomycin for 120 min using live-imaging microscopy, and two different nucleic acid dyes, Hoechst 33342, permeant to the cell membrane, and SYTOX Green, an impermeant dye to live cells. At every 2 min, one image frame was acquired for the control and ionomycin-treated cells. All nuclei were automatically categorized in polymorphonuclear, spherical, decondensed and undergoing NETs, according to their size, circularity, and plasmatic membrane loss of integrity (SYTOX green positive) by a set of specific parameters predefined on ImageJ software (Table 1). Figure 1B depicts 3 representative cells of control and ionomycin-treated samples tracking chromatin alterations over time. Control cells remained polymorphonuclear until 120 min (Figure 1B, C and D), whereas ionomycin-treated cells already displayed chromatin changes as early as 8 minutes (Figure 1B, C and D). Control cells were mainly polymorphonuclear (around 80%) at 20 min of incubation (Figure 1B, D) and at the 120 min timepoint, polymorphonuclear cells were still the major population (around 50%), while about 20% of cells displayed spontaneous NETs and around 20% had spherical nuclei (stable from the beginning) (Figure 1D). On the other hand, during the

first 20 min following ionomycin treatment, the nuclei lost their characteristic polymorphism, and became rounded (Figure 1B, E, spherical nuclei). After 20 min of incubation of neutrophils with ionomycin, approximately 35 % of the cells had lost their characteristic polymorphic nucleus, displaying rather a spherical nuclear shape. After one hour, the majority of ionomycin-treated cells (~70 %) presented decondensed chromatin, and after 100 min, the majority of cells (~60 %) had undergone NETosis (Figure 1A, E). Taken together, these results showed that ionomycin treatment leads to a fast remodeling of nuclear shape, with early changes detected in less than 8 minutes after exposure. The extensive chromatin remodeling culminates in loss of cell membrane integrity and NETs release, starting as early as 40 minutes after ionomycin treatment (for about 20 % of cells).

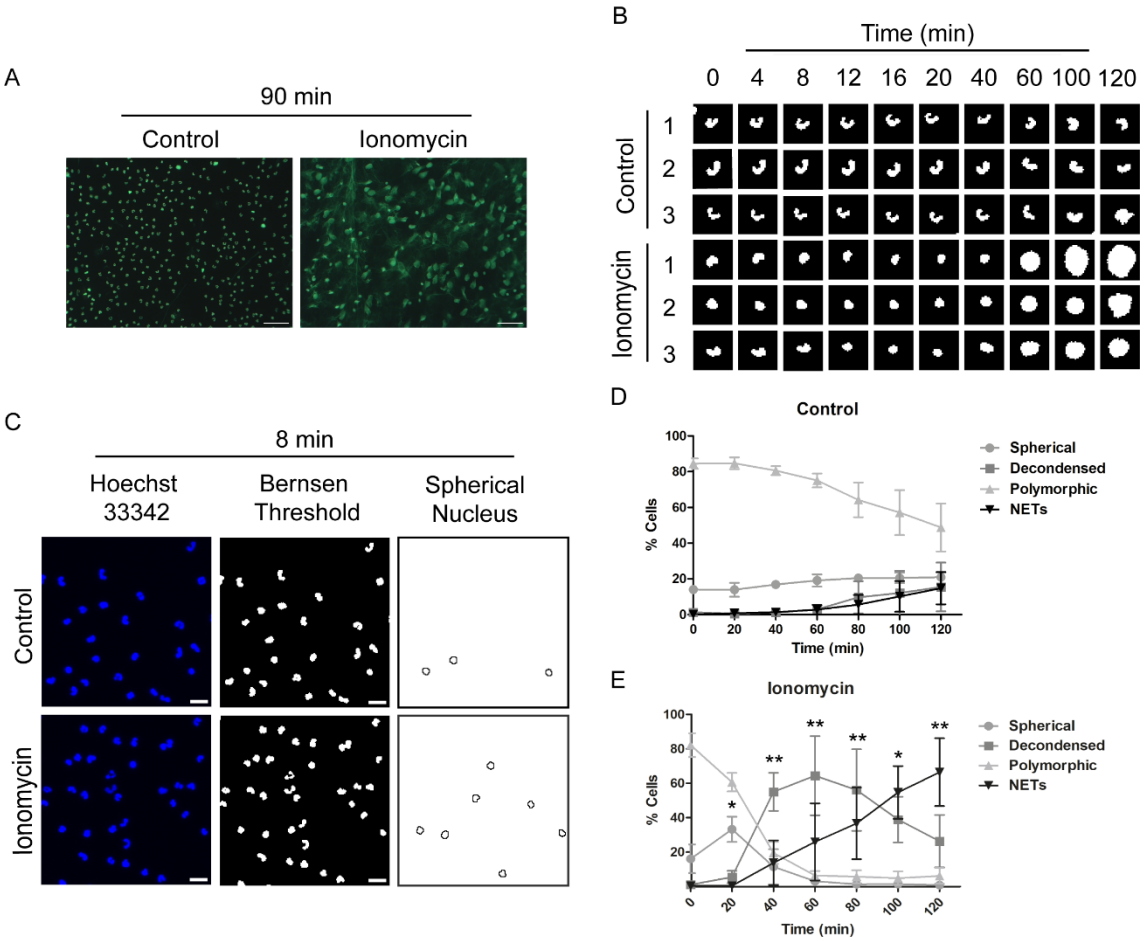

Figure 1. Ionomycin treatment leads to chromatin changes and NETs release. Human neutrophils were treated with vehicle (DMSO) or 6.7 µM ionomycin for 90 min and fixed (A) or monitored (live) for 120 min (B – E) at 37 °C. Images are representative

of three independent experiments. Approximately 200-350 cells from a seeding density of $1,5x10^5$ per well, were monitored per condition. A) After fixation, cells were stained with 500 nM SYTOX Green followed by fluorescence microscopy analysis. Scale bars = 50 µm. B – E). Cells stained with 2 µM Hoechst 33342 and 500 nM SYTOX Green were monitored by live-imaging microscopy. B) 8-bit binary images with *Bernsen* local threshold of three representative cells from control (top) and ionomycin (bottom) groups over time. C) Microscope images of control (upper panel) and ionomycin-treated neutrophils (bottom panel) at 8 min of incubation. From left to right: fluorescence images, 8-bit binary images with *Bernsen* local threshold of all cells >26 µm and circularity 0 - 1.0, and outlines of cells with 26-50 µm and circularity 0.94 - 1.0 (spherical nucleus). Scale bars = 20 µm. D) Percentage of control (n = 3) and E) Ionomycin-treated neutrophils (n = 3) quantified in *Phansalkar* thresholded images with spherical (26-50 µm and circularity 0.94-1.0), decondensed (only Hoechst 33342 (+), > 94 µm and circularity 0-1.0) or polymorphic (>26 µm and circularity 0-1.0) nucleus, or NETotic cells (Sytox Green (+), > 94 µm and circularity 0-1.0). * Denotes P value <0.05, and ** P value < 0.01, after one-way ANOVA followed by Tukey posttest.

3.2 Ionomycin treatment triggers a rapid communication with the environment

The results obtained by live cell imaging highlighted the fast intracellular changes unraveled upon ionomycin treatment. We next sought to evaluate if the intracellular changes were paralleled by release of signaling proteins to the extracellular environment. To tackle that, we performed a proteomic study of the secretome of neutrophils 2 minutes after treatment with ionomycin (Figure 2A, Supplemental Tables 1A and 1B). Proteins with at least a 2-fold difference between ionomycin-treated and control cells ($Log_2 \geq 1$), and with a P value < 0.05 after a multiple comparison adjusted t-test were considered differentially secreted.

Remarkably, after 2 minutes of ionomycin exposure, neutrophils had already secreted proteins crucial for an inflammatory response, such as myeloperoxidase (MPO), neutrophil elastase (ELANE) and azurocidin (AZU1) (Figure 2A). Pathway enrichment analysis showed that early on after ionomycin stimulus, neutrophils secrete proteins related to their activation, phagocytosis and regulation of cytokine production (Figure 2B, Supplemental Table 1C). On the other hand, the secretome of control cells

showed the presence of proteins such as actins (ACTC1/ACTA1/2, ACTB), vimentin (VIM), and cofilin-1 (CFL1, an actin binder), proteins found as pertaining to extracellular exosomes and/or extracellular space in addition to other intracellular compartments. Secretome of control cells also showed proteins related to neutrophil mediated immunity, although in a much weaker enrichment ratio when comparing with ionomycin-treated cells (Figure 2C, Supplemental Table 1D). This is not surprising, once neutrophils are isolated from blood, and although extreme care is taken during the isolation/incubation process, these immune cells already sense environment alterations that lead to cellular stress. Supplemental Table 1A shows all the differentially regulated proteins found for control and ionomycin-treated cells. Importantly, ionomycin-treated cells secreted proteins distinct from those secreted by neutrophils treated with 1 μM fMLP, a known chemotactic factor that leads to neutrophil degranulation but not to NETosis [38] (Supplemental Figures 1, 2, and Supplemental Tables 1B, E). Interestingly, some of the proteins increased in fMLP-treated cells when compared with ionomycin treatment were the same as those found for control-treated cells compared with ionomycin stimulus (for instance, ACTB, ACTC1/ACTA1/2 and VIM). The most enriched biological process relate to fMLP activation was cell redox homeostasis (Supplemental Figure 2B and Supplemental Table 1F), while for ionomycin treatment, granulocyte activation was the most enriched biological process (Supplemental Figure 2C and Supplemental Table 1G). Of note, at 2 min of incubation, the secretome of fMLP-treated neutrophils was very similar to the secretome of control cells (Supplemental Figure 2 and Supplemental Table 1H).

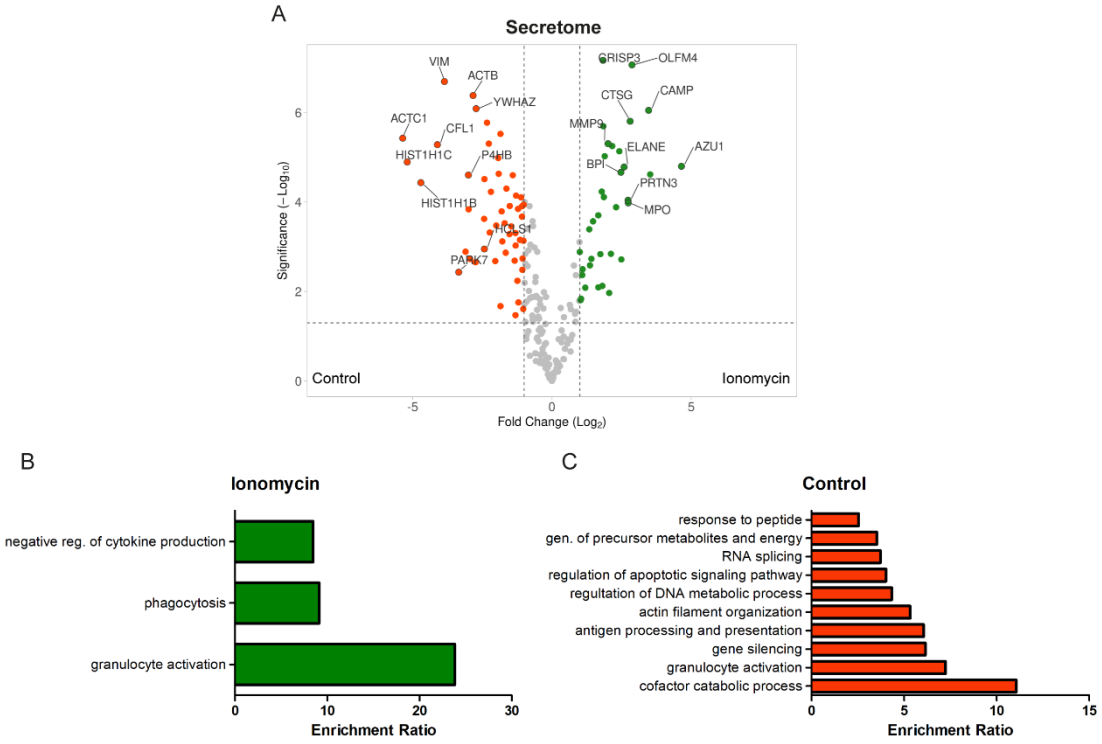

Figure 2. Ionomycin-treated neutrophils secrete proteins related to phagocytosis and granulocyte activation. The secretome of human neutrophils treated with the vehicle (DMSO) or 6.7 µM ionomycin for 2 min at 37 °C was analyzed by mass spectrometry. A) Differentially regulated proteins obtained comparing control and ionomycin-treated neutrophils. For each protein, the -$\log_{10}$ of the P-value from t-test followed by multiple comparisons adjustment is plotted against the $\log_2$ fold change between control and ionomycin groups. This result was obtained for neutrophils isolated from one subject but is representative of 3 independent experiments. Proteins more abundant in the secretome of ionomycin-treated neutrophils are displayed to the right of the value 1 in the x-axis (dashed line), while less abundant proteins are displayed to the left of the -1 value. Pathway enrichment analysis of unique and enriched proteins with FDR $\leq$ 0.05 found in B) ionomycin and C) control groups. For each enriched biological process (y-axis), the enrichment ratio (the number of observed proteins over the expected value, x-axis) was calculated.

3.3 The nucleus at early stages of NETosis is engaged in cytoskeleton organization and inflammatory response

Our results showed ionomycin treatment leads to early changes in the nucleus of activated neutrophils (Figure 1), and that they communicate these changes very quickly to the surrounding environment (Figure 2). A key question that remained was regarding the inner signals leading to the early chromatin changes seen in these cells. To address this matter, after treating neutrophils for 2 minutes with ionomycin, we first

collected the secretome (Figure 2), and then the cells were lysed by nitrogen cavitation, followed by a centrifugation-based fractionation of cell compartments. The sequential centrifugation procedure yielded three distinct fractions, a nucleus-enriched, an organelle-enriched, and a soluble proteins-enriched fraction, in addition to the secretome fraction that was collected before cell lysis. Alterations in the proteome of the fractions were investigated by mass spectrometry. Importantly, independent experiments using neutrophils of three different donors were performed. Noteworthy, Figures 3A-C bring the results obtained with neutrophils isolated from one subject, but very similar results were obtained analyzing the fractionated neutrophil's nuclear proteome derived from the other two subjects (Supplemental Figure 4). Thus, several proteins were highly increased in the nuclear fraction of ionomycin-treated neutrophils when compared with controls (Figure 3A, Supplemental Tables 2A, B). Among these proteins, ANXA1 [39] (Annexin A1, Figure 3B, 4-fold increase), ARHGDIB [40] (Rho GDP-dissociation inhibitor 2, Figure 3C, 3-fold increase), GAPDH [41] (Glyceraldehyde-3-phosphate dehydrogenase, Figure 3D, 4-fold increase) and TMSB4X [42] (Thymosin beta-4, Figure 3E, nearly 4-fold increase) have been described to function on actin cytoskeleton organization. Additionally, S100P (Protein S100-P, Figure 3F, 7-fold increase) and ANXA3 (Annexin A3, Figure 3G, 10-fold increase) were also highly enriched in the nucleus of ionomycin-treated neutrophils. The S100-P is a Ca^{2+} transduction signal protein [43] that interacts with the actin reorganization proteins [44], [45] and the protein ANXA3 is involved in caspase-3 suppression [46], [47], and granule-granule, and granule-phagosome fusion [48], [49] in neutrophils. Importantly, all selected proteins displayed in Figures 3B-G were enriched in the nuclear fraction of ionomycin-treated neutrophils in at least 2 out of 3 individuals. Pathway enrichment analysis (Figure 3H, supplemental Table 2C) showed

that ionomycin-treated cells display proteins related to neutrophil mediated immunity as the most enriched biological process in their nuclear fraction. Interestingly, actin filament organization and regulation of cytoskeleton organization are two highly enriched processes in the nucleus of these cells. These results are in line with our previous findings (Figure 1) of early chromatin remodeling as a key factor preceding NETosis.

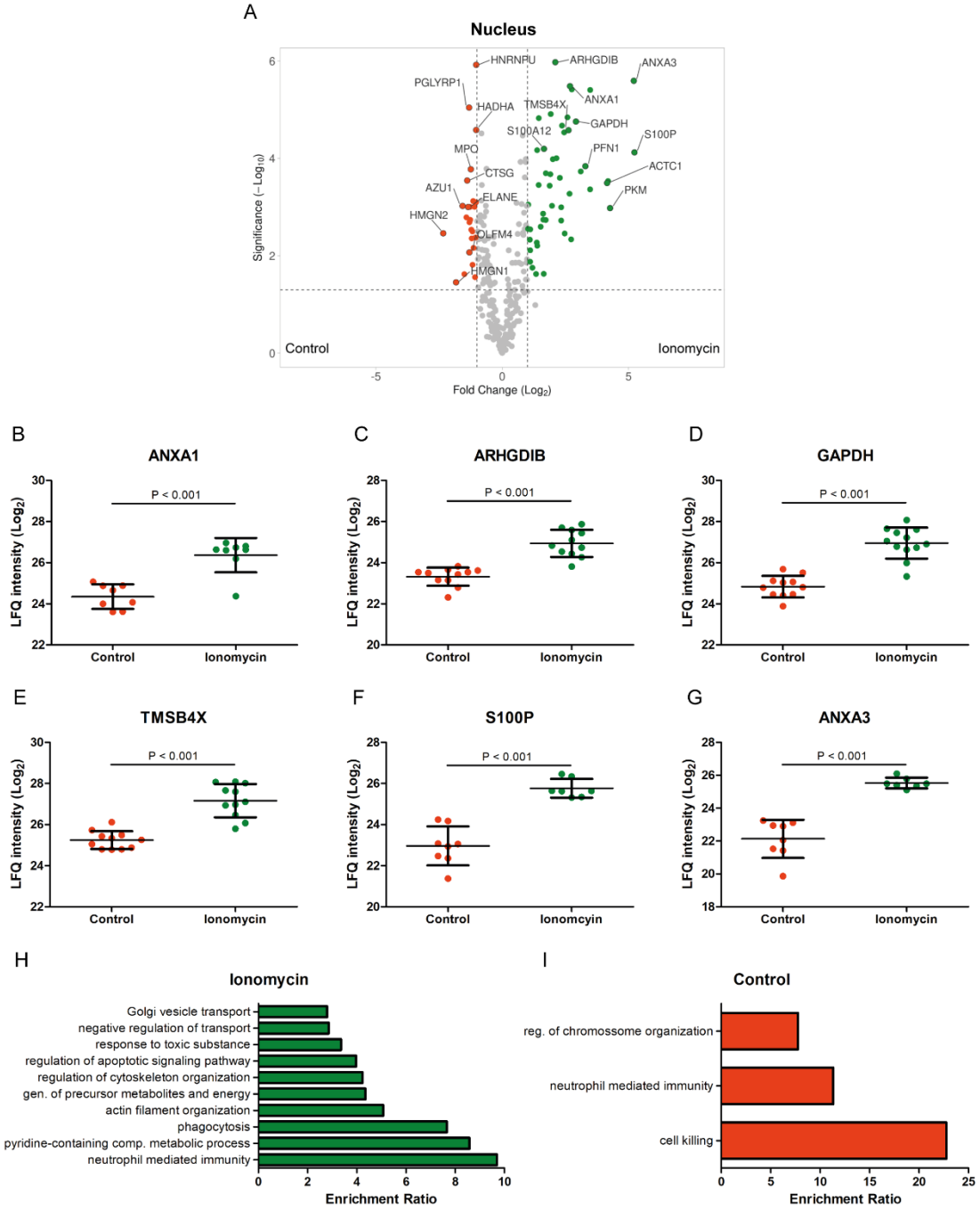

Figure 3. Proteins involved with cytoskeleton organization and immune response are enriched in the nucleus of ionomycin-treated neutrophils. Proteins belonging to the nuclear-enriched fraction of human neutrophils treated with the vehicle (DMSO) or 6.7 µM ionomycin for 2 min at 37 °C were analyzed by mass spectrometry. A) Differentially regulated proteins obtained comparing control and ionomycin-treated neutrophils. For each protein, the $-\log_{10}$ of the P-value from t-test adjusted for multiple comparisons is plotted against the $\log_2$ fold change between control and ionomycin groups. This result was obtained for neutrophils isolated from one subject but is representative of 3 independent experiments. Proteins more abundant in the ionomycin-treated neutrophils nucleus are displayed to the right of the value 1 in the x-axis (dashed line), while less abundant proteins are displayed to the left of the -1 value. B – G) Box plots of selected proteins from neutrophils of 3 individuals with a fold change > 2 and P-value < 0.05 after t-test followed by multiple comparison adjustment in the nucleus of ionomycin-treated group compared to the controls. LFQ intensities (Log_2) for the proteins D) ANXA1, E) ARHGDIB, F) GAPDH, G) TMSB4X, H) S100P, I) ANXA3) found enriched in the nucleus of ionomycin-treated neutrophils of at least 2 out of 3 subjects. The line in the middle is the mean of the LFQ intensities and the error bars represent the standard deviation. Pathway enrichment analysis of unique and more abundant proteins found in the H) ionomycin and I) control groups. For each enriched biological process (y-axis), the enrichment ratio (the number of observed proteins over the expected value, x-axis) was calculated.

Of note, in this study we used differential centrifugation to obtain fractions enriched for proteins derived from specific cell compartments (nucleus, organelles, soluble proteins, and secreted proteins). However, we did not attempt to purify such fractions, given the massive amount of starting material needed. Thus, we expected to have some overlap between the fractions. For instance, we can observe (Figure 3A) a few proteins commonly found in the neutrophil's granules such as MPO, ELANE, CTSG, AZU1, and olfactomedin-4 (OLFM4) [50], enriched in the control's nuclear fraction. This can also be seen in the pathway enrichment analysis of nucleus of control cells (Figure 3I and Supplemental Table 2D), with cell killing and neutrophil mediated immunity as enriched processes.

3.4 Actin remodeling-related processes are predominant in nucleus and organelles fractions of NETotic neutrophils

Taking a more holistic view of the cell status, we looked for changes in protein distribution across the 4 different cellular fractions. Thus, for each treatment, the

percentage of a protein in a given fraction (nucleus, organelles, soluble proteins and secreted) was calculated in relation to the total amount found in all 4 fractions. Accordingly, we observed that many proteins were present in a significantly higher proportion in the nucleus (Figure 4A) and organelles (Figure 4B) of ionomycin-treated cells, compared with unstimulated neutrophils. On the other hand, for the majority of proteins, a similar proportion was found in the soluble fraction of control and ionomycin-stimulated neutrophils (Figure 4C). Interestingly, the majority of secreted proteins were found in higher proportion in control cells when compared with ionomycin treatment (Figure 4D).

The unbalanced protein distribution seen across the 4 different fractions (Figure 4A-D) for control and ionomycin-stimulated cells led us to investigate the identity of these proteins, as well as their unique fractionation pattern for each of the 2 different treatments. Thus, for every protein, we calculated the fold change in proportion (ionomycin treatment over control) for each of the 4 different fractions (Supplemental Table 3A).

Interestingly, the results showed that the proportion of many proteins in the ionomycin-treated neutrophil nucleus and organelles was substantially higher (> 2-fold change) than that found for unstimulated neutrophils. These results prompt us to check if those same proteins were decreased on another cellular fraction of ionomycin-treated cells. To accomplish this task, we filtered only for those proteins with a ratio ionomycin/control > 2 in the nucleus and/or organelles fractions, and < 0.5 in the soluble proteins and/or secretome fractions (Supplemental Table 3B). Importantly, only proteins with an adjusted P-value < 0.05 were considered for the analyses.

Out of the 41 proteins that met our criteria, we selected twelve proteins (Figure 4E-J, and Supplemental Figure 5) to show their distribution within the cellular fractions

of ionomycin-treated or unstimulated neutrophils. The annexin proteins, ANXA1 (Annexin A1, Figure 4E), ANXA3 (Annexin A3, Figure 4F) and ANXA6 (Annexin A6, Supplemental Figure 5A), known Ca^{2+} dependent phospholipid and membrane-binding proteins [51], [52], were found enriched on nuclear and organellar fractions of the ionomycin-treated group. ANXA1 (Figure 4E) had an increase of over 4 times in the nucleus and organelles fractions, ANXA3 (Figure 4F) had an increase of 21.4 times in the nucleus, and of 8.8 times in the organelles, and ANXA6 (Supplemental Figure 5A) had an increase of 2.3 times in the nucleus and of 3.6 times in the organelles of ionomycin-treated neutrophils. The highly homologous actin proteins ACTC1/ACTA1/2 (alpha-cardiac actin / alpha-actin-1 / alpha-actin-2, Figure 4G), structural constituents of cytoskeleton, were also found enriched in the nucleus and in the organelles of ionomycin-treated neutrophils. Thus, ACTC1/ACTA1/2 increased roughly 22 times in the nucleus, and 4 times in the organelles. Of note, the actin binding proteins [53] PFN1 (Profilin-1, Figure 4H), CFL1 (Cofilin-1, Figure 5I) and TMSB4X (thymosin beta-4, Figure 4J) were also enriched in the nucleus/organelles of ionomycin group. PFN1 (Figure 4H) had an increase of 21 times in the nucleus and 3.8 times in the organelles, CFL1 (Figure 4I) had an increase of 3.7 times in the nucleus (and was not enriched in the organelles), while TMSB4X (Figure 4J) had an increase of 6.4 times in the nucleus and 3.3 times in the organelles. Interestingly, all these proteins were secreted in a higher proportion by control cells, when compared to the proportion of these proteins secreted by ionomycin-treated neutrophils (Figure 4E-J). Lastly, the actin-binding protein CAP1 (Adenylyl cyclase-associated protein 1, Supplemental Figure 5B) was also proportionally increased in nuclear and organellar fractions of neutrophils treated with ionomycin. CAP1 accelerates CFL1-dependent filament depolymerization [54]. In agreement with what was seen in the nucleus of ionomycin-treated neutrophils (Figure

3H), the biological process “actin filament organization” was also found in the pathway enrichment analysis of the proteins that were proportionally increased in the nucleus (Figure 4K) and/or organelles (Figure 4L), and decreased in the soluble proteins fraction and/or secretome of treated cells.

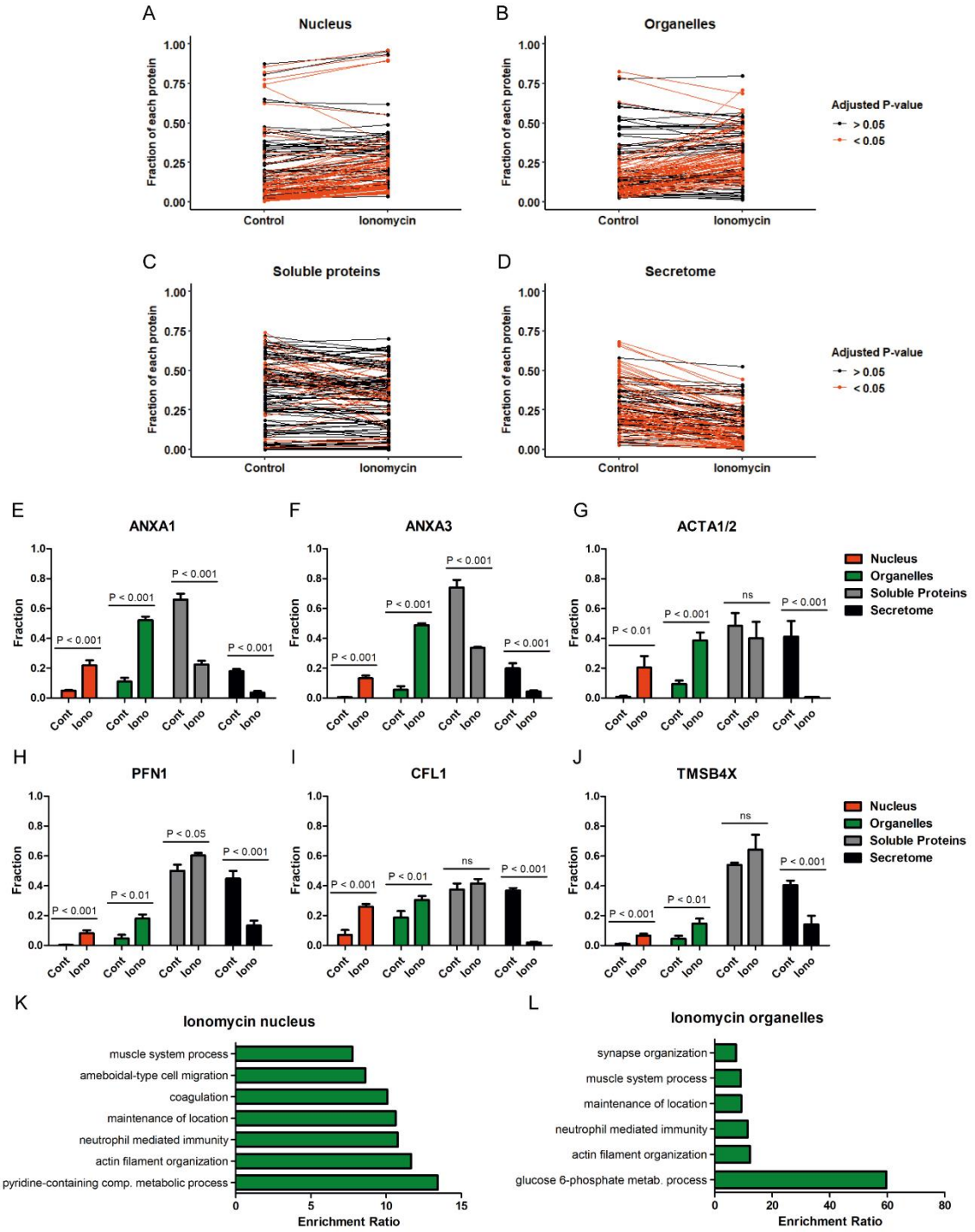

Figure 4. Protein distribution across cellular compartments in neutrophils treated with vehicle (DMSO) or 6.7 µM ionomycin for 2 min at 37 °C, fractionated in 4 different fractions (nucleus, organelles, soluble proteins and secretome), and analyzed by mass

spectrometry. The results are from 1 experiment but representative of 3 subjects. Comparison of proteins proportions found for control and ionomycin-treated groups in the fractions of A) nucleus, B) organelles, C) soluble proteins and D) secretome. Orange lines represent proteins significantly different (adjusted P-value < 0.05) for each of the 4 cellular fractions after an unpaired t-test. E) – J) Selected proteins with ratio ionomycin/control > 2 in the nucleus and/or organelles fractions, and < 0.5 in the soluble proteins and/or secretome fractions. P-values are FDR adjusted after unpaired t-test of each protein in each of the 4 cellular fractions. Error bars represent the standard deviation. Pathway enrichment analysis of unique and more abundant proteins found in the K) nucleus and L) organelles fractions of ionomycin-treated neutrophils. For each enriched biological process (y-axis), the enrichment ratio (number of observed proteins over the expected value (x-axis) was calculated.

Of note, nucleus and organelles fraction of ionomycin-treated neutrophils also show enriched processes related respectively to metabolism of pyridine-containing components, and metabolism of glucose 6-phosphate. Looking for the proteins pertaining to these biological processes (Supplemental Tables 3C, D), we found the pentose phosphate pathway enzymes TALDO1 (Transaldolase, Supplemental Figure 5C), PKM (Pyruvate kinase, Supplemental Figure 5D), PGD (6-phosphogluconate dehydrogenase, Supplemental Figure 5E), and G6PD (Glucose-6-phosphate 1-dehydrogenase, Supplemental Figure 5F), all proportionally increased in the nucleus and organelles of ionomycin-exposed neutrophils.

Taken together, these results suggest that actin remodeling, and energy metabolism are relevant processes around and in the nucleus in the early stages of NETosis induced by ionomycin.

3.5 Citrullination of actin and nuclear structural proteins is an early step in ionomycin-induced NETosis

It is well known that peptidylarginine deiminases (PADs) are activated by an increase on cellular Ca^{2+} concentration [55], and one particular PAD, namely PAD4, has been implicated in NETosis [21]. This enzyme catalyzes the

deimination/citrullination of arginine residues in histones and other proteins. Therefore, we sought to investigate the presence of citrullinated proteins among the enriched fractions of nucleus, organelles, soluble proteins and secretome after 2 min of exposure to ionomycin or DMSO (control).

Overall, we identified 89 citrullinated peptides from 44 proteins (Figure 5 and Supplemental Table 4A) present in at least 2 individuals. Of these, 32 (36%) were peptides shared between ionomycin and control groups, 54 (60.7%) were peptides exclusive pertaining to the ionomycin group, and 3 (3.4%) were exclusive to the control group (Figure 5).

The shared citrullinated peptides between ionomycin and control groups, as well as those that were unique to each group, were found to originate from similar cellular compartments (Figure 5). It is noteworthy that the majority of citrullinated peptides belonged to the ionomycin group. Interestingly, 32 citrullinated peptides exclusively found in ionomycin-treated neutrophils belong to ten different proteins involved in actin filament and cytoskeleton organization: AIF1 (Allograft inflammatory factor 1), CAP1 (Adenylyl cyclase-associated protein 1), CNN2 (Calponin-2), CORO1A (Coronin-1A), HCLS1 (Hematopoietic lineage cell-specific protein), LASP1 (LIM and SH3 domain protein 1), LSP1 (lymphocyte-specific protein 1), TLN1 (Talin-1), VASP (vasodilator-stimulated phosphoprotein), and VIM (vimentin) (Supplemental Table 4A).

It is worth mentioning that VIM had six citrullinated peptides, four of which were exclusively present in the ionomycin group, and from the 2 common citrullinated VIM peptides, one was significantly enriched in the ionomycin-treated neutrophils (Supplemental Tables 4A and 4B). VIM is a type III IF protein that forms networks throughout the cytoplasm and surrounds the nucleus [56], where it is responsible for its stability and structure [57], [58].

Besides the VIM common peptide, ionomycin-stimulated neutrophils also presented a citrullinated peptide from neutrophil elastase (ELANE) enriched in the secretome, and a citrullinated peptide from histone H1.4 significantly enriched in the nuclear fraction. Interestingly, histone H3.1 was found exclusively citrullinated in the nucleus of ionomycin-treated samples from one subject and enriched in the nucleus of ionomycin-treated neutrophils of another subject (Supplemental Table 4B). Missing values from the analysis with neutrophils derived from the third subject precluded statistical analysis, but we found relevant to report increased citrullination in H3.1 from neutrophils of two different subjects treated with ionomycin , since it is frequently assigned as a hallmark of NETosis triggered by calcium ionophores [9], [11], [59]. Only one peptide from the protein Adenylosuccinate synthetase isozyme 2 (ADSS) was found enriched in the soluble protein fraction of the control group (Supplemental Table 4B).

Furthermore, the nuclear-enriched fraction of ionomycin-treated neutrophils contained the unique citrullinated proteins H1FX (Histone H1.10), LBR (Delta (14)-sterol reductase LBR), and LMNB1 (Lamin B1) (Supplemental Table 4A). H1FX stabilizes chromatin compaction due to its interaction with the DNA region between nucleosome cores [60]. LBR, also known as Lamin B receptor, is an inner nuclear membrane protein which interacts with heterochromatin and Lamin B [61], [62] and it is responsible for the lobulated nucleus found in granulocytes [62]. LMNB1 is a type V intermediate filament (IF) protein that forms thin organized networks crucial to structure and elasticity of the nucleus [63].

The majority of previous studies focus exclusively in the citrullination of histone proteins in NETosis[9], [11], [14]. Thus, we specifically looked for the presence of citrullinated histones, regardless if the modification was differentially regulated in

controls and ionomycin-treated neutrophils or not. The results showed that besides the citrullination of histones H1.4, H3.1 and H1FX found in ionomycin-treated neutrophils, both groups displayed citrullination in histones H1.5, H1.4, H2A type 1-C and type 2-C.

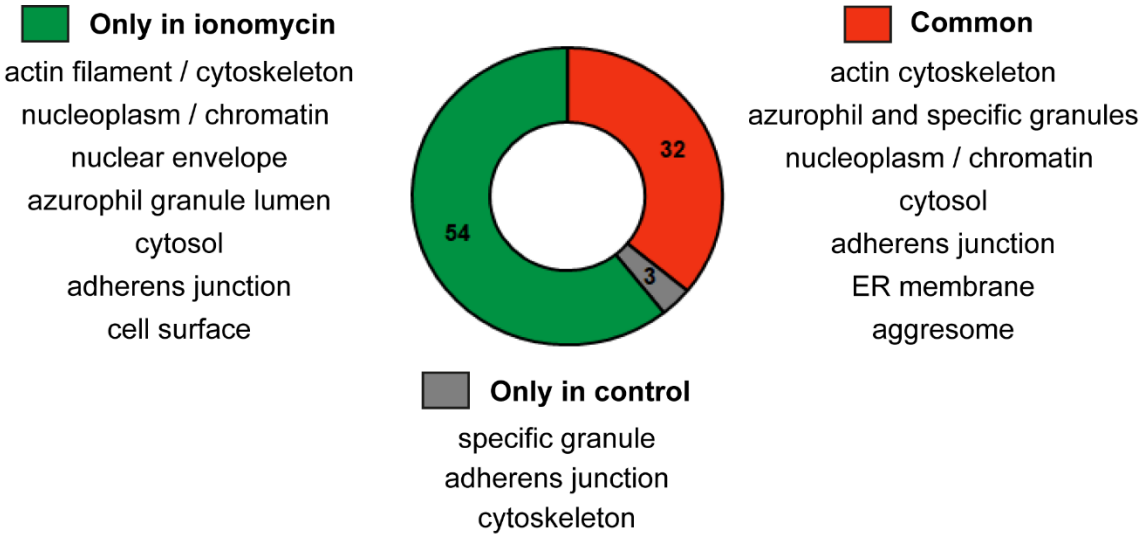

Figure 5. 60.7 % of the citrullinated peptides were unique to the ionomycin group. 89 citrullinated peptides from 44 distinct proteins were identified uniquely present in any of both groups or commonly found between them. In the figure contains a summary of the cellular components found after searching in the Gene Ontology database.

Taken together, our results show that proteins related to actin reorganization are enriched in the nuclear and organellar fractions of ionomycin-activated cells, and these proteins, together with chromatin structural proteins, were also targeted for citrullination. Thus, actin reorganization, as well as citrullination of the actin-ligand proteins (*i.e.,* AIF1, CAP1, CNN2, CORO1A, HCLS1, LASP1, LSP1, TLN1, VASP, and VIM), and of structural proteins in the nucleus and chromatin (H1FX, LBR, and LMNB1) are all early events leading to NETosis.

4. Discussion

NETosis occurs through a sequence of highly organized events leading to chromatin decondensation, rupture of nuclear and cellular membranes and extracellular DNA release. Previous studies have used multiple microscopy imaging techniques to characterize the morphological changes associated with these cellular events [21], [23]. Here, by using a combination of fluorescent and live cell imaging microscopy, cell fractionation and proteomics, we provided a comprehensive overview of the biochemical processes involved in the initial cellular events that culminates in NETosis.

We showed that before ionomycin-stimulated neutrophils release NETs, (1) they rapidly (in 2 min) communicate with the surrounding medium, releasing crucial proteins related to immune response; (2) alterations occur around and in their nucleus, with cytoskeleton reorganization, nuclear redistribution of actin-remodeling related proteins, and citrullination of actin-ligand and nuclear structural proteins; (3) these events culminate in nuclei losing their characteristic polymorphic shape becoming spherical (in less than 8 min). The rapid biochemical and morphological changes characterized in this work subsequently culminate in the well-studied events of membrane rupture and the release of NETs.

The release of microvesicles by neutrophils was described as a first step in NETosis. By using immunostaining for six different proteins, Thiam *et al* [21] identified neutrophil granular proteins as components of the microvesicles. In our work, we have confirmed these results, and expanded the understanding of the secreted proteins in the onset of NETosis. Our secretome analysis shows that proteins belonging to azurophilic, secondary and tertiary granules are secreted by neutrophils stimulated by ionomycin. Because degranulation is a hallmark of fMLP-stimulated neutrophils [64]–

[66], and because in our work fMLP did not incuded NETosis (supplemental figure 1), we have compared the proteins secreted upon ionomycin treatment with those secreted after fMLP stimulation. The results showed that differently from the rapid degranulation induced by ionomycin, at the first moments after fMLP activation, the secretome of neutrophils is mainly enriched in proteins related to redox homeostasis. The rapid response of neutrophils to ionomycin may be a signal of cellular stress. Of note, consistent with Yuen *et al.*, (2016) [38], our study found that neutrophils treated with fMLP 1 µM did not release NETs. However, other studies have reported the presence of NETs in neutrophils after fMLP treatment at this concentration, and the reasons for these discrepancies are unknown [67], [68].

The current model for calcium ionophores-induced NETosis postulates that chromatin decondensation occurs by the action of PAD4 enzyme [14]. Core histones were first identified as substrates for this nuclear enzyme [69], [70]. Thus, citrullination of arginine residues by PAD4 causes a loss of attractive forces between the citrullinated histones and DNA. Recently, Christophorou *et. al.* showed citrullination of the linker histone H1 by PAD4 is involved in the regulation of pluripotency [71]. They showed that PAD4 mediates chromatin decondensation by inhibiting the compaction mediated by linker histone H1, known to be involved in generation of compact chromatin [72]. We showed histone H1.10 was exclusively citrullinated and that citrullinated histone H1.4 was found significantly altered in ionomycin-activated neutrophils, thus supporting a role for citrullination of histone H1 in chromatin decondensation also in neutrophils. Thus, citrullination of linker histone H1, together with previously reported citrullination of core histones may play a key role for chromatin decondensation in calcium ionophores-driven NETosis.

Importantly, we have shown citrullination is not restricted to histones, but rather affects proteins involved in the organization of the nucleus and chromatin, such as LMNB1, LBR, and VIM, as well as proteins related to the actin filament organization (AIF1, CAP1, CNN2, CORO1A, HCLS1, LASP1, LSP1, TLN1, and VASP). Citrullination of other proteins distinct from histones in neutrophils stimulated by calcium ionophores was also seen by other studies [4], [5], [32], [73]. Interestingly, Gobwein and collaborators suggested citrullination of proteins of the nuclear lamina and core facilitates their proteolysis by calpain, likely by altering polar interactions that might facilitate inter-domain cleavage by this protease [74].

In this regard, it is possible that citrullination of LMNB1, LBR and VIM, all crucial proteins for stability of the nucleus, impair their ability to maintain the nuclear integrity [57], [58], [61], [62], [75], and may contribute to the loss of the nuclear segmentation seen in Figure 1. Thus, neutrophils from patients with the Pelger-Huët genetic anomaly display low levels of LBR, and have an ovoid or hypolobulated nucleus [76]. Moreover, HL-60/S4 cells knockdown for LBR failed to display nuclear lobulation after 4 days of treatment with the differentiation agent retinoic acid [62]. $Vim^{-/-}$ mouse embryonic fibroblasts had a lower volume round-shaped nucleus which is more susceptible to rupture after a mechanical stress [58]. Also, PAD4 depletion delays the disassembly of vimentin intermediate filaments in ionomycin-induced NETosis [21].

Furthermore, the presence of citrullinated proteins and histones in NETs may act as autoantigens that can stimulate the body to produce anti-citrullinated protein autoantibodies (ACPA) which are related to the progression of rheumatoid arthritis (RA) [77]–[79]. Interestingly, some of the unique citrullinated proteins found in the ionomycin group, such as CAP1, VIM, myeloid cell nuclear differentiation antigen (MNDA), H1FX, high mobility group protein B2 (HMGB2), neutrophil cytosol factor 1

(NCF1), and LBR, have been identified in the synovial fluid samples from RA patients [80], [81].

Similar to calcium ionophore treatment, human neutrophils or neutrophil-like cells (differentiated HL-60) treated with monosodium urate (MSU), C. albicans, TNF, LPS, f-MLP, H_2O_2, or lipoteichoic acid (LTA) released citrullinated NETs [14], [82], [83]. Although this study and others have detected citrullinated proteins and histones [4], [9], [11], [32], [74], [83], the causal involvement of PAD4 activity and citrullinations for the occurrence of NETosisis still a topic of intense debate. Thus, three independent strategies were used to test the requirement of citrullination in NETosis, but with conflicting results. First, experiments with neutrophils from PAD4 knockout mice [21] showed that, at least in mice, PAD4 is a requirement for NETs formation. Second, by using PAD4-deficient HL-60 neutrophil-like cells, Thiam and collaborators showed PAD4 nuclear localization and enzymatic activity are required for efficient chromatin decondensation and NETosis, although a small fraction of the cells was still able to complete NETosis [21]. Contrasting with these two first observations, three different inhibitors of PAD proteins were used in experiments with human neutrophils, and the results showed ionomycin-induced NETosis was not affected by any of these inhibitors, although some histone H3 citrullination still occurs [11]. Other selective PAD4 inhibitors showed partial inhibition of NETs in human neutrophils, while fully inhibiting mouse NETosis [84]. On one hand, NETosis may be differentially regulated in mouse and humans, explaining the differences obtained with mouse models. It is also possible that “neutrophil-like” HL-60 cultured cells do not fully reflect the NETotic process that occurs in circulating neutrophils. On the other hand, studies with inhibitors [84] that bind a calcium-deficient form of the PAD4 suggest calcium may alter substrate specificity and activity of PAD4, adding a new layer of complexity to understand PAD4

role in NETosis. Thus, only studies that provide a full understanding on the actions and functionalities of PAD4 may provide the answers regarding its requirement during NETosis.

Besides citrullination of histones, actin-related and nuclear structural proteins, our work also revealed a fast protein redistribution across cellular fractions as an event preceding NETs release. Thus, two main protein classes were proportionally increased in nucleus and organelles fractions from activated neutrophils. First, the nuclear and organelles enrichment of the actin-related proteins PFN1, CFL1, TMSB4X, CAP1, as well as the annexins A1, A3 and A6 [52] point to the extensive dynamic remodeling of the actin cytoskeleton. Our results obtained using proteomics to uncover proteins related to actin remodeling supports the results regarding quick morphological changes obtained by live cell tracking experiments. These studies showed that within minutes after neutrophil stimulation and preceding chromatin decondensation, reorganization of actin filaments occurs. Second, proteins related to the energy metabolism (TALDO1, PKM, PGD and G6PD) in the nucleus and organelles fractions of ionomycin-treated neutrophils corroborates the need of biochemical energy before chromatin swelling in NETosis [23].

Altogether, in this work we have highlighted some of the key players in the early events driving NETs release, but we also provided an extensive list of proteins that participates in the onset of NETosis, playing roles in the communication with the environment and in the active remodeling across cell fractions. Therefore, in ionomycin-stimulated neutrophils, citrullination of proteins responsible for the regulation of the chromatin changes, and of cytoskeleton remodeling occurs. Our results also place actin dynamics regulation as another early event preceding membrane rupture and DNA release.

5. Acknowledgments

We are grateful for Dr. Mariana Pereira Massafera for her technical assistance. The Redox Proteomics Core of the Mass Spectrometry Resource at Institute of Chemistry, University of São Paulo is acknowledged for access to state-of-the-art MS instrumentation

6. References

[1] E. Kolaczkowska and P. Kubes, “Neutrophil recruitment and function in health and inflammation,” *Nat. Rev. Immunol.*, vol. 13, no. 3, pp. 159–175, 2013, doi: 10.1038/nri3399.

[2] W. M. Nauseef, “How human neutrophils kill and degrade microbes: An integrated view,” *Immunol. Rev.*, vol. 219, no. 1, pp. 88–102, 2007, doi: 10.1111/j.1600-065X.2007.00550.x.

[3] V. Brinkmann, “Neutrophil Extracellular Traps Kill Bacteria,” *Science (80-.).*, vol. 303, no. 5663, pp. 1532–1535, 2004, doi: 10.1126/science.1092385.

[4] E. A. Chapman *et al.*, “Caught in a trap? Proteomic analysis of neutrophil extracellular traps in rheumatoid arthritis and systemic lupus erythematosus,” *Front. Immunol.*, vol. 10, no. 423, pp. 1–20, 2019, doi: 10.3389/fimmu.2019.00423.

[5] A. Petretto *et al.*, “Neutrophil extracellular traps (NET) induced by different stimuli: A comparative proteomic analysis,” *PLoS One*, vol. 14, no. 7, pp. 1–18, 2019, doi: 10.1371/journal.pone.0218946.

[6] T. A. Fuchs *et al.*, “Novel cell death program leads to neutrophil extracellular traps,” *J. Cell Biol.*, vol. 176, no. 2, pp. 231–241, 2007, doi: 10.1083/jcb.200606027.

[7] T. Hoppenbrouwers *et al.*, “In vitro induction of NETosis: Comprehensive live imaging comparison and systematic review,” *PLoS One*, vol. 12, no. 5, pp. 1–29, 2017, doi: 10.1371/journal.pone.0176472.

[8] A. B. Guimarães-Costa, M. T. C. Nascimento, A. B. Wardini, L. H. Pinto-Da-Silva, and E. M. Saraiva, “ETosis: A microbicidal mechanism beyond cell death,” *J. Parasitol. Res.*, vol. 2012, no. 929743, pp. 1–11, 2012, doi: 10.1155/2012/929743.

[9] C. M. De Bont, W. J. H. Koopman, W. C. Boelens, and G. J. M. Pruijn, “Stimulus-dependent chromatin dynamics, citrullination, calcium signalling and ROS production during NET formation,” *BBA - Mol. Cell Res.*, vol. 1865, no. 11, pp. 1621–1629, 2018, doi: 10.1016/j.bbamcr.2018.08.014.

[10] M. F. Konig and F. Andrade, “A critical reappraisal of neutrophil extracellular traps and NETosis mimics based on differential requirements for protein citrullination,” *Front. Immunol.*, vol. 7, no. 461, pp. 1–18, 2016, doi: 10.3389/fimmu.2016.00461.

[11] E. F. Kenny *et al.*, “Diverse stimuli engage different neutrophil extracellular trap pathways,” *Elife*, vol. 6, no. e24437, pp. 1–21, 2017, doi: 10.7554/eLife.24437.

[12] H. Parker, M. Dragunow, M. B. Hampton, A. J. Kettle, and C. C. Winterbourn, “Requirements for NADPH oxidase and myeloperoxidase in neutrophil extracellular trap formation differ depending on the stimulus,” *J. Leukoc. Biol.*, vol. 92, no. 4, pp. 841–849, 2012, doi: 10.1189/jlb.1211601.

[13] M. van Der Linden, G. H. A. Westerlaken, M. van Der Vlist, J. van Montfrans, and L. Meyaard, “Differential Signalling and Kinetics of Neutrophil Extracellular Trap Release Revealed by Quantitative Live Imaging,” *Sci. Rep.*, vol. 7, no. 6259, pp. 1–11, 2017, doi: 10.1038/s41598-017-06901-w.

[14] Y. Wang *et al.*, “Histone hypercitrullination mediates chromatin decondensation and neutrophil extracellular trap formation,” *J. Cell Biol.*, vol. 184, no. 2, pp. 205–213, 2009, doi: 10.1083/jcb.200806072.

[15] V. Papayannopoulos, K. D. Metzler, A. Hakkim, and A. Zychlinsky, “Neutrophil elastase and myeloperoxidase regulate the formation of neutrophil extracellular traps,” *J. Cell Biol.*, vol. 191, no. 3, pp. 677–691, 2010, doi: 10.1083/jcb.201006052.

[16] H. R. Thiam, S. L. Wong, D. D. Wagner, and C. M. Waterman, “Cellular Mechanisms of NETosis,” *Annu. Rev. Cell Dev. Biol.*, vol. 36, pp. 191–218, 2020, doi: 10.1146/annurev-cellbio-020520-111016.

[17] A. K. Gupta, S. Giaglis, P. Hasler, and S. Hahn, “Efficient Neutrophil Extracellular Trap Induction Requires Mobilization of Both Intracellular and Extracellular Calcium Pools and Is Modulated by Cyclosporine A,” *PLoS One*, vol. 9, no. 5, pp. 1–12, 2014, doi: 10.1371/journal.pone.0097088.

[18] L. Staali, H. Monteil, and D. A. Colin, “The Staphylococcal Pore-forming Leukotoxins Open Ca 2 + Channels in the Membrane of,” *J. Membr. Biol.*, vol. 162, no. 3, pp. 209–216, 1998, doi: 10.1007/s002329900358.

[19] V. Finck-barban, O. Meunier, and D. A. Colin, “Pore formation by a two-component leukocidin from Staphylococcus aureus within the membrane of human polymorphonuclear leukocytes,” *Biochim. Biophys. Acta*, vol. 1182, no. 3, pp. 275–282, 1993, doi: 10.1016/0925-4439(93)90069-d.

[20] K. D. Metzler, C. Goosmann, A. Lubojemska, and A. Zychlinsky, “A Myeloperoxidase-Containing Complex Regulates Neutrophil Elastase Release and Actin Dynamics during NETosis,” *CellReports*, vol. 8, no. 3, pp. 883–896, 2014, doi: 10.1016/j.celrep.2014.06.044.

[21] H. R. Thiam, L. Wong, Siu, R. Qiu, M. Kittisopikul, A. Vahabikashi, and A. E. Goldman, “NETosis proceeds by cytoskeleton and endomembrane

disassembly and PAD4-mediated chromatin decondensation and nuclear envelope rupture," *PNAS*, vol. 117, no. 13, pp. 7326–7337, 2020, doi: 10.1073/pnas.1909546117.

[22] B. Amulic *et al.*, "Cell-Cycle Proteins Control Production of Neutrophil Extracellular Traps Article Cell-Cycle Proteins Control Production of Neutrophil Extracellular Traps," *Dev. Cell*, vol. 43, no. 4, pp. 449-462.e5, 2017, doi: 10.1016/j.devcel.2017.10.013.

[23] E. Neubert *et al.*, "Chromatin swelling drives neutrophil extracellular trap release," *Nat. Commun.*, vol. 9, no. 3767, pp. 1–13, 2018, doi: 10.1038/s41467-018-06263-5.

[24] G. Sollberger *et al.*, "Gasdermin D plays a vital role in the generation of neutrophil extracellular traps," *Sci. Immunol.*, vol. 3, no. 26, 2018, doi: 10.1126/sciimmunol.aar6689.

[25] W. M. Nauseef and S. Kremserova, "Isolation of Human Neutrophils From Venous Blood," *Methods Mol. Biol.*, vol. 2087, pp. 33–42, 2020, doi: 10.1007/978-1-0716-0154-9_3.

[26] V. Brinkmann, C. Goosmann, L. I. Kühn, and A. Zychlinsky, "Automatic quantification of in vitro NET formation," *Front. Immunol.*, vol. 3, no. 413, pp. 1–8, 2013, doi: 10.3389/fimmu.2012.00413.

[27] M. S. Klempner, R. B. Mikkelsen, D. H. Corfman, and J. Andre-schwartz, "Neutrophil Plasma Membranes I . High-Yield Purification of Human Neutrophil Plasma Membrane Vesicles by Nitrogen Cavitation and Differential Centrifugation," *J. Cell Biol.*, vol. 86, no. 1, pp. 21–28, 1980, doi: 10.1083/jcb.86.1.21.

[28] G. H. H. Borner, D. N. Itzhak, and S. Tyanova, "Global, quantitative and dynamic mapping of protein subcellular localization," *Elife*, vol. 5:e16950, pp. 1–36, 2016, doi: 10.7554/eLife.16950.

[29] J. Rappsilber, M. Mann, and Y. Ishihama, "Protocol for micro-purification, enrichment, pre-fractionation and storage of peptides for proteomics using StageTips," *Nat. Protoc.*, vol. 2, no. 8, pp. 1896–1906, 2007, doi: 10.1038/nprot.2007.261.

[30] J. Cox and M. Mann, "MaxQuant enables high peptide identification rates, individualized p.p.b.-range mass accuracies and proteome-wide protein quantification," *Nat. Biotechnol.*, vol. 26, no. 12, pp. 1367–1372, 2008, doi: 10.1038/nbt.1511.

[31] J. Cox, N. Neuhauser, A. Michalski, R. A. Scheltema, J. V. Olsen, and M. Mann, "Andromeda: A peptide search engine integrated into the MaxQuant environment," *J. Proteome Res.*, vol. 10, no. 4, pp. 1794–1805, 2011, doi: 10.1021/pr101065j.

[32] R. Chaerkady *et al.*, "Characterization of Citrullination Sites in Neutrophils and Mast Cells Activated by Ionomycin via Integration of Mass Spectrometry and

Machine Learning," *J. Proteome Res.*, vol. 20, no. 6, pp. 3150–3164, 2021, doi: 10.1021/acs.jproteome.1c00028.

[33] M. Y. Hein, C. A. Luber, I. Paron, N. Nagaraj, and M. Mann, "Accurate proteome-wide label-free quantification by delayed normalization and maximal peptide ratio extraction, termed MaxLFQ," *Mol. Cell. Proteomics*, vol. 13(9), pp. 2513–2526, 2014, doi: 10.1074/mcp.M113.031591.

[34] S. Tyanova *et al.*, "The Perseus computational platform for comprehensive analysis of (prote) omics data," *Nat. Methods*, vol. 13, no. June, pp. 731–740, 2016, doi: 10.1038/nmeth.3901.

[35] J. Goedhart and M. S. Luijsterburg, "VolcaNoseR is a web app for creating, exploring, labeling and sharing volcano plots," *Sci. Rep.*, vol. 10(1):2056, pp. 1–5, 2020, doi: 10.1038/s41598-020-76603-3.

[36] Y. Liao, J. Wang, E. J. Jaehnig, Z. Shi, and B. Zhang, "WebGestalt 2019: gene set analysis toolkit with revamped UIs and APIs," *Nucl. Acids Res.*, vol. 47, no. W1, pp. W199–W205, 2019, doi: 10.1093/nar/gkz401.

[37] B. Yates, B. Braschi, K. A. Gray, R. L. Seal, S. Tweedie, and E. A. Bruford, "Genenames.org: The HGNC and VGNC resources in 2017," *Nucleic Acids Res.*, vol. 45, no. D1, pp. D619–D625, 2017, doi: 10.1093/nar/gkw1033.

[38] J. Yuen *et al.*, "NETosing neutrophils activate complement both on their own NETs and bacteria via alternative and non-alternative pathways," *Front. Immunol.*, vol. 7, no. 137, pp. 1–14, 2016, doi: 10.3389/fimmu.2016.00137.

[39] S. Ernst, C. Lange, A. Wilbers, V. Goebeler, V. Gerke, and U. Rescher, "An Annexin 1 N-Terminal Peptide Activates Leukocytes by Triggering Different Members of the Formyl Peptide Receptor Family," *J. Immunol.*, vol. 172, no. 12, pp. 7669–7676, 2004, doi: 10.4049/jimmunol.172.12.7669.

[40] H. Leffers *et al.*, "Identification of two human Rho GDP dissociation inhibitor proteins whose overexpression leads to disruption of the actin cytoskeleton," *Experimental Cell Research*, vol. 209, no. 2. pp. 165–174, 1993. doi: 10.1006/excr.1993.1298.

[41] C. Tristan, N. Shahani, T. W. Sedlak, and A. Sawa, "The diverse functions of GAPDH: Views from different subcellular compartments," *Cell. Signal.*, vol. 23, no. 2, pp. 317–323, 2011, doi: 10.1016/j.cellsig.2010.08.003.

[42] A. Makowiecka *et al.*, "Changes in biomechanical properties of A375 cells due to the silencing of TMSB4X expression are not directly correlated with alterations in their stemness features," *Cells*, vol. 10, no. 4, pp. 1–25, 2021, doi: 10.3390/cells10040769.

[43] R. Donato, "S100: A multigenic family of calcium-modulated proteins of the EF-hand type with intracellular and extracellular functional roles," *Int. J. Biochem. Cell Biol.*, vol. 33, pp. 637–668, 2001, doi: 10.1016/S1357-2725(01)00046-2.

[44] A. Heil *et al.*, "S100P is a novel interaction partner and regulator of IQGAP1," *J.*

Biol. Chem., vol. 286, no. 9, pp. 7227–7238, 2011, doi: 10.1074/jbc.M110.135095.

[45] M. Koltzcher, C. Neumann, S. König, and V. Gerke, “Ca2+-dependent Binding and Activation of Dormant Ezrin by Dimeric S100P,” *Mol. Biol. Cell*, vol. 14, pp. 2372–2384, 2003, doi: 10.1091/mbc.E02.

[46] L. Wang *et al.*, “Cancer-associated fibroblasts contribute to cisplatin resistance by modulating ANXA3 in lung cancer cells,” *Cancer Sci.*, vol. 110, pp. 1609–1620, 2019, doi: 10.1111/cas.13998.

[47] R. Xu, “Annexin A3 depletion overcomes resistance to oxaliplatin in colorectal cancer via the MAPK signaling pathway,” *J. Cell. Biochem.*, vol. 120, pp. 14585–14593, 2019, doi: 10.1002/jcb.28720.

[48] V. L. E. Cabec and I. Maridonneau-parini, “Annexin 3 is associated with cytoplasmic granules in neutrophils and monocytes and translocates to the plasma membrane in activated cells,” *Biochem. J.*, vol. 303, no. Pt 2)(Pt 2, pp. 481–487, 1994, doi: 10.1042/bj3030481.

[49] J. D. Ernst, E. Hoye, R. A. Blackwood, and D. Jaye, “Purification and Characterization of an Abundant Cytosolic Protein from Human Neutrophils That Promotes Ca2+ -dependent Aggregation of Isolated Specific Granules,” *J. Clin. Invest.*, vol. 85, no. 4, pp. 1065–1071, 1990, doi: 10.1172/JCI114537.

[50] J. B. Cowland and N. Borregaard, “Granulopoiesis and granules of human neutropophils,” *Immunol. Rev.*, vol. 273, pp. 11–28, 2016, doi: 10.2214/ajr.155.2.2115276.

[51] U. Rescher and V. Gerke, “Annexins – unique membrane binding proteins with diverse functions,” *J. Cell Sci.*, vol. 117, pp. 2631–2639, 2004, doi: 10.1242/jcs.01245.

[52] V. Gerke and S. E. Moss, “Annexins: From Structure to Function,” *Physiol. Rev.*, vol. 82, pp. 331–371, 2002, doi: 10.1152/physrev.00030.2001.

[53] T. D. Pollard and J. A. Cooper, “Actin, a Central Player in Cell Shape and Movement,” *Science (80-.).*, vol. 326, pp. 1208–1212, 2009, doi: 10.1126/science.1175862.

[54] E. Bertling, P. Hotulainen, P. Mattila, K, T. Matilainen, M. Salminen, and P. Lappalainen, “Cyclase-associated Protein 1 (CAP1) Promotes Cofilin- induced Actin Dynamics in Mammalian Nonmuscle Cells,” *Mol Biol Cell*, vol. 15, pp. 2324–2334, 2004, doi: 10.1091/mbc.E04.

[55] K. L. Bicker and P. R. Thompson, “The Protein Arginine Deiminases: Structure, Function, Inhibition, and Disease,” *Biopolymers*, vol. 99, no. 2, pp. 155–163, 2012, doi: 10.1002/bip.22127.

[56] J. Lowery, E. R. Kuczmarski, H. Herrmann, and R. D. Goldma, “Intermediate filaments play a pivotal role in regulating cell architecture and function,” *J. Biol. Chem.*, vol. 290, no. 28, pp. 17145–17153, 2015, doi:

10.1074/jbc.R115.640359.

[57] I. Dupin, Y. Sakamoto, and S. Etienne-Manneville, “Cytoplasmic intermediate filaments mediate actin-driven positioning of the nucleus,” *J. Cell Sci.*, vol. 124, no. 6, pp. 865–872, 2011, doi: 10.1242/jcs.076356.

[58] A. E. Patteson *et al.*, “Vimentin protects cells against nuclear rupture and DNA damage during migration,” *J. Cell Biol.*, vol. 218, no. 12, pp. 4079–4092, 2019, doi: 10.1083/JCB.201902046.

[59] M. Leshner *et al.*, “PAD4 mediated histone hypercitrullination induces heterochromatin decondensation and chromatin unfolding to form neutrophil extracellular trap-like structures,” *Front. Immunol.*, vol. 3, no. OCT, pp. 1–11, 2012, doi: 10.3389/fimmu.2012.00307.

[60] J. C. Hansen, “Conformational dynamics of the chromatin fiber in solution: Determinants, mechanisms, and functions,” *Annu. Rev. Biophys. Biomol. Struct.*, vol. 31, pp. 361–392, 2002, doi: 10.1146/annurev.biophys.31.101101.140858.

[61] E. Nikolakaki, I. Mylonis, and T. Giannakouros, “Lamin B receptor: Interplay between structure, function and localization,” *Cells*, vol. 6, no. 3, pp. 1–17, 2017, doi: 10.3390/cells6030028.

[62] A. L. Olins, A. Ernst, M. Zwerger, H. Herrmann, and D. E. Olins, “An in vitro model for Pelger-Huët anomaly,” *Nucleus*, vol. 1, no. 6, pp. 506–512, 2010, doi: 10.4161/nucl.1.6.13271.

[63] J. Camps, M. R. Erdos, and T. Ried, “The role of lamin B1 for the maintenance of nuclear structure and function,” *Nucleus*, vol. 6, no. 1, pp. 8–14, 2015, doi: 10.1080/19491034.2014.1003510.

[64] C. D. Sadik, N. D. Kim, and A. D. Luster, “Neutrophils cascading their way to inflammation,” *Trends Immunol.*, vol. 32, no. 10, pp. 452–460, 2012, doi: 10.1016/j.it.2011.06.008.Neutrophils.

[65] S. Rørvig *et al.*, “Ficolin-1 is present in a highly mobilizable subset of human neutrophil granules and associates with the cell surface after stimulation with fMLP,” *J. Leukoc. Biol.*, vol. 86, no. 6, pp. 1439–1449, 2009, doi: 10.1189/jlb.1008606.

[66] V. Videm and E. Strand, “Changes in Neutrophil Surface-Receptor Expression After Stimulation with FMLP , Endotoxin , Interleukin-8 and Activated Complement Compared to Degranulation,” *Scand. J. ofImmunology*, vol. 59, pp. 25–33, 2004, doi: 10.1111/j.0300-9475.2004.01351.x.

[67] M. P. Pruchniak and U. Demkow, “Potent NETosis inducers do not show synergistic effects in vitro,” *Cent. Eur. J. Immunol.*, vol. 44, no. 1, pp. 51–58, 2019, doi: 10.5114/ceji.2019.84017.

[68] O. Rodríguez-Espinosa, O. Rojas-Espinosa, M. M. B. Moreno-Altamirano, E. O. López-Villegas, and F. J. Sánchez-García, “Metabolic requirements for

neutrophil extracellular traps formation," *Immunology*, vol. 145, no. 2, pp. 213–224, 2015, doi: 10.1111/imm.12437.

[69] K. Nakashima, T. Hagiwara, and M. Yamada, "Nuclear localization of peptidylarginine deiminase V and histone deimination in granulocytes," *J. Biol. Chem.*, vol. 277, no. 51, pp. 49562–49568, 2002, doi: 10.1074/jbc.M208795200.

[70] T. Hagiwara, Y. Hidaka, and M. Yamada, "Deimination of histone H2A and H4 at arginine 3 in HL-60 granulocytes," *Biochemistry*, vol. 44, no. 15, pp. 5827–5834, 2005, doi: 10.1021/bi047505c.

[71] M. A. Christophorou *et al.*, "Citrullination regulates pluripotency and histone H1 binding to chromatin," *Nature*, vol. 507, no. 7490, pp. 104–108, 2014, doi: 10.1038/nature12942.

[72] M. Buttinelli, G. Panetta, D. Rhodes, and A. Travers, "The role of histone H1 in chromatin condensation and transcriptional repression," *Genetica*, vol. 106, no. 1–2, pp. 117–124, 1999, doi: 10.1023/a:1003745315540.

[73] C. Carmona-rivera *et al.*, "Synovial fibroblast-neutrophil interactions promote pathogenic adaptive immunity in rheumatoid arthritis," *Sci. Immunol.*, vol. 2, no. 10, p. eaag3358, 2017, doi: 10.1126/sciimmunol.aag3358.

[74] S. Gößwein *et al.*, "Citrullination licenses calpain to decondense nuclei in neutrophil extracellular trap formation," *Front. Immunol.*, vol. 10, no. OCT, pp. 1–15, 2019, doi: 10.3389/fimmu.2019.02481.

[75] Y. Li, M. Li, B. Weigel, M. Mall, V. P. Werth, and M. Liu, "Nuclear envelope rupture and NET formation is driven by PKCα-mediated lamin B disassembly," *EMBO Rep.*, vol. 21, no. 8, pp. 1–19, 2020, doi: 10.15252/embr.201948779.

[76] K. Hoffmann *et al.*, "Mutations in the gene encoding the lamin B receptor produce an altered nuclear morphology in granulocytes (Pelger-Huët anomaly)," *Nat. Genet.*, vol. 31, no. 4, pp. 410–414, 2002, doi: 10.1038/ng925.

[77] L. I. Sakkas, D. P. Bogdanos, C. Katsiari, and C. D. Platsoucas, "Autoimmunity Reviews Anti-citrullinated peptides as autoantigens in rheumatoid arthritis — relevance to treatment," *Autoimmun. Rev.*, vol. 13, no. 11, pp. 1114–1120, 2014, doi: 10.1016/j.autrev.2014.08.012.

[78] S. Muller and M. Radic, "Citrullinated Autoantigens: From Diagnostic Markers to Pathogenetic Mechanisms," *Clin. Rev. Allergy Immunol.*, vol. 49, pp. 232–239, 2015, doi: 10.1007/s12016-014-8459-2.

[79] D. A. Fox, "Citrullination: A Specific Target for the Autoimmune Response in Rheumatoid Arthritis," *J. Immunol.*, vol. 195, no. 1, pp. 5–7, 2020, doi: 10.4049/jimmunol.1501021.

[80] F. Wang *et al.*, "Identification of citrullinated peptides in the synovial fluid of patients with rheumatoid arthritis using LC-MALDI-TOF/TOF," *Clin. Rheumatol.*, vol. 35, no. 9, pp. 2185–2194, 2016, doi: 10.1007/s10067-016-

3247-4.

[81] K. Van Steendam, K. Tilleman, M. De Ceuleneer, F. De Keyser, D. Elewaut, and D. Deforce, “Citrullinated vimentin as an important antigen in immune complexes from synovial fluid of rheumatoid arthritis patients with antibodies against citrullinated proteins,” *Arthritis Res. Ther.*, vol. 12, no. R132, pp. 1–10, 2010, doi: 10.1186/ar3070.

[82] I. Neeli, S. N. Khan, and M. Radic, “Histone Deimination As a Response to Inflammatory Stimuli in Neutrophils,” *J. Immunol.*, vol. 180, no. 3, pp. 1895–1902, 2008, doi: 10.4049/jimmunol.180.3.1895.

[83] C. L. Holmes, D. Shim, J. Kernien, C. J. Johnson, J. E. Nett, and M. A. Shelef, “Insight into Neutrophil Extracellular Traps through Systematic Evaluation of Citrullination and Peptidylarginine Deiminases,” *J. Immunol. Res.*, vol. 2019, no. Article ID 2160192, pp. 1–11, 2019, doi: 10.1155/2019/2160192.

[84] H. D. Lewis *et al.*, “Inhibition of PAD4 activity is sufficient to disrupt mouse and human NET formation,” *Nat. Chem. Biol.*, vol. 11, no. 3, pp. 189–191, 2015, doi: 10.1038/nchembio.1735.

7. Web references

Webgestalt, WEB-based GEne SeT AnaLysis Toolkit. http://www.webgestalt.org/, 2022 (accessed 30 december, 2022)

VolcanoseR – exploring volcano plots. https://huygens.science.uva.nl/VolcaNoseR/, 2022 (accessed 25 november, 2022)

8. Appendix list (CHAPTER 1)

- **Supplemental Figure 1:** Neutrophils treated with fMLP were not able to produce NETs
- **Supplemental Figure 2:** The secretome of ionomycin-treated neutrophils differs from fMLP stimulated cells
- **Supplemental Figure 3:** The secretome of control neutrophils is similar to the secretome of fMLP-treated neutrophils

- **Supplemental Figure 4:** Actin filament organization and neutrophil mediated immunity are common biological process found for ionomycin-treated neutrophils isolated from three different subjects
- **Supplemental Figure 5:** Proteins involved in neutrophil mediated immunity, metabolism of pyridine-containing components and metabolism of glucose 6-phosphate are more abundant in the nucleus and/or organelles of ionomycin-treated neutrophils
- **Supplemental Table 1A:** Volcano plot data of the secretome of control and ionomycin-treated neutrophils
- **Supplemental Table 1B:** Proteins exclusively found in the secretome of control, ionomycin-treated and fMLP-treated neutrophils
- **Supplemental Table 1C:** Secretome enrichment results of unique and enriched proteins on ionomycin-treated neutrophils in comparison with control neutrophils
- **Supplemental Table 1D:** Secretome enrichment results of unique and enriched proteins on control neutrophils in comparison with the ionomycin-treated neutrophils
- **Supplemental Table 1E:** Volcano plot data of the secretome of fMLP- and ionomycin-treated neutrophils
- **Supplemental Table 1F:** Secretome enrichment results of unique and enriched proteins on fMLP-treated neutrophils in comparison with the neutrophils treated with ionomycin
- **Supplemental Table 1G:** Secretome enrichment results of unique and enriched proteins on ionomycin-treated neutrophils in comparison with the neutrophils treated with fMLP

- **Supplemental Table 1H:** Volcano plot data of the secretome of control and fMLP-treated neutrophils
- **Supplemental Table 2A:** Volcano plot data of the nucleus of control and ionomycin-treated neutrophils
- **Supplemental Table 2B:** Unique proteins found in the nucleus of control and ionomycin-treated neutrophils
- **Supplemental Table 2C:** Enrichment results of unique and enriched proteins on ionomycin-treated neutrophils nucleus
- **Supplemental Table 2D:** Enrichment results of unique and enriched proteins on control neutrophils nucleus
- **Supplemental Table 3A:** Protein distribution across different fractions of control and ionomycin-treated neutrophils
- **Supplemental Table 3B:** Proteins found in higher proportion on the nucleus and/or organelles fractions but reduced on the soluble proteins fraction and/or in the secretome of ionomycin-treated neutrophils
- **Supplemental Table 3C:** Enrichment results of proteins that are proportionally enriched in the nucleus and proportionally reduced in the secretome and/or soluble proteins fraction of ionomycin-treated neutrophils
- **Supplemental Table 3D:** Enrichment results of proteins that are proportionally enriched in the organellar fraction and proportionally reduced in the secretome and soluble proteins fraction of ionomycin-treated neutrophils

The above supplemental tables can be found at: https://github.com/Lore-rocha/Early-events-in-ionomycin-induced-NETosis

9. Appendix - supplemental figures (CHAPTER 1):

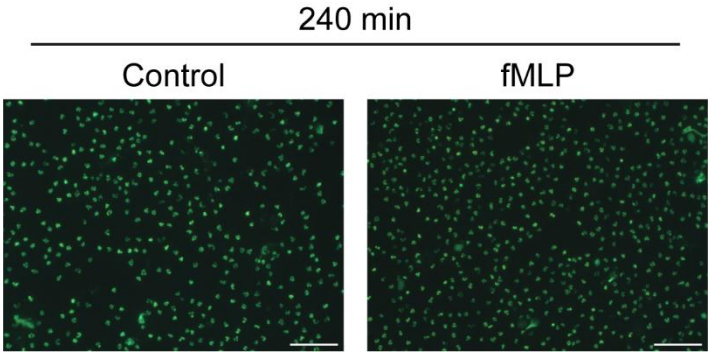

Supplemental Figure 1. Neutrophils treated with fMLP were not able to produce NETs. Human neutrophils were treated with DMSO or 1 µM fMLP for 240 min, fixed, stained with 500 nM SYTOX green, and visualized by fluorescence microscopy analysis. Scale bars = 50 µm.

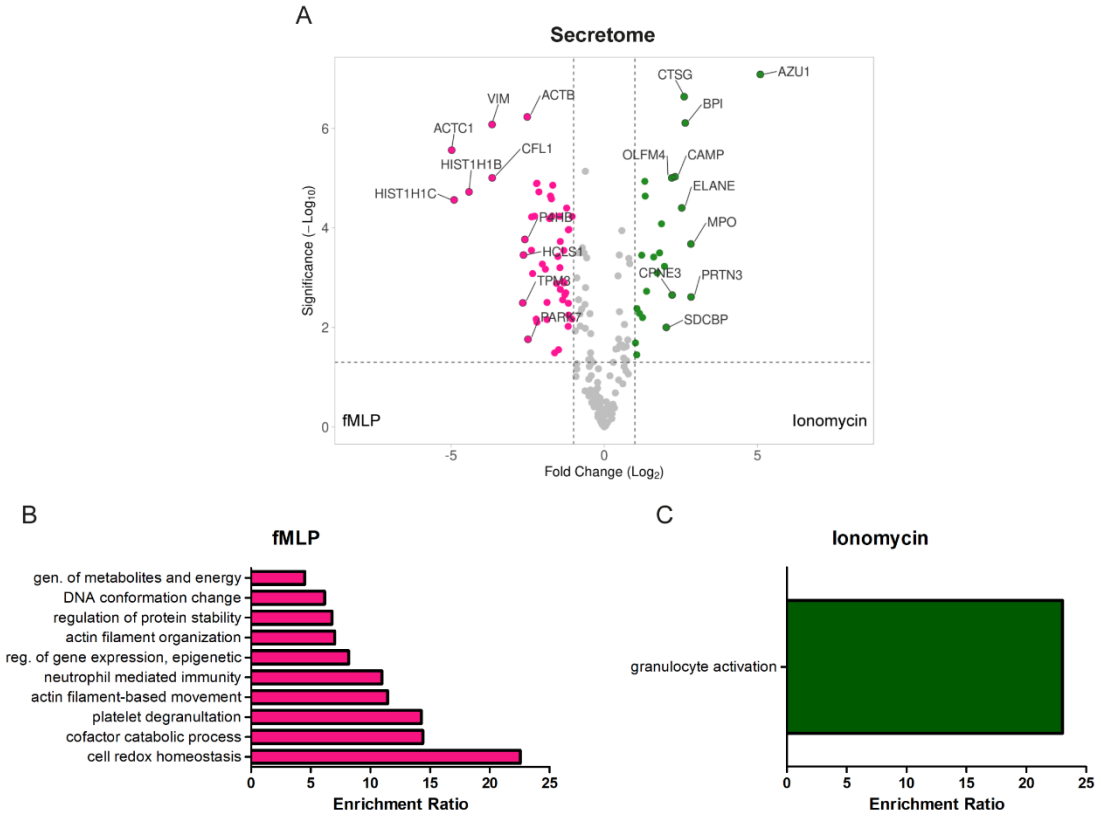

Supplemental Figure 2. The secretome of ionomycin-treated neutrophils differs from fMLP stimulated cells. The secretome of human neutrophils treated with 6.7 µM ionomycin or 1 µM fMLP was analyzed by mass spectrometry**.** A) Differentially secreted proteins obtained comparing fMLP and ionomycin-treated neutrophils. For each protein, the -log10 of the P-value from t-test followed by multiple comparisons adjustment is plotted against the log2 fold change between fMLP and ionomycin groups of 1 representative of 3 independent experiments. Proteins more abundant in the ionomycin-treated neutrophils secretome are displayed to the right of the value 1 in the x-axis (dashed line), while less abundant proteins are displayed to the left of the

-1 value. Enrichment analysis of exclusive and more abundant proteins found in the B) fMLP and C) ionomycin groups. For each enriched biological process (y-axis), the enrichment ratio (the number of observed genes over the expected value, x-axis) was calculated.

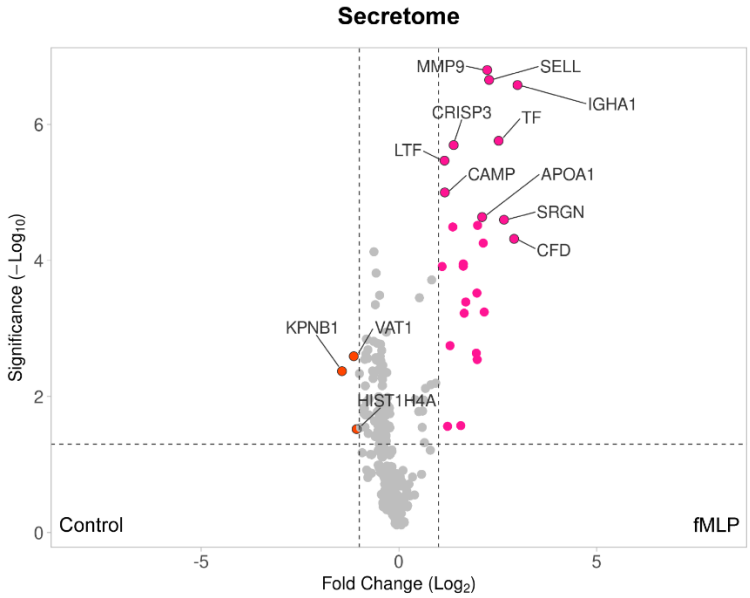

Supplemental Figure 3. The secretome of control neutrophils is similar to the secretome of fMLP-treated neutrophils. The secretome of human neutrophils treated with the vehicle (DMSO) or fMLP 1 µM for 2 min at 37 °C was analyzed by mass spectrometry, and differentially secreted proteins obtained comparing control and fMLP-treated neutrophils are displayed in the graph. For each protein, the -log10 of the P-value from t-test after multiple comparisons adjustment is plotted against the log2 fold change between control and fMLP groups of 1 representative of 3 independent experiments. Proteins more abundant in the fMLP-treated neutrophils secretome are displayed to the right of the value 1 in the x-axis (dashed line), while less abundant proteins are displayed to the left of the -1 value.

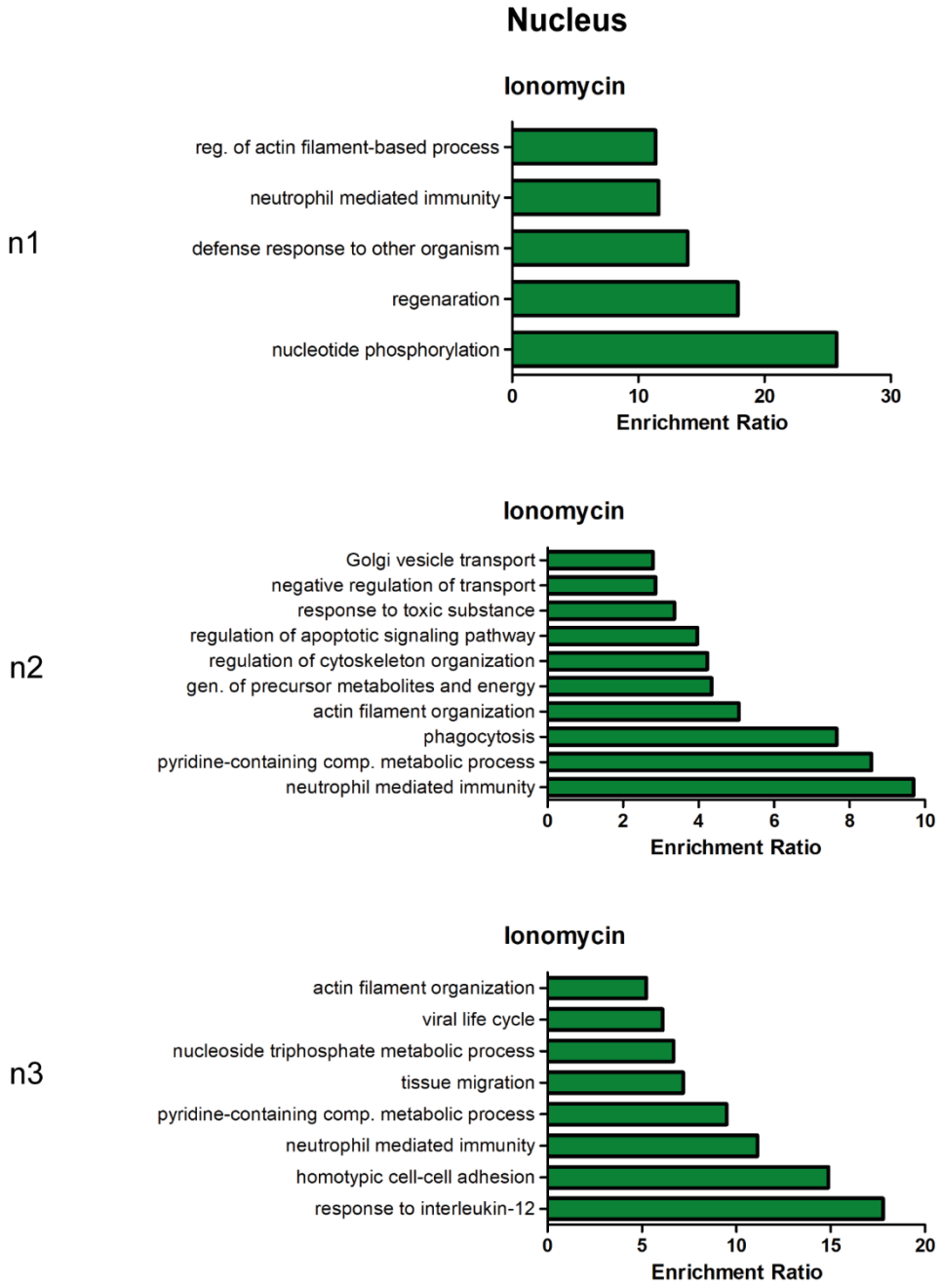

Supplemental Figure 4. Actin filament organization and neutrophil mediated immunity are common biological process found for ionomycin-treated neutrophils isolated from three different subjects. The nuclear proteins of human neutrophils treated with 6.7 µM ionomycin for 2 min at 37 °C were analyzed by mass spectrometry. Comparison of the enrichment analysis of unique and enriched proteins found in the ionomycin-treated neutrophils of each of the individual subjects (n = 3). For each enriched biological process (y-axis), the enrichment ratio (the number of observed genes over the expected value, x-axis) was calculated.

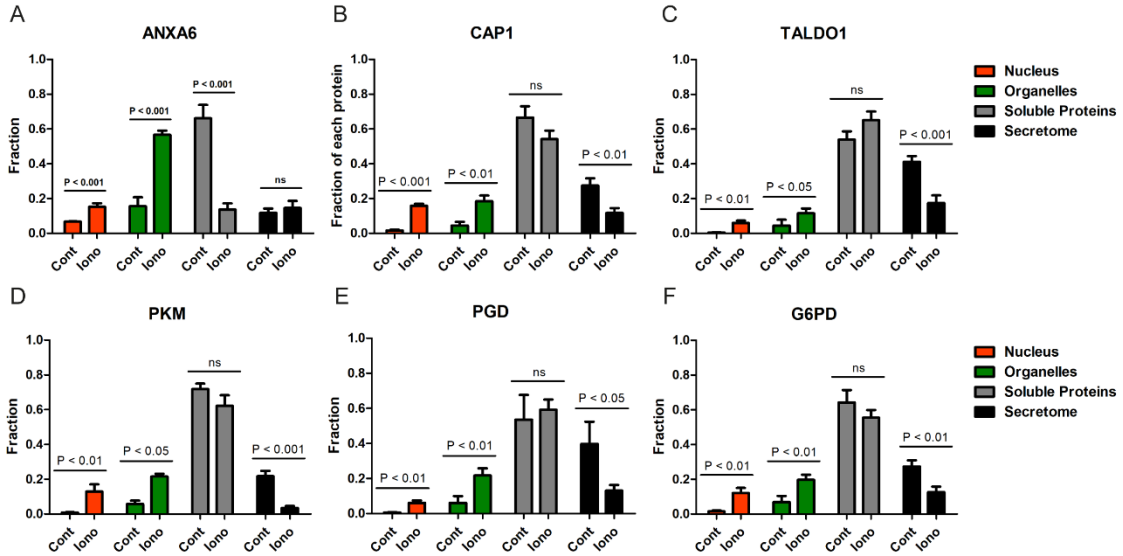

Supplemental Figure 5. Proteins involved in neutrophil mediated immunity, metabolism of pyridine-containing components and metabolism of glucose 6-phosphate are more abundant in the nucleus and/or organelles of ionomycin-treated neutrophils. Human neutrophils were treated with the vehicle (DMSO) or 6,7 µM ionomycin, fractionated in nucleus, organelles, soluble proteins and secretome-enriched fractions and analyzed by mass spectrometry. The results presented are from one experiment representative of 3 subjects. A) - H) Selected proteins with ratio ionomycin/control > 2 in the nucleus and/or organelles fractions, and < 0.5 in the soluble proteins and/or secretome fractions. P-values are FDR adjusted after unpaired t-test of each protein in each of the 4 cellular fractions. Comparison of the fractions of the proteins A) ANXA6, B) CAP1, C) TALDO1, D) PKM, E) PGD, and F) G6PD in the control and ionomycin groups. Error bars represent the standard deviation.

CHAPTER 2: Neutrophil's response before NETs release is stimulus-dependent

Abbreviations

(ROS) – Reactive oxygen species

(NETs) – Neutrophil extracellular traps

(PMA) - Phorbol-12-myristate-13-acetate

(PKC) – Protein kinase C

(DAG) – Diacylglycerol

(ELANE) – Neutrophil elastase

(fMLP) - N-formylmethionyl-leucyl-phenylalanine

(PAD4) – Protein arginine deiminase 4

(ITGAM/CD11b) – Integrin alpha-M

(ITGB2/CD18) – Integrin beta-2

(MPO) – Myeloperoxidase

(PRTN3) – Proteinase 3

(CAMP) – Cathelicidin

(DMSO) – Dimethylsulfoxide

(LTF) – Lactotransferrin

(PTPRJ) - Receptor-type tyrosine-protein phosphatase eta

(LRG1) - Leucine-rich alpha-2-glycoprotein

(CD177) - CD177 antigen

(MMP8) – Neutrophil collagenase

(MMP9) – Matrix metalloproteinase-9

(LYZ) – Lysozyme

(S100A8) – Protein S100-A8

(S100A9) – Protein S100-A9

(OLFM4) – Olfactomedin-4

Abstract

Neutrophil extracellular traps (NETs) are web-like structures composed of chromatin along with microbicidal proteins, released by activated neutrophils and capable of killing pathogens. Many different stimuli are able to induce NETs release, and recent evidences suggest multiple mechanisms might be involved in this process. Thus, some stimuli, such as phorbol-12-myristate-13-acetate (PMA) induce NETs activating the NADPH oxidase, while this enzyme participation upon other stimulus, such as the calcium ionophore ionomycin, is debatable. Interestingly, other stimuli, such as the chemotactic peptide n-formylmethionyl-leucyl-phenylalanine (fMLP) activate the NADPH oxidase, but the release of NETs after fMLP treatment is controversial. Here, a careful examination of the initial response following neutrophil activation by three common stimuli, namely PMA, ionomycin and fMLP was provided by using live-imaging microscopy and proteomics. Our results demonstrated that PMA- and fMLP-stimulated cells were able to activate NADPH oxidase, in contrast to ionomycin-stimulated neutrophils. Even without NADPH oxidase activation, ionomycin-treated cells release NETs with a much faster kinetics when comparing with PMA-treated neutrophils. More interestingly, even though ionomycin and PMA induced NETs generation (albeit with different kinetics), the signals and mediators released by stimulated cells to the environment before the onset of NETs were distinct. Thus, cells treated with ionomycin released higher levels of cytotoxic proteins whereas PMA-treated neutrophils released more proteins associated with cell adhesion, migration and superoxide generation. In conclusion, despite leading to the same final outcome, PMA and ionomycin treatments trigger different responses in neutrophils.

Keywords: Neutrophil extracellular traps, NADPH oxidase activation, degranulation, PMA, ionomycin, and fMLP.

1. Introduction

Neutrophils are highly specialized cells of the innate immune system that eliminate pathogens using a range of microbicidal proteins, with or without the assistance of reactive oxygen species (ROS) generated by NADPH oxidase [1]–[3]. These microbicidal proteins are primarily stored in five distinct compartments called granules within neutrophil cytosol [4], and they can be released either intracellularly into the phagosome compartment or extracellularly, through degranulation or in association with neutrophil extracellular traps (NETs) [5], [6]. NETs are chromatin webs that can trap bacteria, fungi, and virus, and eventually eliminate them using their cytotoxic protein content derived from neutrophil granules, nucleus and cytosol [6]–[11]. Upon activation, neutrophils begin degranulating within minutes [1], [12] and tend to release NETs instead of undergoing phagocytosis in response to large pathogens like *Candida albicans* hyphae [8].

NETs can be released from neutrophils resulting in a form of cell death distinct from necrosis or apoptosis (suicidal NETosis) [13] , or they can be released from living cells (vital NETosis) [14]. Neutrophils can undergo NETosis in response to various sterile or infectious stimuli [15]–[17], and recent studies have suggested that suicidal NETosis may involve stimulus-dependent mechanisms that differ in their ability to activate superoxide production by NADPH oxidase [18]–[20]. The stimuli phorbol-12-myristate-13-acetate (PMA) and the calcium ionophore ionomycin, possibly represent these two distinct mechanisms of suicidal NETosis [19].

PMA directly activates protein kinase C (PKC) by mimicking the action of diacylglycerol (DAG), which acts phosphorylating the NADPH oxidase subunits, allowing for their assembly and activation [21], [22]. PMA induces neutrophil degranulation [23], mildly intracellular Ca^{2+} oscillations [18], and causes chromatin

swelling and decondensation [24], partially via the degrading action of ELANE on histones [25], [26]. Finally, this process culminates in the release of NETs on average after 1h30 min to 3 hours [20], [27], [28]. The actions of PMA and of the chemotactic peptide n-formylmethionyl-leucyl-phenylalanine (fMLP) in neutrophils are somewhat similar. Both are known to activate the superoxide production by NADPH oxidase [29], increase intracellular Ca^{2+} [30], elicit degranulation [34, 35], and increase expression of surface receptors such as β_2-integrins (CD18/ITGB2) [31]. While it is well-established that PMA treatment induces NETosis, there is currently no consensus on whether fMLP has the same effect on neutrophils [32], [33].

Neutrophils treated with Ca^{2+} ionophores such as ionomycin, have a substantial increase in their intracellular Ca^{2+} levels (above 1 μM) [34]. This increase elicits degranulation and hyperactivates the proteins arginine deiminases 2 and 4 (PAD2 and PAD4) [35], that catalyze the citrullination (also called deimination) of arginine residues modifying protein net charge, which in histones promotes chromatin decondensation [36]. These effects ultimately lead to NETosis on average after 1h30min [18], [20]. However, there is still confounding evidence in the literature regarding the requirements of NADPH oxidase in Ca^{2+} ionophores-activated NETosis [20], [27], [37].

Thus, neutrophil responses to PMA, ionomycin and fMLP, intersect in two aspects: increase in intracellular Ca^{2+} and degranulation. Degranulation occurs through the fusion of granule membranes with the phagocytic or plasma membranes [38], [39]. There are five types of granules in neutrophils cytosol – secretory vesicles, ficolin-1-rich granules, tertiary/gelatinase granules, secondary/specific granules, and primary/azurophilic granules - which mainly differ in their protein content and sensitivity to calcium [40]–[43]. Secretory vesicles are enriched in pathogen-recognition receptors and adhesion molecules, such as the integrin Mac-1 (CD11b/CD18 or ITGAM/ITGB2)

[44]. Ficolin-1-rich granules have ficolin-1, a lectin that acts as a pattern-recognition receptor [43]. Specific and tertiary granules have similar protein content of secretory vesicles but have different pathogen-recognition receptors and additional adhesion molecules [44], [45]. Furthermore, they contain proteins that make the surrounding tissue inhospitable for pathogens, such as gelatinase and collagenase, and a few microbicidal proteins [44]. Azurophilic granules have the highest content of microbicidal proteins including oxidant-producing enzymes, such as MPO, proteases, membrane-permeabilizing proteins, and defensins [44], [46].

Ca^{2+}-mediated signaling plays a crucial role in several neutrophil functions, including degranulation and NETosis [47]. Neutrophil granules exhibit a descending order of sensitivity to Ca^{2+}, with the secretory granules being the most responsive and secreted among them [4], [48]. Moreover, chelating intracellular or extracellular Ca^{2+} stores impaired NETosis after PMA or ionomycin treatment [19], [49].

The uncontrolled release of several granule proteins, including MPO, proteinase 3 (PRTN3), and cathelicidin (CAMP), either alone or in association with NETs, can act as autoantigens in systemic autoimmune diseases such as antineutrophil cytoplasmic antibody (ANCA)-associated vasculitis and systemic lupus erythematosus (SLE) [50]–[52]. Furthermore, they can cause damage to endothelial cells and contribute to the progression of other diseases like atherosclerosis and thrombosis [53], [54]. While some studies have identified proteins associated with NETs under different stimuli, the proteins secreted before NETs release are not yet fully known [55]–[57].

Therefore, we used live-imaging microscopy and mass spectrometry-based proteomics to examine neutrophil's response to distinct stimuli prior to NETs release. Our results showed only neutrophils treated with PMA and ionomycin were able to produce NETs, although with distinct kinetics. On the other hand, only fMLP- and PMA-

treated neutrophils produced NADPH oxidase-dependent superoxide. Neutrophils treated with fMLP and PMA secreted similar proteins, involved in processes related to neutrophil adhesion and migration, and in the superoxide production. In contrast, neutrophils treated with ionomycin released more cytotoxic proteins from azurophilic granules. Thus, this work demonstrated that the release of NETs following treatment with PMA or ionomycin involves distinct preceding events despite leading to the common final outcome of cell death by NETs release.

2. Materials and methods

2.1. Materials

Dextran, Hystopaque, ammonium bicarbonate, tris(hydroxymethyl)aminomethane hydrochloride (Tris-HCl), sodium deoxycholate (SDC), dimethylsulfoxide (DMSO), ionomycin, phorbol 12-myristate 13-acetate (PMA), phenylmethanesulfonyl fluoride (PMSF), Amicon® Ultra 0.5 mL 10 kDa centrifugal filter units, Tween® 20, Urea, Benzonase® nuclease, and trifluoroacetic acid (TFA) were obtained from Sigma (St. Louis, MO, USA). SYTOX™ green, Hoechst 33342, and Pierce™ BCA protein assay kit were purchased from Invitrogen (Waltham, MA, USA). Dithiothreitol (DTT) and iodoacetamide (IAA) were purchased from Bio-Rad laboratories (Hercules, CA, USA). Poly-D-Lysine, acetonitrile, and 0.1% formic acid were obtained from Merck (Darmstadt, Germany). Trypsin was obtained from Promega (Madison, WI, USA). fMLP (?) – add.

2.2. Neutrophil Isolation

Human neutrophils were isolated from healthy volunteers' heparinized blood using Dextran sedimentation, density centrifugation with Hystopaque 1.077 g/mL, and erythrocyte lysis with a hypotonic solution. Neutrophils were then resuspended in either

PBS with 5.5 mM glucose or RPMI medium without phenol red [58]. Blood collection was authorized by the Research Ethics Committee of the Faculty of Pharmaceutical Sciences at the University of São Paulo (CAAE 60860016.5.0000.0067).

2.3. Measurement of extracellular superoxide

Extracellular superoxide release was measured by monitoring cytochrome c reduction [59]. Neutrophils ($1x10^6$) were exposed to DMSO 0,005% (v/v, vehicle), fMLP 1 μM, PMA 20 nM or ionomycin 6,7 μM with 40 μM cytochrome C and 5 nM Taurine in PBS with 5.5 mM glucose. Absorbances in 550 nm were obtained in 51 s intervals over a period of 30 min at 37 °C, using a microplate reader (Synergy H1, Biotek). The rate of superoxide release was calculated from the slope obtained using the linear part of the curves.

2.4. Live-imaging microscopy

To visualize neutrophils behavior, cells ($1.5x10^5$) were seeded onto a 24-well plate coated with 0.001% poly-D-lysine and allowed to settle for 20 minutes at 37°C in RPMI 1640 medium without phenol red, supplemented with 1% antibiotic and 2 μM Hoechst 33342. Neutrophils were then treated with 0.005% DMSO (vehicle), 1 μM fMLP, 20 nM PMA or 6.7 μM ionomycin, followed by 500 nM SYTOX green addition. Fluorescent images for Hoechst 33342 and SYTOX Green were automatically captured every 2 minutes for 120 minutes at 37°C with 5% CO2 using a 20x/0.4 objective on a Leica DMi8 widefield microscope coupled with the LASX Application Software (Leica Microsystems).

2.5. NETs quantification

The method of quantification described here has been described in detail [60], and was based on previous methods [28], [61]. Briefly, images obtained from live-

imaging microscopy of neutrophils in the presence of Hoechst 33342 and SYTOX Green (respectively, a permeant and an impermeant dye to the cell membranes) were processed using ImageJ software (version 1.52p). This involved adjusting the auto local threshold of the 8-bit images generated and using the watershed function to separate cells, followed by cell categorization based on their size and loss of plasma membrane integrity (SYTOX green positive cells). To determine the percentage of NETs, we calculated the ratio of cells with NETs (SYTOX green plus Hoechst 33342 positive cells) to the total number of cells (the sum of SYTOX green plus Hoechst 33342 positive cells and Hoechst 33342-only positive cells), and then multiplied by 100. Cells had to be larger than 26 μm^2 to be counted (this procedure excludes any possible debris).

2.6. Secretome collection

Neutrophils ($2x10^6$/mL) in RPMI 1640 medium without phenol red, supplemented with 1% of antibiotic, were allowed to settle for 30 min at 37 °C in 0.001% poly-D-lysine coated 12-well plates. Next, cells were exposed to 0.005% v/v DMSO (vehicle), 1 µM fMLP, 20 nM PMA or 6.7 µM ionomycin for 30 or 90 min at 37 °C with 5 % CO_2. Following the designated time period, the supernatant was collected and kept on ice. Cells were separated from the secretome through a 10-min centrifugation at 400 x *g* and 4°C. Afterwards, 100 nM PMSF was added to the secretome, and proteins were concentrated by two cycles of centrifugation at 14,000 x *g* for 15 min at 4 °C, using previously passivated 10 kDa centrifugal filter units [62]. Finally, proteins obtained from secretome were incubated twice with 12.5 U of benzonase for 45 min at 37 °C and 300 rpm.

2.7. Filter-aided sample preparation (FASP) for mass spectrometry

The concentration of proteins in the secretome samples was measured by the bicinchoninic acid assay (BCA). Ten µg of secretome proteins were added to previously passivated 10 kDa centrifugal filter units [62], followed by three cycles of centrifugation at 14,000 x *g* for 20 min with 500 µL 8 M Urea in 25 mM $(NH_4)HCO_3$. Proteins were reduced with 450 µL of 10 mM DTT in 25 mM $(NH_4)HCO_3$ for 30 min at 30 °C and 600 rpm, centrifuged at 14,000 x *g* for 20 min, alkylated with 450 µL of 20 mM IAA in 25 mM $(NH_4)HCO_3$ for 45 min at 600 rpm and 25 °C in the dark, and then centrifuged 14,000 x *g* for 20 min. Next, DTT and IAA were removed by 4 cycles of 450 µL 25 mM $(NH_4)HCO_3$ addition followed by centrifugation at 14,000 x *g* for 20 min (except for the last centrifugation, that took 2 min). Proteins were digested overnight at 37 °C and 100 rpm with trypsin (1:25 w/w). Peptides were eluted into a clean microtube after centrifugation at 14,000 x *g* and 20 °C for 25 min, followed by two cycles of 150 µL 5 mM $(NH_4)HCO_3$ addition and centrifugation at 14,000 x *g* for 20 min [63], [64]. Finally, the samples were lyophilized at 25 °C, and stored at –80 °C until injection into the mass spectrometer. Before injection, each sample was resuspended in 100 µL of 0.1% formic acid.

2.8. LC-MS/MS measurements

The peptides were analyzed using a Nano EASY-nLC 1200 coupled to an Orbitrap Fusion Lumos mass spectrometer (Thermo Fisher Scientific, Bremen, Germany). To begin the analysis, each sample was injected into a trap column (nano Viper C18, 3 µm, 75 µm × 2 cm, Thermo Scientific) with 12 µL of solvent A (0.1% formic acid in water) at a pressure of 500 bar. The peptides were then eluted onto a C18 column (nano Viper C18, 2 µm, 75 µm × 15 cm, Thermo Scientific) at a flow rate of 300 nL/min. A linear gradient of solvent A (0.1% formic acid in water) and solvent B (0.1%

formic acid in 20:80 water: acetonitrile, v/v) was used to elute the peptides from the column. The gradient began with 5% solvent B and increased to 28% over 80 minutes, followed by an increase to 40% B for 10 minutes. The column was then washed by increasing the solvent B percentage to 95% in 2 minutes, and maintaining this percentage for 12 minutes. To prepare for the next injection, the system was re-equilibrated with 100% solvent A.

After elution, the peptides were ionized under positive electrospray conditions and subjected to data-dependent acquisition mode for analysis. The most intense ions were selected for fragmentation by the quadrupole after a full scan (400-1600 *m/z*) with a resolution of 120,000. A quadrupole transmission window of 1.2 *m/z* was used to filter the ions, which were then subjected to HCD fragmentation with a normalized collision energy of 30. The fragments were detected by the orbitrap mass analyzer with a resolution of 30,000. The analysis process involved the use of a new cycle of MS followed by MS2 events at every 3 seconds. To minimize interference, monocharged ions or ions with undetermined charges were excluded from fragmentation.

2.9. Data analysis and study design

The raw files of all proteomic experiments were processed using MaxQuant software [65], with proteins identified through the Andromeda algorithm [66] against the Homo sapiens Uniprot database (downloaded March, 2022; 20,401 entries). The precursor and fragment error mass tolerances were set at 4.5 ppm and 20 ppm, respectively, with cysteine carbamidomethylation as the fixed modification. Variable modifications, including methionine oxidation, and *N*-terminal acetylation, were also set. The identification process was conducted with a semi-tryptic digestion mode, allowing a maximum of 2 missed cleavages, and a maximum FDR of 1% was permitted for both peptides and proteins identification. For proteins, the false discovery rate

(FDR) was calculated using a decoy database. Protein abundance was calculated using the LFQ algorithm [67] present in MaxQuant software. For a protein to be considered present, at least two peptides, one of which was unique, needed to be detected. The match between runs option was enabled, and all other parameters were maintained at their default settings.

The proteomic analysis was conducted using neutrophils from three different donors. Altogether, we used eight replicates per treatment (control (DMSO), fMLP, PMA, and ionomycin), and all of them were run into MaxQuant software simultaneously. We used Perseus software (version 1.6.15.0) [68] to analyze the protein data, and the resulting figures were generated using either GraphPad Prism (version 6.01), Perseus or R (version 4.0.0). To investigate enriched pathways, we employed the WebGestalt platform (http://www.webgestalt.org/) with over-representation analysis and default settings, while controlling for a false discovery rate (FDR) of less than 0.05 [12]. Subsequently, we conducted an in-depth analysis of the biological processes identified by WebGestalt with an FDR<0.05 using the STRING and UniProt platforms (https://string-db.org/ and https://www.uniprot.org/id-mapping). Pathway enrichment analyzes were performed combining the enriched and unique proteins. The enriched biological processes were summarized using the weighted-set cover method.

Prior to statistical analysis, label-free quantification (LFQ) intensities were preprocessed in Perseus software. Reverse peptides and potential contaminants were removed via filtering, and the data were log2-transformed. Missing values were filtered using the criteria of at least 7 valid values in each group. A protein was considered unique (exclusive) to a group if it had at least 3 out of 8 valid values in that group and 0, 1, or 2 valid values in the other groups.

Preparation of data for principal component analysis (PCA) and hierarchical clustering was also conducted using Perseus software. Before PCA, the remaining missing values after filtration were imputed with values from the normal distribution (width: 0.3 and down shift 1.8). PCA calculations and graphics were performed on R (version 4.0.0). Hierarchical clustering was performed without imputation, and after z-score transformation of statistically significant data ($P < 0.05$, after controlling for multiple comparisons, FDR based permutation <0.05). The Euclidean distance was used, and the average linkage method was employed to construct the rows and columns tree.

Protein symbols were derived from gene symbols as per the recommendations of the Human Genome Organization Gene Nomenclature Committee [69], and were written in all capital letters and not italicized.

2.10. Statistical analysis

For live imaging microscopy experiments, after quantifying NETs, a 2-way analysis of variance (ANOVA) was conducted, followed by a Bonferroni *post hoc* test to compare each group against the control at the different time points using GraphPad Prism software.

To compare significantly secreted proteins according to neutrophil's distinct treatments, ANOVA was performed with P-value adjustment based on a permutation-based FDR of 0.05 using Perseus software.

2.11. Data statement

As part of our commitment to transparent and reproducible research, the corresponding author can provide the data that support the findings of this study upon reasonable request.

3. Results

3.1. NADPH oxidase activation is stimulus-dependent

Neutrophils challenged with 0.005% (v/v) DMSO (control), 1 μM fMLP, 6.7 μM ionomycin or 20 nM PMA were first compared regarding their ability to generate extracellular superoxide. The production of extracellular superoxide was assed using the cytochrome c reduction assay. Thus, neutrophils treated with fMLP exhibited a superoxide release rate of 0.9 ± 0.2 μM/min, which was slightly higher than the control and ionomycin rates of 0.2 ± 0.1 μM/min (Figure 1). In contrast, neutrophils treated with PMA released superoxide at a much higher rate of 4.9 ± 1.3 μM/min. Consistent with previous reports [20], [70], our findings show PMA is a strong activator of NADPH oxidase. Additionally, fMLP was also able to activate NADPH oxidase, albeit with a weaker response, and in the conditions of our experiment, ionomycin treatment did not induce NADPH oxidase activation.

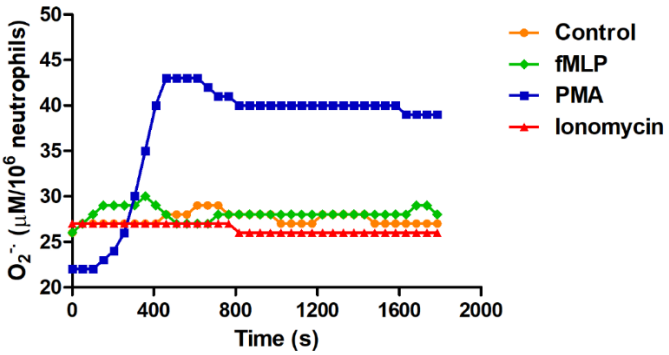

Figure 1. Neutrophil's superoxide production is stimulus-dependent. Neutrophils were treated with 0.005 % (v/v) DMSO, 1 μM fMLP, 20 nM PMA or 6.7 μM ionomycin and the superoxide production was measured through the reduction of 40 μM cytochrome C at 37 °C in the presence of 5 nM Taurine. Superoxide concentration was calculated by dividing the absorbance at 550 nm by the molar absorptivity of 21,000 M^{-1} . cm^{-1}, and considering the path length of 1 cm. Absorbance measurements were taken at intervals of 51 s.

3.2. Kinetics of NETs release depend on neutrophil stimulus

Given the striking differences regarding NADPH oxidase activation and superoxide production upon different stimuli, we next sought to study the ability of each stimulus to induce NETs release. With that in mind, neutrophils treated with 0.005% (v/v) DMSO, 1 μM fMLP, 6.7 μM ionomycin or 20 nM PMA in the presence of Hoechst 33342 and SYTOX Green were monitored with live-imaging microscopy for 120 min (Figure 2A). This experimental design allowed us to observe the release of NETs, as indicated by the uptake of the impermeant SYTOX Green dye, while also visualizing the morphology of the cells using the permeant Hoechst 33342 dye. Thus, our results demonstrate that both PMA and ionomycin are capable of inducing NETosis, albeit with different kinetics (Figure 2A, B). Notably, neutrophils treated with ionomycin began to display NETs at 60 min (Figure 2B), and by 90 min (Figure 2A), all ionomycin-treated cells exhibited either a decondensed nucleus (loss of the polymorphic shape) or the presence of NETs. In contrast, after 90 minutes of treatment with PMA, only a few neutrophils exhibited NETs, while many still displayed the characteristic polymorphic nucleus (Figure 2A). Only at 120-min a statistically significant increase in NETs was observed in PMA-treated neutrophils compared to the control group (Figure 2B). Only a few neutrophils released NETs after 120 min incubation with fMLP, and this small number of NETs formed was not statistically different from the control group. These findings demonstrate that PMA and ionomycin are potent inducers of NETosis, with ionomycin-treated neutrophils exhibiting a faster release of NETs.

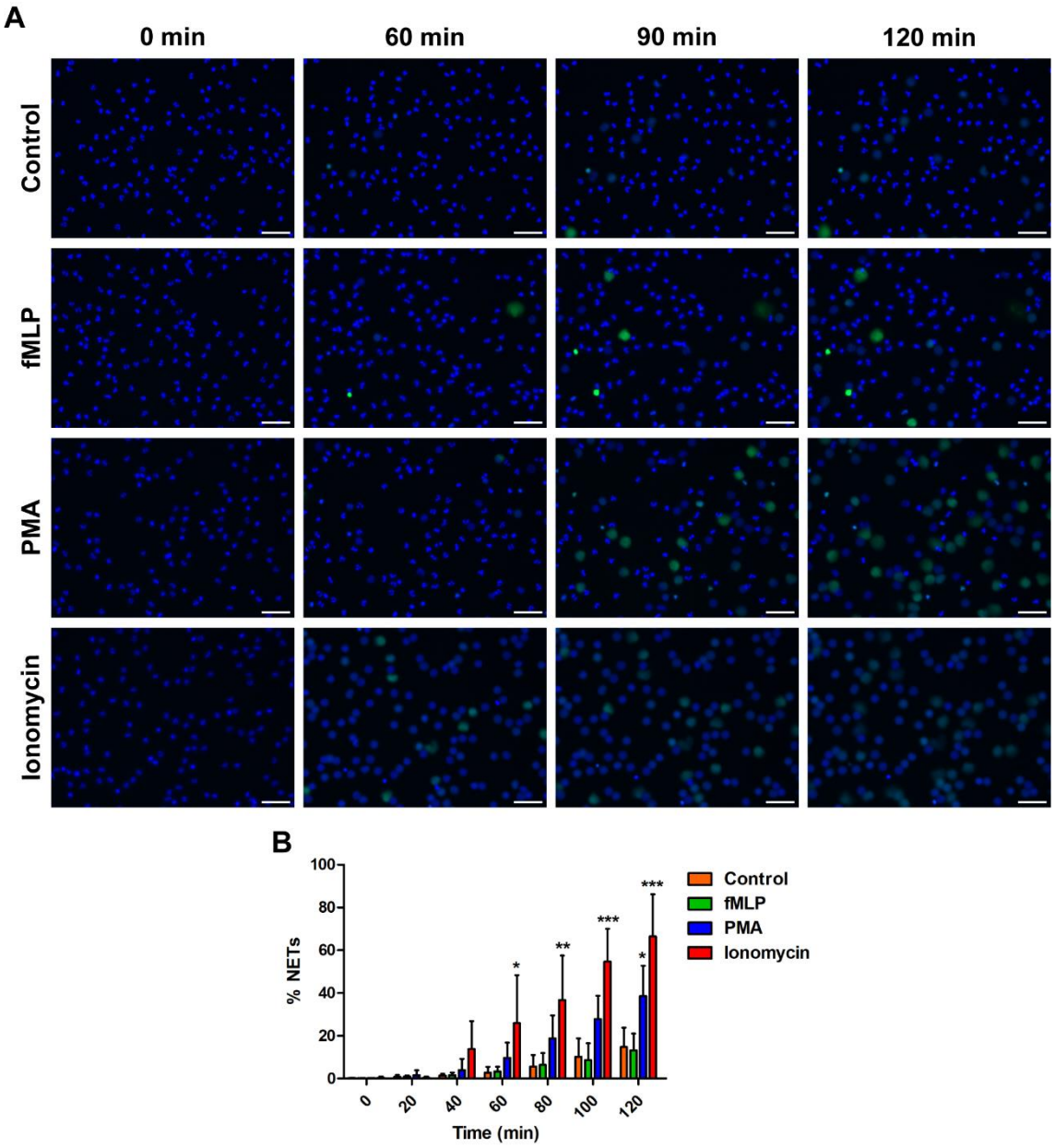

Figure 2. The ability to generate NETs and the kinetics of their release are stimulus-dependent. Neutrophils were treated with 0.005 % v/v DMSO, 1 μM fMLP, 20 nM PMA or 6.7 μM ionomycin, stained with 2 μM Hoechst 33342 (blue, cell permeant dye) and 500 nM Sytox Green (green, cell impermeant dye), and monitored for 120 min at 37 °C and 5 % CO_2 in the microscope. Images are representative of three independent experiments with neutrophils isolated from different volunteers. A) Microscope images of untreated and treated neutrophils at different time-points. Scale bars represent 50 μm. B) The percentage of neutrophils that released NETs, defined as Hoechst 33342 and SYTOX Green (+) cells was calculated over time with respect to all neutrophils (all cells > 26 μm^2 that were either Hoechst 33342 (+) only, or Hoechst 33342 + SYTOX Green (+)).

3.3. The neutrophil´s response after activation is stimulus-dependent

The results obtained so far pointed to a dissimilar response of neutrophils to distinct stimuli, summarized by the early NADPH oxidase activation and late NETs release upon PMA stimulation, contrasting with the lack of superoxide anion generation, and fast NETs release upon ionomycin treatment, and with the inability of fMLP to induce NETosis. The heterogeneous response obtained upon distinct stimuli lead us to hypothesize that the communication with the environment and neutrophil´s response might also be distinct. To test this hypothesis, we used a proteomic approach to investigate the proteins secreted by neutrophils treated with 0.005% (v/v) DMSO, 1 μM fMLP, 6.7 μM ionomycin or 20 nM PMA for 30 and 90 min.

Initially, a dimensionality reduction analysis revealed two main clusters in our dataset, the first was composed of the neutrophils stimulated for 30 and 90 minutes with either PMA and fMLP, and the second main cluster was composed of samples obtained after treatment with ionomycin for 30 and 90 minutes, together with controls for both time points (Figure 3A). Notably, fMLP and PMA groups are in closer proximity in the PCA than control and ionomycin-treated groups. The first two components explained approximately 62 % of the variance of the whole dataset. This first exploratory analysis already revealed that communication with environment is an early event upon cells activation (regardless the stimulus), since 30 and 90 min- time points are in relatively close proximity in the principal component analysis.

The unsupervised hierarchical clustering of the significantly different proteins ($P < 0.05$ after ANOVA adjusted for multiple comparisons, FDR<0.05) (Figure 3B) revealed the separation of samples into two major treatment clusters (columns). Thus, the first cluster is composed of the secretome of neutrophils treated with PMA and fMLP (either for 30 or 90 min), and the second cluster comprises the ionomycin-

stimulated neutrophil's secretome plus the control group. This result corroborates the outcome of the PCA, but provide a more detailed analysis, revealing a further separation between the secretome of ionomycin-treated and control groups. The protein abundances across treatments (rows) were partitioned into five clusters, comprising proteins enriched in the control and ionomycin groups (cluster 1), those enriched only in the control group (cluster 2), those enriched in the ionomycin group (cluster 3), those enriched in both, fMLP and PMA groups (cluster 4), and those enriched in the ionomycin, fMLP, and PMA groups (cluster 5). We also categorized the number of unique and shared proteins among treatments using a Venn diagram (Figure 3C), which revealed that the majority of the secreted proteins are shared among them.

Aiming to understand the biological processes and the cellular communication present upon activation of neutrophils with distinct stimuli, pathway enrichment analyses were conducted combining the proteins obtained from each cluster in Figure 3B and Supplemental Table 1A with the unique proteins identified in the Venn diagram (Figure 3C and Supplemental Table 1A). For example, proteins from cluster 1 in Figure 3B (proteins enriched in ionomycin and control treatments) were combined with proteins exclusively found in control and ionomycin samples (n=60, figure 3C) and a pathway enrichment analysis was performed. The results show that ionomycin-stimulated neutrophils and controls commonly secrete proteins linked to immune response, cellular structure organization, regulation of peptidase activity, and metabolism. Specifically, the immune response associated with this cluster was characterized by the involvement in the interleukin-12 mediated signaling pathway, regulated exocytosis, neutrophil degranulation, and migration (Figure 3D and Supplemental Table 1B).

Data from cluster 2 (Figure 3B, Supplemental Table 1A), representing proteins secreted in higher abundance by the control group, were combined with proteins exclusively secreted by the control cells (n=86, Figure 3C, Supplemental Table 1A). The proteins in this cluster (Figure 3E and Supplemental Table 1C) are involved in biological processes related to protein regulation and modification, phagocytosis, neutrophil degranulation, cytoskeleton and membrane organization, cellular metabolism, response to stimuli, and Ras protein signal transduction. Much like the enrichment analysis found for the proteins secreted by neutrophils treated with ionomycin and controls described above, control neutrophils secrete proteins related to the immune response committed to interleukin-12 mediated signaling pathway (Supplemental Table 1C).

The proteins described in “response to IL-12” also participate in other biological processes, including positive regulation of podosome assembly, regulation of protein kinase activity, T cell activation, and apoptotic process. These proteins were observed in cluster 1 (control and ionomycin-treated neutrophils, Supplemental Table 1B). Additionally, in cluster 2 (control neutrophils, Supplemental Table 1C) the “response to IL-12” englobes proteins involved in actin cytoskeleton organization, nuclear migration, and positive regulation of endopeptidase activity. Notably, in neutrophils treated with IL-12 an increase in Ca^{2+} intracellular concentration from intra- and extracellular stores, accompanied with increase actin polymerization and tyrosine phosphorylation was observed [71]. Therefore, it can be suggested that there was an overlap between the biological processes “response to interleukin-12” and calcium-mediated signaling pathways [47], [72], [73].

The joint analysis of proteins from cluster 3 (Figure 3B and Supplemental Table 1A), and proteins secreted only by ionomycin-activated neutrophils (n= 60, Figure 3C

and Supplemental Table 1A), shows that ionomycin treatment led to secreted proteins related to immune response, vesicle transport, and carbohydrate catabolism (Figure 3F and Supplemental Table 1D). The secreted proteins associated with the biological processes "non-recombinational repair", "viral life cycle", and "regulation of body fluid levels" (Figure 3F) are also involved in stress response, vesicle-mediated transport, and regulation of DNA repair. Within this cluster, the immune response was characterized by regulated exocytosis and neutrophil degranulation (Supplemental Table 1D).

The secretome of neutrophils treated with PMA and fMLP was highly similar, with 77% of their secreted proteins being shared between the two treatments (Supplemental Figure 1). This similarity was further supported by the clustering of their enriched proteins (cluster 4, Figure 3B), indicating that there were no significant differences in protein abundance between them. The enrichment analysis obtained by combining proteins of cluster 4 (Figure 3B and Supplemental Table 1A) with common proteins secreted by PMA and fMLP-treated neutrophils (n=11, Figure 3C and Supplemental Table 1A) showed “interaction with symbiont”, “granulocyte activation” and “phagocytosis” as the most enriched biological process in response to PMA and fMLP stimuli (Figure 3G). The biological processes within this cluster englobe proteins related to immune response, regulation of vesicle-mediated transport, and leukocyte differentiation. Specifically, the immune response in this group concerns the proteins involved in phagocytosis, positive regulation of prostaglandin-E synthesis, positive regulation of signaling from Fc-gamma and Toll-like 4 receptors, positive regulation of superoxide anion generation, and neutrophil degranulation (Supplemental Table 1E).

Finally, the enrichment analysis of proteins commonly found for PMA, fMLP, and ionomycin treatments (cluster 5, Figure 3B and Supplemental Table 1A) together with

proteins found exclusively in these treatments but not in control, (n=3, Figure 3C and Supplemental Table 1A) showed biological processes associated with neutrophil-mediated immunity, particularly in relation to neutrophil degranulation (Figure 3H and supplemental Table 1F).

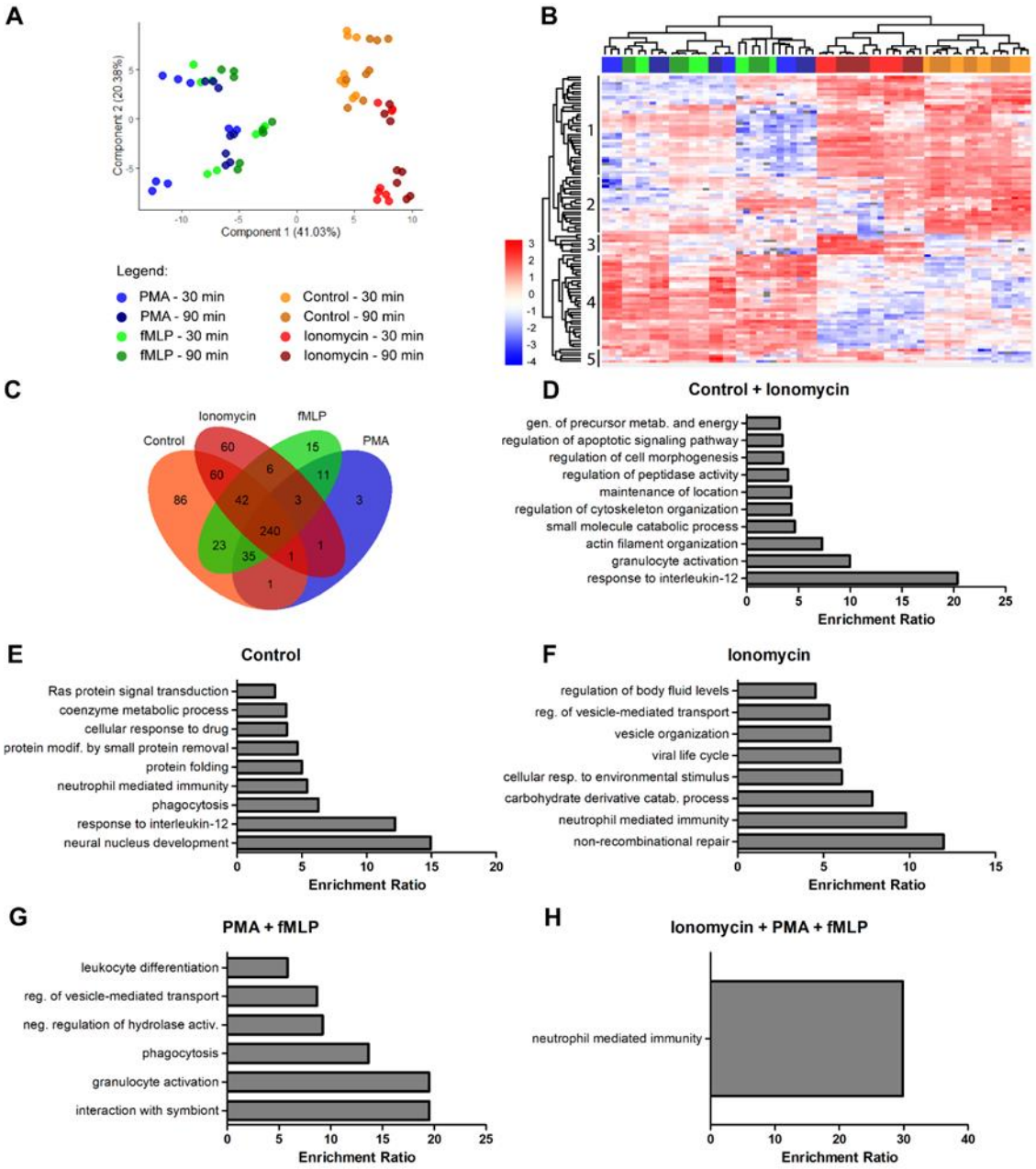

Figure 3. Neutrophils treated with fMLP, PMA, or ionomycin secreted proteins involved in cell homeostasis, and immune response. The secretome of neutrophils treated with 0.005 % v/v DMSO, 1 µM fMLP, 20 nM PMA or 6.7 µM ionomycin for 30 and 90 min at 37 °C was collected and analyzed by mass spectrometry. A) Principal component analysis (PCA) of the secretome of neutrophills exposed to different stimuli by 30 and 90 minutes. B) Hierarchical clustering of significantly altered proteins (ANOVA correcting for multiple comparisons using FDR<0.05). C) Venn diagram of

proteins identified in each group. Pathway enrichment analysis of the unique and enriched proteins found in the D) control and ionomycin groups, E) control group, F) ionomycin group, G) PMA and ionomycin groups, and H) ionomycin, PMA, and fMLP groups. For each enriched biological process (y-axis), the enrichment ratio (the number of observed genes over the expected value, x-axis) was calculated. Only biological processes with FDR < 0.05 were displayed. Secretome proteins were acquired from neutrophils in three independent experiments.

In summary, proteins associated with the neutrophil degranulation process were found in all clusters. Neutrophils that underwent treatment demonstrated varied immune responses, despite their shared process of vesicle-mediated transport. Specifically, upon exposure to PMA and fMLP, neutrophils exhibited upregulation of Fc-receptor and Toll-like receptor 4, whereas upon exposure to ionomycin or in the absence of stimulation, neutrophils secreted more proteins involved in regulation of cytoskeleton organization, modification and processing of proteins, and cellular metabolism. Moreover, the ionomycin-treated group had additional proteins involved in DNA repair and stress response. Importantly, only the treatment groups showed enrichment for neutrophil bactericidal proteins, including MPO, ELANE, PRTN3, and LTF (Supplemental Table 1A). Finally, as corroborated by Figure 1A, the PMA- and fMLP-treated group demonstrated positive regulation of superoxide anion generation.

3.4. Ionomycin- and PMA- treated neutrophils exhibited a different pattern of degranulation

Our global analysis of the secretome of stimulated neutrophils showed that their released proteins vary according to the stimulus, regardless the time that has passed (although we were careful to choose time points before the majority of neutrophils underwent cell rupture and could release NETs). Intriguingly, our results also showed ionomycin-stimulated cells release NETs much faster than PMA-activated neutrophils. The majority of ionomycin-treated neutrophils had already released NETs by 90 min, while PMA-treated cells were mostly polymorphic (Fig 2A and B). Therefore, we

investigated if PMA-activated neutrophils are slower in the process of NETosis, but are still releasing the same mediators as ionomycin-treated neutrophils, or if the entire process is different. To gain insights into this question, we performed a subgroup analysis comparing the secretome of ionomycin-activated neutrophils after 30 minutes with that obtained after 90 minutes of PMA activation, i.e., time-points before NETs release by these stimuli. Five hundred and twenty secreted proteins were identified in these two groups (Figure 4A and Supplemental Table 2A). From this total, 313 proteins (60.2%) were common between the groups, 129 proteins (24.8%) were exclusive to the ionomycin group, and 78 proteins (15%) were exclusive to the PMA group. We then tested if the abundance of the common proteins secreted after 30 minutes of ionomycin treatment was the same when comparing with proteins secreted after 90 minutes of PMA stimulus (Figure 4B and Supplemental Table 2B). All proteins with a fold-change greater than 2 ($Log_2 > 1$) and significantly altered ($P < 0.05$) after a multiple comparison adjusted t-test, were color-coded either red (ionomycin group) or blue (PMA group). Following a 90-minute treatment with PMA, neutrophils' secretome exhibited significant enrichment in proteins that play a crucial role in neutrophil adhesion and migration, including ITGAM (Integrin alpha-M, 15-fold increase), ITGB2 (Integrin beta-2, 15-fold increase), PTPRJ (Receptor-type tyrosine-protein phosphatase eta, 4-fold increase), LRG1 (Leucine-rich alpha-2-glycoprotein, 4.7-fold increase), and CD177 (CD177 antigen, 3-fold increase) (Figure 4B and Supplemental Tables 2B). Notably, ITGAM, ITGB2, and CD177 also positively regulate superoxide generation by NADPH oxidase [5, 6]. The PMA-treated cells' secretome also showed an increase in MMP8 (Neutrophil collagenase, 2.5-fold increase) and MMP9 (Matrix metalloproteinase-9, 2.5-fold increase), extracellular matrix proteases that degrade collagenase and gelatinase [76], facilitating neutrophil extravasation (Figure 4B and Supplemental Tables 2B).

Conversely, ionomycin-treated neutrophils exhibited a 39-fold enrichment in BPI (Bactericidal permeability-increasing protein), and a 5.5- fold enrichment in MPO (Myeloperoxidase), proteins present in the neutrophil's azurophilic granule and with a microbicidal activity (Figure 4B and Supplemental Tables 2B). LYZ (Lysozyme), another granular bacteriolytic protein showed a 6.7-fold increase in the secretome of ionomycin-stimulated neutrophils. They also show an 8-fold increase in the calprotectin subunits S1008 (Protein S100-A8) and S1009 (Protein S100-A9), that extracellularly also have antimicrobial activity (Figure 4B and Supplemental Tables 2B).

To gain a better understanding of the cellular function of the proteins being secreted by each group, we combined the enriched (Figure 4B and Supplemental Table 2B) and unique proteins (Figure 4A and Supplemental Table 2A) of each group and performed a cellular component analysis (Figure 4C, 4D, and Supplemental Tables 2C and 2D). The results show the secretome of neutrophils after 30 min exposure to ionomycin is enriched with proteins from the azurophil, secretory, and ficolin-1-rich granules, as well as proteins from the actin cytoskeleton, extracellular exosome, cell projections, and focal adhesion (Figure 4C and Supplemental Table 2C). In contrast, after 90 min, the secretome of PMA-treated neutrophils is enriched with proteins from the proteasome complex, secretory, ficolin-1-rich, tertiary, and specific granules, as well as proteins from the endoplasmic reticulum-Golgi intermediate compartment, cell surface, receptor complex and focal adhesion (Figure 4D and Supplemental Table 2D).

In summary, both treatment groups secrete proteins derived from the secretory and ficolin-1-rich granules, as well as proteins from the cell surface and focal adhesion. However, ionomycin-treated neutrophils released more proteins from the azurophil granule and actin cytoskeleton in their secretome, while the secretome of PMA-treated neutrophils was enriched with proteins from the proteasome complex, specific and

tertiary granules, and endoplasmic reticulum-Golgi intermediate compartment. Thus, ionomycin-treated neutrophils released a higher level of antibacterial proteins, while PMA-treated neutrophils released proteins associated with cell adhesion and superoxide production. The observed differences in degranulation between the treatment groups is another evidence that NETosis triggered by PMA or ionomycin are distinct.

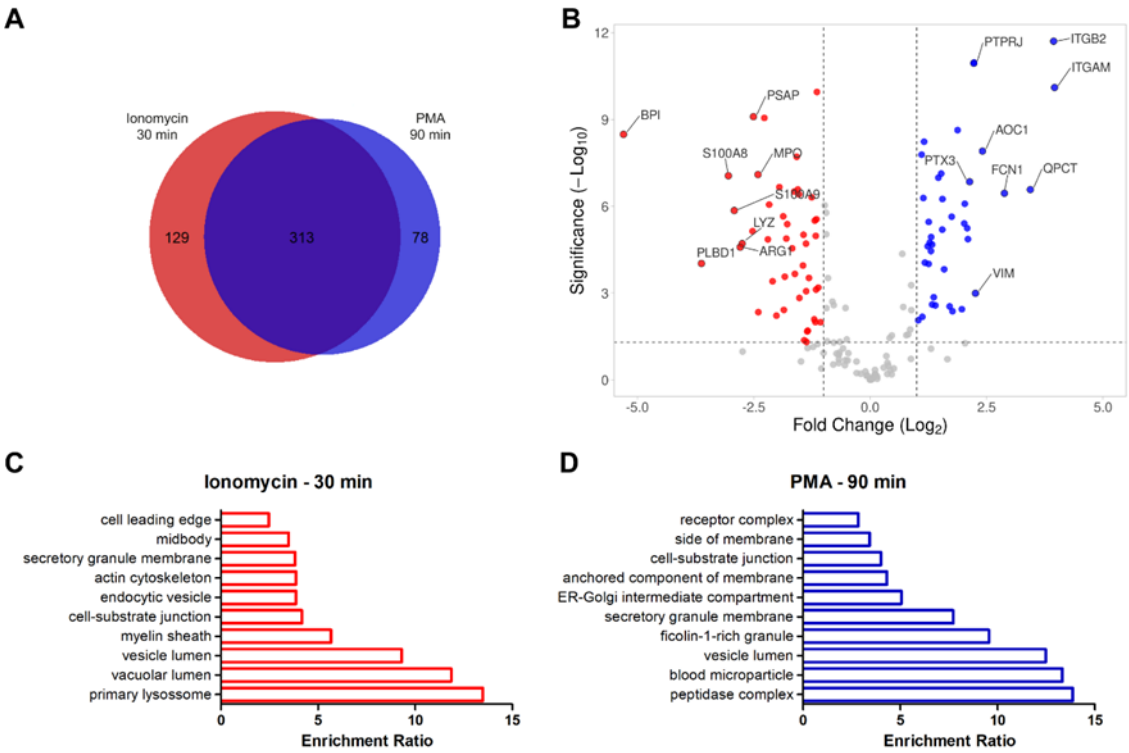

Figure 4. Different patterns of degranulation are seen in ionomycin- and PMA-treated neutrophils. The secretome of human neutrophils treated with 6.7 µM ionomycin for 30 min or 20 nM PMA for 90 min at 37 °C was analyzed by mass spectrometry. A) Venn diagram of proteins comonly or exclusively identified in the secretome of neutrophils treated with ionomycin for 30 min or PMA for 90 minutes. B) Differentially regulated proteins obtained comparing ionomycin- and PMA-treated neutrophils at 30 and 90 min, respectively. The log2 fold change between the ionomycin and PMA treatment groups is plotted against the -log10 of the P-value obtained from the t-test, which was followed by multiple comparisons adjustment. Proteins more abundant in the secretome of ionomycin-treated neutrophils are displayed to the left of the value -1 in the x-axis (dashed line), while proteins more abundant in the PMA group are displayed to the right of the 1 value. Cellular component analysis of the unique and enriched proteins found in the secretome of ionomycin C) or D) PMA stimulated neturophils. For each enriched (y-axis), the enrichment ratio (the number of observed genes over the expected value, x-axis) was

calculated. Only cellular components with FDR < 0.05 were displayed. Secretome proteins were acquired from neutrophils in three independent experiments.

4. Discussion

Upon activation, neutrophils can release their arsenal of cytotoxic proteins stored in their granules either within the phagosome compartment, externally or in association with NETs [1, 2]. Although they are also released in sterile conditions [78], [79] NETs have been shown to be highly effective against a broad range of pathogens [6], [9], [10]. In both scenarios, their excessive release may pose a risk to the host due to their cytotoxic content, which mainly originates from the neutrophil granules [80]. Previous studies have explored the protein content of NETs, but they were performed in later time-points, i.e., after neutrophil's membrane rupture [55]–[57]. Therefore, our goal was to elucidate the secretome from NADPH oxidase-dependent and -independent NETosis, prior to the terminal process of NETs release. Using live-imaging microscopy and mass spectrometry we were able to determine the kinetics of the NETotic process, as well as to unravel the cytotoxic proteins that were secreted in response to each specific stimulus.

Our results showed that although neutrophils stimulated with ionomycin and PMA will commonly end up releasing NETs, the processes that precede this final event were quite diverse, since (1) PMA- and fMLP-treated neutrophils were able to activate the NADPH oxidase, in contrast to ionomycin-stimulated neutrophils; (2) neutrophils treated with ionomycin- quickly release NETs (around 60 min), while it takes twice longer for PMA-stimulated cells to get to this final event; (3) the cell communication with the environment before NETs release, was distinct; (5) neutrophils response to the stress was also dissimilar; cells treated with ionomycin released higher levels of

cytotoxic proteins whereas PMA-treated neutrophils released more proteins associated with cell adhesion, migration and superoxide generation.

Consistent with earlier reports, treatment of neutrophils with PMA resulted in generation of superoxide by NADPH oxidase, and the release of NETs after 120 min [18], [20], [27]. A similar response was described in neutrophils treated with a variety of pathogens, including *P. aeruginosa*, *S.aureus*, and *E.coli* [13], [20]. The requirement of NADPH oxidase activation for PMA-triggered NETosis was confirmed using neutrophils from individuals with chronic granulomatous disease (CGD), who cannot produce superoxide by NADPH oxidase, and from neutrophils treated with the flavoprotein inhibitor diphenyleneiodonium (DPI) before exposure to PMA. In both scenarios, PMA-induced NETs are diminished [13], [20]. In contrast, neutrophils treated with ionomycin were not able to activate the NADPH oxidase, but they still released. The independence of NADPH oxidase activation for NETosis has already been described for calcium ionophores such as ionomycin and A23187 [18], [19], [81], and a similar response was observed in neutrophils treated with the potassium ionophore nigericin [19], as well as, treated with C. albicans [82], soluble immune complexes [83], S. aureus, or monosodium urate crystals [28].

As previously reported [22] and discussed above, the treatment of neutrophils with either PMA or fMLP resulted in the activation of the NADPH oxidase pathway. In addition, before the onset of NETs release, these treatments triggered a similar pattern of neutrophil degranulation, as evidenced by the clustering of common proteins (Figures 1, 3A and B). Interestingly, the proteomic analysis revealed that both stimuli upregulate the secretion of proteins involved in pathogen recognition and elimination, including those related to superoxide anion generation, signaling from Fc- and Toll-like 4 receptors, prostaglandin-E synthesis, and the secretion of integrins Mac-1

(ITGAM/ITGB2) (Figure 3F and Supplemental Table 1A). However, it is worth to point out that in comparison with PMA, neutrophils treated with fMLP displayed a weaker NADPH oxidase response [3] and, in the condition of our study, did not released NETs. The ability of fMLP-treated neutrophils to release NETs is still a topic of debate. Thus, using the same concentration of fMLP that we used in our study (1 μM) Pruchniak and Demkow (2019) [32], and Rodríguez-Espinosa *et al.* (2015) [84], reported the release of NETs, while Yuen *et al.* (2016) [33], did not. Vorobjeva *et al.* (2017, 2020)[84, 85], have argued that NADPH oxidase activation by fMLP stimulus is dependent on mitochondrial reactive oxygen species (mtROS), which in turn requires the opening of the mitochondrial permeability transition pore (mPTP). Nevertheless, further discussion on the distinction of PMA and fMLP activation is still absent. In our study, we employed live-imaging microscopy and automatic quantification of NETs-positive cells up to 120 minutes to demonstrate the absence of NETs after fMLP treatment. In agreement, NETs were not observed in fixed cell imaging experiments until 240 min (data not shown).

Control and ionomycin-treated neutrophils commonly secreted proteins related to cytoskeleton organization, protein processing and modification, as well proteins involved in cellular metabolism. However, ionomycin-treated neutrophils also secrete proteins related to stress response, DNA-repair and cytotoxic proteins such MPO, PRTN3, ELANE and OLFM4 (Supplemental Tables 1D and 1F). Previous reports have shown that neutrophils treated with calcium ionophores can raise their intracellular calcium levels above 1 μM [34], leading to the release of all neutrophil granules [87], [88]. Importantly, in our work we have confirmed and extended these observations, since quantification of the secreted granular proteins showed after 30 minutes of ionomycin treatment, neutrophils released more proteins from azurophilic granules

than neutrophils stimulated with PMA for a much longer period of time (90 minutes, Figures 4B, 4C, and Supplemental Table 2C). Meanwhile, after 90 minutes, neutrophils treated with PMA released considerably more proteins from tertiary and specific granules (Figure 4B, 4D, and Supplemental Table 2D). Thus, our study showed the secretome of ionomycin-treated neutrophils had a greater cytotoxic potential seen by the enrichment of proteins from the azurophilic granules as well as other microbicidal proteins such as LYZ, S100A8 and S100A9. In contrast, the secretome of PMA-treated neutrophils showed enrichment of proteins involved in neutrophil adhesion and migration, as well as proteins involved in regulating superoxide generation by NADPH oxidase. Interestingly, regardless of the stimulus, there are a set of secreted proteins which their abundances did not change over time.

In summary, our work has shown that although both PMA and ionomycin treatments result in the release of NETs, the events preceding the final event are quite distinct. Thus, we have shown NETs release upon ionomycin stimulation is a fast process, preceded by release of cytotoxic proteins to the media. In contrast, PMA-activated neutrophils take longer to release NETs, and before the conclusion of the process, the cells are more concerned to release to the environment proteins related to cell adhesion and migration. Our study highlights that the resolution of infection by neutrophils begins prior to the release of NETs, and this process varies depending on the stimulus.

5. References

[1] C. Yin and B. Heit, “Armed for destruction: formation, function and trafficking of neutrophil granules,” *Cell Tissue Res.*, vol. 371, no. 3, pp. 455–471, 2018, doi: 10.1007/s00441-017-2731-8.

[2] N. Borregaard, O. E. Sørensen, and K. Theilgaard-Mönch, “Neutrophil granules: a library of innate immunity proteins,” *Trends Immunol.*, vol. 28, no. 8, pp. 340–345, 2007, doi: 10.1016/j.it.2007.06.002.

[3] C. C. Winterbourn, A. J. Kettle, and M. B. Hampton, “Reactive Oxygen Species and Neutrophil Function,” *Annu. Rev. Biochem.*, vol. 85, pp. 765–792, 2016, doi: 10.1146/annurev-biochem-060815-014442.

[4] N. Borregaard and J. B. Cowland, “Granules of the human neutrophilic polymorphonuclear leukocyte.,” *Blood*, vol. 89, no. 10, pp. 3503–3521, 1997, doi: 10.1182/blood.V89.10.3503.

[5] W. M. Nauseef, “How human neutrophils kill and degrade microbes: An integrated view,” *Immunol. Rev.*, vol. 219, no. 1, pp. 88–102, 2007, doi: 10.1111/j.1600-065X.2007.00550.x.

[6] V. Brinkmann, “Neutrophil Extracellular Traps Kill Bacteria,” *Science (80-.).*, vol. 303, no. 5663, pp. 1532–1535, 2004, doi: 10.1126/science.1092385.

[7] V. Brinkmann and A. Zychlinsky, “Neutrophil extracellular traps: Is immunity the second function of chromatin?,” *J. Cell Biol.*, vol. 198, no. 5, pp. 773–783, 2012, doi: 10.1083/jcb.201203170.

[8] N. Branzk *et al.*, “Neutrophils sense microbe size and selectively release neutrophil extracellular traps in response to large pathogens,” *Nat. Immunol.*, vol. 15, no. 11, pp. 1017–1025, 2014, doi: 10.1038/ni.2987.

[9] C. F. Urban, U. Reichard, V. Brinkmann, and A. Zychlinsky, “Neutrophil extracellular traps capture and kill Candida albicans and hyphal forms,” *Cell. Microbiol.*, vol. 8, no. 4, pp. 668–676, 2006, doi: 10.1111/j.1462-5822.2005.00659.x.

[10] T. Saitoh *et al.*, “Neutrophil extracellular traps mediate a host defense response to human immunodeficiency virus-1.,” *Cell Host Microbe*, vol. 12, no. 1, pp. 109–116, 2012, doi: 10.1016/j.chom.2012.05.015.

[11] G. A. Funchal *et al.*, “Respiratory syncytial virus fusion protein promotes TLR-4-dependent neutrophil extracellular trap formation by human neutrophils,” *PLoS One*, vol. 10, no. 4, pp. 1–14, 2015, doi: 10.1371/journal.pone.0124082.

[12] W. H. Chou *et al.*, “Neutrophil protein kinase Cδ as a mediator of stroke-reperfusion injury,” *Journal of Clinical Investigation*, vol. 114, no. 1. pp. 49–56, 2004. doi: 10.1172/JCI200421655.

[13] T. A. Fuchs *et al.*, “Novel cell death program leads to neutrophil extracellular traps,” *J. Cell Biol.*, vol. 176, no. 2, pp. 231–241, 2007, doi: 10.1083/jcb.200606027.

[14] B. G. Yipp, P. Kubes, W. Dc, B. G. Yipp, and P. Kubes, “NETosis: how vital is it?,” *Blood*, vol. 122, no. 16, pp. 2784–2794, 2013, doi: 10.1182/blood-2013-04-457671.

[15] T. Hoppenbrouwers *et al.*, “In vitro induction of NETosis: Comprehensive live imaging comparison and systematic review,” *PLoS One*, vol. 12, no. 5, pp. 1–29, 2017, doi: 10.1371/journal.pone.0176472.

[16] A. B. Guimarães-Costa, M. T. C. Nascimento, A. B. Wardini, L. H. Pinto-Da-Silva, and E. M. Saraiva, “ETosis: A microbicidal mechanism beyond cell death,” *J. Parasitol. Res.*, vol. 2012, no. 929743, pp. 1–11, 2012, doi: 10.1155/2012/929743.

[17] V. Delgado-Rizo, M. A. Martínez-Guzmán, L. Iñiguez-Gutierrez, A. García-Orozco, A. Alvarado-Navarro, and M. Fafutis-Morris, “Neutrophil extracellular traps and its implications in inflammation: An overview,” *Frontiers in Immunology*, vol. 8, no. 81. pp. 1–20, 2017. doi: 10.3389/fimmu.2017.00081.

[18] C. M. De Bont, W. J. H. Koopman, W. C. Boelens, and G. J. M. Pruijn, “Stimulus-dependent chromatin dynamics, citrullination, calcium signalling and ROS production during NET formation,” *BBA - Mol. Cell Res.*, vol. 1865, no. 11, pp. 1621–1629, 2018, doi: 10.1016/j.bbamcr.2018.08.014.

[19] E. F. Kenny *et al.*, “Diverse stimuli engage different neutrophil extracellular trap pathways,” *Elife*, vol. 6, no. e24437, pp. 1–21, 2017, doi: 10.7554/eLife.24437.

[20] H. Parker, M. Dragunow, M. B. Hampton, A. J. Kettle, and C. C. Winterbourn, “Requirements for NADPH oxidase and myeloperoxidase in neutrophil extracellular trap formation differ depending on the stimulus,” *J. Leukoc. Biol.*, vol. 92, no. 4, pp. 841–849, 2012, doi: 10.1189/jlb.1211601.

[21] N. O. Christiansen and N. Borregaard, “Translocation of Protein Kinase C to Subcellular Fractions of Human Neutrophils,” *Scand. J. Immunol.*, vol. 29, no. 1989, pp. 409–416, 1989.

[22] S. A. Belambri, R. Houssam, and R. Margarita, “NADPH oxidase activation in neutrophils: Role of the phosphorylation of its subunits,” *Eur. J. Clin. Invest.*, vol. 48, no. January, pp. 1–9, 2018, doi: 10.1111/eci.12951.

[23] M. Faurschou, O. E. Sørensen, A. H. Johnsen, J. Askaa, and N. Borregaard, “Defensin-rich granules of human neutrophils: Characterization of secretory properties,” *Biochim. Biophys. Acta - Mol. Cell Res.*, vol. 1591, no. 1–3, pp. 29–35, 2002, doi: 10.1016/S0167-4889(02)00243-4.

[24] E. Neubert *et al.*, “Chromatin swelling drives neutrophil extracellular trap release,” *Nat. Commun.*, vol. 9, no. 3767, pp. 1–13, 2018, doi: 10.1038/s41467-018-06263-5.

[25] V. Papayannopoulos, K. D. Metzler, A. Hakkim, and A. Zychlinsky, “Neutrophil elastase and myeloperoxidase regulate the formation of neutrophil extracellular traps,” *J. Cell Biol.*, vol. 191, no. 3, pp. 677–691, 2010, doi: 10.1083/jcb.201006052.

[26] K. D. Metzler, C. Goosmann, A. Lubojemska, and A. Zychlinsky, “A Myeloperoxidase-Containing Complex Regulates Neutrophil Elastase Release and Actin Dynamics during NETosis,” *CellReports*, vol. 8, no. 3, pp. 883–896, 2014, doi: 10.1016/j.celrep.2014.06.044.

[27] A. Muth *et al.*, “Diverse stimuli engage different neutrophil extracellular trap pathways,” pp. 1–21, 2017, doi: 10.7554/eLife.24437.

[28] M. van Der Linden, G. H. A. Westerlaken, M. van Der Vlist, J. van Montfrans, and L. Meyaard, “Differential Signalling and Kinetics of Neutrophil Extracellular Trap Release Revealed by Quantitative Live Imaging,” *Sci. Rep.*, vol. 7, no. 6259, pp. 1–11, 2017, doi: 10.1038/s41598-017-06901-w.

[29] G. M. Bokoch, “Chemoattractant Signaling and Leukocyte Activation,” *Blood*, vol. 86, no. 5, pp. 1649–1660, 1995, doi:

10.1182/blood.V86.5.1649.bloodjournal8651649.

[30] T. Sato, T. Hongu, M. Sakamoto, Y. Funakoshi, and Y. Kanaho, “Molecular Mechanisms of N -Formyl-Methionyl-Leucyl-Phenylalanine- Induced Superoxide Generation and Degranulation in Mouse Neutrophils : Phospholipase D Is Dispensable,” *Mol. Cell. Biol.*, vol. 33, no. 1, pp. 136–145, 2013, doi: 10.1128/MCB.00869-12.

[31] V. Videm and E. Strand, “Changes in Neutrophil Surface-Receptor Expression After Stimulation with FMLP , Endotoxin , Interleukin-8 and Activated Complement Compared to Degranulation,” *Scand. J. ofImmunology*, vol. 59, pp. 25–33, 2004, doi: 10.1111/j.0300-9475.2004.01351.x.

[32] M. P. Pruchniak and U. Demkow, “Potent NETosis inducers do not show synergistic effects in vitro,” *Cent. Eur. J. Immunol.*, vol. 44, no. 1, pp. 51–58, 2019, doi: 10.5114/ceji.2019.84017.

[33] J. Yuen *et al.*, “NETosing neutrophils activate complement both on their own NETs and bacteria via alternative and non-alternative pathways,” *Front. Immunol.*, vol. 7, no. 137, pp. 1–14, 2016, doi: 10.3389/fimmu.2016.00137.

[34] R. Gennaro, T. Pozzant, and D. Romeo, “Monitoring of cytosolic free Ca2+ in C5a-stimulated neutrophils: Loss of receptor-modulated Ca2+ stores and Ca2+ uptake in granule-free cytoplasts,” *Proc. Natl. Acad. Sci.*, vol. 81, no. March, pp. 1416–1420, 1984, doi: 10.1073/pnas.81.5.1416.

[35] E. Tarcsa, L. N. Marekov, G. Mei, G. Melino, S.-C. Lee, and P. M. Steinert, “Protein Unfolding by Peptidylarginine Deiminase,” *J. Biol. Chem.*, vol. 271, no. 48, pp. 30709–30716, 1996, doi: 10.1074/jbc.271.48.30709.

[36] Y. Wang *et al.*, “Histone hypercitrullination mediates chromatin decondensation and neutrophil extracellular trap formation,” *J. Cell Biol.*, vol. 184, no. 2, pp. 205–213, 2009, doi: 10.1083/jcb.200806072.

[37] H. R. Thiam, S. L. Wong, D. D. Wagner, and C. M. Waterman, “Cellular Mechanisms of NETosis,” *Annu. Rev. Cell Dev. Biol.*, vol. 36, pp. 191–218, 2020, doi: 10.1146/annurev-cellbio-020520-111016.

[38] R. Sutton, D. Fasshauer, R. Jahn, and A. T. Brunger, “Crystal structure of a SNARE complex involved in synaptic exocytosis at 2.4 Å resolution,” *Nature*, vol. 395, pp. 347–353, 1998, doi: 10.1038/26412.

[39] C. Hu, M. Ahmed, T. J. Melia, T. Mayer, and J. E. Rothman, “Fusion of Cells by Flipped SNAREs,” *Science (80-.).*, vol. 300, no. 2003, pp. 1745–1749, 2003, doi: 10.1126/science.1084909.

[40] N. Borregaard, L. Kjeldsen, K. Rygaard, L. Bastholm, M. H. Nielsen, and H. Sengelev, “Stimulus-dependent secretion of plasma proteins from human neutrophils . Stimulus-dependent Secretion of Plasma Proteins from Human Neutrophils,” *J. Clin. Invest.*, vol. 90, no. 1, pp. 86–96, 1992, doi: 10.1172/JCI115860.

[41] O. Nüsse and M. Lindau, “The Dynamics of Exocytosis in Human Neutrophils,” *J. Cell Biol.*, vol. 107, no. 6, pp. 2117–2123, 1988, doi: 10.1083/jcb.107.6.2117.

[42] D. P. Lew, “Receptor signalling and intracellular calcium in neutrophil

activation," *Eur. J. Clin. Invest.*, vol. 19, pp. 338–346, 1989, doi: 10.1111/j.1365-2362.1989.tb00240.x.

[43] S. Rørvig *et al.*, "Ficolin-1 is present in a highly mobilizable subset of human neutrophil granules and associates with the cell surface after stimulation with fMLP," *J. Leukoc. Biol.*, vol. 86, no. 6, pp. 1439–1449, 2009, doi: 10.1189/jlb.1008606.

[44] S. Rørvig, O. Østergaard, N. H. H. Heegaard, and N. Borregaard, "Proteome profiling of human neutrophil granule subsets , secretory vesicles , and cell membrane : correlation with transcriptome profiling of neutrophil precursors," *J. Leukoc. Biol.*, vol. 94, no. October, pp. 711–721, 2013, doi: 10.1189/jlb.1212619.

[45] B. Dewald, U. Bretz, and M. Baggiolini, "Release of Gelatinase from a Novel Secretory Compartment of Human Neutrophils," *J. Clin. Invest.*, vol. 70, no. September, pp. 518–525, 1982, doi: 10.1189/jlb.1212619.

[46] E. Feuk-lagerstedt, C. Movitz, C. Dahlgren, and A. Karlsson, "Lipid raft proteome of the human neutrophil azurophil granule," *Proteomics*, vol. 7, pp. 194–205, 2007, doi: 10.1002/pmic.200600482.

[47] J. Hann, J. L. Bueb, F. Tolle, and S. Bréchard, "Calcium signaling and regulation of neutrophil functions: Still a long way to go," *J. Leukoc. Biol.*, vol. 107, no. 2, pp. 285–297, 2020, doi: 10.1002/JLB.3RU0719-241R.

[48] B. J. Bentwood and P. M. Henson, "The sequential release of granule constitutents from human neutrophils," *J. Immunol.*, vol. 12, no. 2, pp. 855–862, 1980.

[49] A. K. Gupta, S. Giaglis, P. Hasler, and S. Hahn, "Efficient Neutrophil Extracellular Trap Induction Requires Mobilization of Both Intracellular and Extracellular Calcium Pools and Is Modulated by Cyclosporine A," *PLoS One*, vol. 9, no. 5, pp. 1–12, 2014, doi: 10.1371/journal.pone.0097088.

[50] J. C. Jennette, H. Xiao, and R. J. Falk, "Pathogenesis of Vascular Inflammation by Anti-Neutrophil Cytoplasmic Antibodies," *Front. Nephrol.*, vol. 3, pp. 1235–1242, 1985, doi: 10.1681/ASN.2005101048.

[51] K. Kessenbrock *et al.*, "Netting neutrophils in autoimmune small-vessel vasculitis," *Nat. Med.*, vol. 15, no. 6, pp. 623–625, 2009, doi: 10.1038/nm.1959.

[52] G. S. Garcia-romo *et al.*, "Netting Neutrophils Are Major Inducers of Type I IFN Production in Pediatric Systemic Lupus Erythematosus," *Sci. Transl. Med.*, vol. 3, no. 73, p. 73ra20, 2011, doi: 10.1126/scitranslmed.3001201.

[53] Z. An *et al.*, "Neutrophil extracellular traps induced by IL-8 aggravate atherosclerosis via activation NF- κ B signaling in macrophages Neutrophil extracellular traps induced by IL-8 aggravate atherosclerosis via activation NF-κ B signaling in macrophages," *Cell Cycle*, vol. 18, no. 21, pp. 2928–2938, 2019, doi: 10.1080/15384101.2019.1662678.

[54] A. S. Savchenko *et al.*, "Neutrophil extracellular traps form predominantly during the organizing stage of human venous thromboembolism development," *J. Thromb. Haemost.*, vol. 12, no. 6, pp. 860–870, 2014, doi:

10.1111/jth.12571.

[55] E. A. Chapman *et al.*, “Caught in a trap? Proteomic analysis of neutrophil extracellular traps in rheumatoid arthritis and systemic lupus erythematosus,” *Front. Immunol.*, vol. 10, no. 423, pp. 1–20, 2019, doi: 10.3389/fimmu.2019.00423.

[56] A. Petretto *et al.*, “Neutrophil extracellular traps (NET) induced by different stimuli: A comparative proteomic analysis,” *PLoS One*, vol. 14, no. 7, pp. 1–18, 2019, doi: 10.1371/journal.pone.0218946.

[57] M. Bruschi *et al.*, “Neutrophil Extracellular Traps protein composition is specific for patients with Lupus nephritis and includes methyl-oxidized αenolase (methionine sulfoxide 93),” *Sci. Rep.*, vol. 9, no. 7934, pp. 1–13, 2019, doi: 10.1038/s41598-019-44379-w.

[58] W. M. Nauseef and S. Kremserova, “Isolation of Human Neutrophils From Venous Blood,” *Methods Mol. Biol.*, vol. 2087, pp. 33–42, 2020, doi: 10.1007/978-1-0716-0154-9_3.

[59] Y. Chen and W. G. Junger, “Measurement of Oxidative Burst in Neutrophils,” *Methods Mol. Biol.*, vol. 844, pp. 115–124, 2012, doi: 10.1007/978-1-61779-527-5.

[60] L. R. Reis *et al.*, “Citrullination of actin-ligand and nuclear structural proteins, cytoskeleton reorganization and protein redistribution across cellular fractions are early events in ionomycin-induced NETosis,” *Redox Biol.*, vol. 64, no. May, p. 102784, 2023, doi: 10.1016/j.redox.2023.102784.

[61] V. Brinkmann, C. Goosmann, L. I. Kühn, and A. Zychlinsky, “Automatic quantification of in vitro NET formation,” *Front. Immunol.*, vol. 3, no. 413, pp. 1–8, 2013, doi: 10.3389/fimmu.2012.00413.

[62] D. Pellerin, H. Gagnon, J. Dubé, and F. Corbin, “Amicon-adapted enhanced FASP: an in-solution digestion-based alternative sample preparation method to FASP,” *F1000Research*, vol. 4, no. 140, pp. 1–21, 2015, doi: 10.12688/f1000research.6529.1.

[63] J. R. Wiśniewski, “Filter-aided sample preparation for proteome analysis,” *Methods Mol. Biol.*, vol. 1841, pp. 3–10, 2018, doi: 10.1007/978-1-4939-8695-8_1.

[64] J. R. Wiśniewski, “Filter Aided Sample Preparation – A tutorial,” *Anal. Chim. Acta*, vol. 1090, pp. 23–30, 2019, doi: 10.1016/j.aca.2019.08.032.

[65] J. Cox and M. Mann, “MaxQuant enables high peptide identification rates, individualized p.p.b.-range mass accuracies and proteome-wide protein quantification,” *Nat. Biotechnol.*, vol. 26, no. 12, pp. 1367–1372, 2008, doi: 10.1038/nbt.1511.

[66] J. Cox, N. Neuhauser, A. Michalski, R. A. Scheltema, J. V. Olsen, and M. Mann, “Andromeda: A peptide search engine integrated into the MaxQuant environment,” *J. Proteome Res.*, vol. 10, no. 4, pp. 1794–1805, 2011, doi: 10.1021/pr101065j.

[67] M. Y. Hein, C. A. Luber, I. Paron, N. Nagaraj, and M. Mann, “Accurate

proteome-wide label-free quantification by delayed normalization and maximal peptide ratio extraction, termed MaxLFQ," *Mol. Cell. Proteomics*, vol. 13(9), pp. 2513–2526, 2014, doi: 10.1074/mcp.M113.031591.

[68] S. Tyanova *et al.*, "The Perseus computational platform for comprehensive analysis of (prote) omics data," *Nat. Methods*, vol. 13, no. June, pp. 731–740, 2016, doi: 10.1038/nmeth.3901.

[69] B. Yates, B. Braschi, K. A. Gray, R. L. Seal, S. Tweedie, and E. A. Bruford, "Genenames.org: The HGNC and VGNC resources in 2017," *Nucleic Acids Res.*, vol. 45, no. D1, pp. D619–D625, 2017, doi: 10.1093/nar/gkw1033.

[70] J. M. Robinson, "Phagocytic leukocytes and reactive oxygen species," *Histochem. Cell Biol.*, vol. 131, no. 4, pp. 465–469, 2009, doi: 10.1007/s00418-009-0565-5.

[71] K. Collison *et al.*, "Evidence for IL-12-Activated Ca2+ and Tyrosine Signaling Pathways in Human Neutrophils," *J. Immunol.*, vol. 161, no. 7, pp. 3737–3745, 1998, doi: 10.4049/jimmunol.161.7.3737.

[72] J. -S Wang, N. Pavlotsky, A. I. Tauber, and K. S. Zaner, "Assembly dynamics of actin in adherent human neutrophils," *Cell Motil. Cytoskeleton*, vol. 26, no. 4, pp. 340–348, 1993, doi: 10.1002/cm.970260408.

[73] C. K. Huang, "Protein kinases in neutrophils: A review," *Mol. Membr. Biol.*, vol. 8, no. 2, pp. 61–79, 1989, doi: 10.3109/09687688909082261.

[74] P. Bouti *et al.*, "β2 Integrin Signaling Cascade in Neutrophils: More Than a Single Function," *Frontiers in Immunology*, vol. 11. 2021. doi: 10.3389/fimmu.2020.619925.

[75] U. Jerke *et al.*, "Complement receptor Mac-1 is an adaptor for NB1 (CD177)-mediated PR3-ANCA neutrophil activation," *J. Biol. Chem.*, vol. 286, no. 9, pp. 7070–7081, 2011, doi: 10.1074/jbc.M110.171256.

[76] M. Lin *et al.*, "Matrix metalloproteinase-8 facilitates neutrophil migration through the corneal stromal matrix by collagen degradation and production of the chemotactic peptide pro-gly-pro," *Am. J. Pathol.*, vol. 173, no. 1, pp. 144–153, 2008, doi: 10.2353/ajpath.2008.080081.

[77] H. Sengeløv, P. Follin, L. Kjeldsen, K. Lollike, C. Dahlgren, and N. Borregaard, "Mobilization of granules and secretory vesicles during in vivo exudation of human neutrophils.," *J. Immunol.*, vol. 154, no. 8, pp. 4157–4165, 1995, doi: 10.4049/jimmunol.154.8.4157.

[78] N. Sorvillo, D. Cherpokova, K. Martinod, and D. D. Wagner, "Extracellular DNA net-works with dire consequences for health," *Circ. Res.*, vol. 125, no. 4, pp. 470–488, 2019, doi: 10.1161/CIRCRESAHA.119.314581.

[79] S. L. Wong and D. D. Wagner, "Peptidylarginine deiminase 4: a nuclear button triggering neutrophil extracellular traps in inflammatory diseases and aging," *FASEB J.*, vol. 32, pp. 1–13, 2018, doi: 10.1096/fj.201800691R.

[80] V. Mutua and L. J. Gershwin, "A Review of Neutrophil Extracellular Traps (NETs) in Disease: Potential Anti-NETs Therapeutics," *Clin. Rev. Allergy Immunol.*, vol. 61, no. 2, pp. 194–211, 2021, doi: 10.1007/s12016-020-08804-

7.

[81] D. N. Douda, M. A. Khan, H. Grasemann, and N. Palaniyar, “SK3 channel and mitochondrial ROS mediate NADPH oxidase-independent NETosis induced by calcium influx,” *Proc. Natl. Acad. Sci.*, vol. 112, no. 9, pp. 2817–2822, 2015, doi: 10.1073/pnas.1414055112.

[82] A. S. Byrd, X. M. O’Brien, C. M. Johnson, L. M. Lavigne, and J. S. Reichner, “An extracellular matrix-based mechanism of rapid neutrophil extracellular trap formation in response to C. albicans1,” *J Immunol.*, vol. 190, no. 8, pp. 4136–4148, 2013, doi: 10.4049/jimmunol.1202671.

[83] K. Chen *et al.*, “Endocytosis of soluble immune complexes leads to their clearance by FcγRIIIB but induces neutrophil extracellular traps via FcγRIIA in vivo,” *Blood*, vol. 120, no. 22, pp. 4421–4431, 2012, doi: 10.1182/blood-2011-12-401133.

[84] O. Rodríguez-Espinosa, O. Rojas-Espinosa, M. M. B. Moreno-Altamirano, E. O. López-Villegas, and F. J. Sánchez-García, “Metabolic requirements for neutrophil extracellular traps formation,” *Immunology*, vol. 145, no. 2, pp. 213–224, 2015, doi: 10.1111/imm.12437.

[85] N. Vorobjeva *et al.*, “Mitochondrial reactive oxygen species are involved in chemoattractant-induced oxidative burst and degranulation of human neutrophils in vitro,” *Eur. J. Cell Biol.*, vol. 96, no. 3, pp. 254–265, 2017, doi: 10.1016/j.ejcb.2017.03.003.

[86] J. Zielonka *et al.*, “Mitochondria-Targeted Triphenylphosphonium-Based Compounds : Syntheses , Mechanisms of Action , and Therapeutic and Diagnostic Applications,” 2017, doi: 10.1021/acs.chemrev.7b00042.

[87] S. Theander, D. P. Lew, and O. Nüße, “Granule-specific ATP requirements for Ca 2 + -induced exocytosis in human neutrophils. Evidence for substantial ATP-independent release,” *J. Cell Sci.*, vol. 115, no. 14, pp. 2975–2983, 2002, doi: 10.1242/jcs.115.14.2975.

[88] J. Hann, J. L. Bueb, F. Tolle, and S. Bréchard, “Calcium signaling and regulation of neutrophil functions: Still a long way to go,” *Journal of Leukocyte Biology*, vol. 107, no. 2. pp. 285–297, 2020. doi: 10.1002/JLB.3RU0719-241R.

6. Appendix list (CHAPTER 2)

- **Supplemental Figure 1:** PMA- and fMLP-treated neutrophils share the majority of secreted proteins
- **Supplemental Table 1A:** Enriched and unique proteins found in each of the five clusters identified comprising the control, ionomycin, PMA, and fMLP groups

- **Supplemental Table 1B:** Pathway enrichment analysis of unique and enriched proteins in the control and ionomycin groups
- **Supplemental Table 1C:** Pathway enrichment analysis of unique and enriched proteins in the control group
- **Supplemental Table 1D:** Pathway enrichment analysis of unique and enriched proteins in the ionomycin group
- **Supplemental Table 1E:** Pathway enrichment analysis of unique and enriched proteins in the PMA and fMLP groups
- **Supplemental Table 1F:** Pathway enrichment analysis of unique and enriched proteins in the ionomycin, PMA, and fMLP groups
- **Supplemental Table 2A:** Unique proteins found in the secretome of ionomycin- and PMA-treated neutrophils at 30 and 90 min, respectively
- **Supplemental Table 2B:** Volcano plot data of the secretome of ionomycin- and PMA-treated neutrophils at 30 and 90 min, respectively
- **Supplemental Table 2C:** Cellular component analysis of unique and enriched proteins in the ionomcyn group at 30 min when compared with the PMA group at 90 min
- **Supplemental Table 2D:** Cellular component analysis of unique and enriched proteins in the PMA group at 90 min when compared with the ionomycin group at 30 min

The above supplemental tables can be found at: https://github.com/Lore-rocha/CHAPTER2-Neutrophil-s-response-before-NETs-release-is-stimulus-dependent

7. Appendix - supplemental figure (CHAPTER 2)

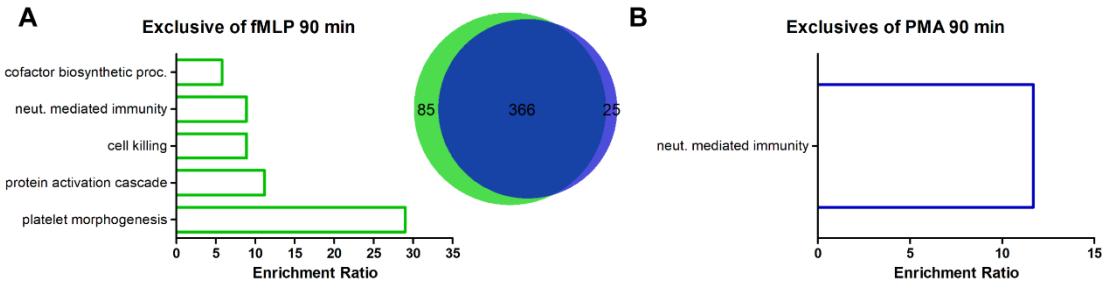

Supplemental Figure 1. PMA- and fMLP-treated neutrophils share the majority of secreted proteins. Cellular component analysis of unique proteins from neutrophils treated with A) 1 µM fMLP or B) 20 nM PMA, for 90 min. For each enriched biological process (y-axis), the enrichment ratio (the number of observed genes over the expected value, x-axis) was calculated. Only biological processes with FDR < 0.05 were displayed. Secreted proteins were acquired from neutrophils in three independent experiments.

Final Remarks

In this thesis, we used high-resolution proteomic analysis and live-imaging microscopy to study the events prior to the release of NETs from two perspectives. First, we investigated the most abundant proteins in the cellular fractions of neutrophils treated for 2 min with ionomycin. Second, we compared the proteins in the secretome of neutrophils treated with fMLP, PMA or ionomycin in the time-points of 30 and 90 min. In addition, we analyzed the chromatin behavior and NETosis kinetics using live-imaging microscopy and the ability to activate NADPH oxidase using the cytochrome c reduction assay.

Thus, neutrophils treated with ionomycin underwent rapid changes in the structure of their nucleus and communicated these changes to the environment secreting proteins crucial for the inflammatory response, such as myeloperoxidase, elastase and azurocidin. Furthermore, extensive protein remodeling occurred among the neutrophil fractions, mainly in the nucleus and organelle enriched fractions, and this effect was accompanied by the citrullination of proteins linked to the cytoskeleton, nuclear structure, and chromatin.

On the other hand, when we compared neutrophils treated with fMLP, PMA, and ionomycin, we saw that they respond differently to each specific stimulus. Neutrophils treated with ionomycin released NETs in 60 min, whereas it took 120 min for neutrophils treated with PMA to reach the same outcome. Although both fMLP and PMA led to NADPH oxidase activation in neutrophils, NETs were not seen in fMLP-treated neutrophils. Proteins related to neutrophil adhesion and migration, as well as upregulation of superoxide production were found enriched in the secretome of neutrophils treated with PMA for 90 min. In

contrast, the secretome of neutrophils treated with ionomycin for 30 min was enriched with microbicidal proteins from the azurophilic granules.

Therefore, this thesis introduced new biochemical mediators involved in the response that triggers the release of NETs as well as in the communication of these activated cells with the environment.